26937

National Library Bibliothèque nationale
of Canada du Canada

CANADIAN THESES
ON MICROFICHE

*THESES CANADIENNES
SUR MICROFICHE*

NAME OF AUTHOR/*NOM DE L'AUTEUR*___MICHAEL CHI-FU TO___

TITLE OF THESIS/*TITRE DE LA THÈSE*___A NEAR IDEAL PID CONTROLLER AND___

___ITS TUNING___

UNIVERSITY/*UNIVERSITÉ*___UNIVERSITY OF ALBERTA___

DEGREE FOR WHICH THESIS WAS PRESENTED/
*GRADE POUR LEQUEL CETTE THÈSE FUT PRÉSENTÉE*___M.Sc.___

YEAR THIS DEGREE CONFERRED/*ANNÉE D'OBTENTION DE CE GRADE*___1975___

NAME OF SUPERVISOR/*NOM DU DIRECTEUR DE THÈSE*___Dr. J F VANELDIK___

DATED/*DATE*___1st Oct, 1975___ SIGNED/*SIGNÉ*_____

PERMANENT ADDRESS/*RÉSIDENCE FIXE*___2911 - 68 St, Edmonton, Alberta___

___Canada___

THE UNIVERSITY OF ALBERTA

A NEAR IDEAL PID CONTROLLER AND ITS TUNING

BY

MICHAEL CHI-FU TO (C)

A THESIS

SUBMITTED TO THE FACULTY OF GRADUATE STUDIES AND RESEARCH

IN PARTIAL FULFILMENT OF THE REQUIREMENTS FOR THE DEGREE

OF MASTER OF SCIENCE

DEPARTMENT OF ELECTRICAL ENGINEERING

FALL, 1975

THE UNIVERSITY OF ALBERTA

FACULTY OF GRADUATE STUDIES AND RESEARCH

The undersigned certify that they have read, and
recommend to the Faculty of Graduate Studies and Research, for
acceptance, a thesis entitled "A Near Ideal PID Controller and its
Tuning" submitted by Michael Chi-Fu To in partial fulfilment of the
requirements for the degree of Master of Science.

....
Supervisor

....

....

....

Date...Oct. 2/1975

Dedication

To my grandmother who could not wait to see the finish of this thesis.

Also, to my wife who has shown great patience and encouragement during the whole process.

ABSTRACT

The objective to design a PID Controller with negligible

parameter interdependency was carried out. As a result the optimum

tuning graphs developed by A.M. Lopez, based on integral of error

criteria, ideal PID algorithm and steepest descent computing technique

can be used in conjunction with this near ideal PID controller. Reset

inhibiting and other convenient features are also incorporated to make

this controller more versatile.

ACKNOWLEDGEMENT

TABLE OF CONTENTS

LIST OF TABLES

LIST OF FIGURES

xiii

NOMENCLATURE

$r(t)$	Set point function
$R(s)$	Laplace transform of set point function
$e(t)$	Error function
$E(s)$	Laplace transform of error function
$m(t)$	Control function
$M(s)$	Laplace transform of control function
$c(t)$	process output function
$c(s)$	Laplace transform of process output function
S	Laplace operator
PID	Proportional, integral, derivative
K_c	Gain constant
T_i	Integral time constant
T_d	Derivative time constant
IVC	Current to voltage converter
VIC	Voltage to current converter
$m'(t)$	Control function before filtering
$m_M(t)$	Manual control function
$m_d(t)$	The sum of control action and disturbance
SW	Switch
K	Process gain constant
Lr	Process reaction time constant
Rr	Process reaction rate constant
θ_o	Dead time delay
τ	Time constant of a 1st order system
ωn	Natural frequency of a 2nd order system

ξ Damping ratio of a 2nd order system

ϕ Figure of merit for integral of error

ϕ_{ITE} Integral of error x time

ϕ_{ISE} Integral of error squared

ϕ_{IAE} Integral of absolute error

ϕ_{ITAE} Integral of absolute error x time

ϕ_{ITSE} Integral of error squared x time

Chapter I

Introduction

The Conventional Continuous PID Controller

In its early days, the design and application of the conventional continuous PID controller was somewhat of an art [1]. The choice of the PID combination itself was guided by intuition and experience. In those early days, the problem caused by dead time delay and physical limitations were great obstacles to analytical study of the system [2]. Hence, it is not surprising to find that even the tuning methods were derived by trial and error. Quite a number of tuning methods are in use. To name a few: Ziegler-Nichols method, Harriot's method, 3-C method etc. Most of these methods were based on the quarter decay ratio (or some other arbitrary constraints which lack solid mathematical justification) as the performance criterion.

To complicate the matter further, most of the conventional PID controllers have their three parameters interrelated [3]. Thus, even if the correct parameter settings were known, it could well take hours to settle down to the final adjustments. It is therefore obvious that optimal tuning of a controller is quite a difficult problem (By optimal tuning is meant that tuning which gives the best performance, judged by a certain mathematically sound performance criterion).

1

Possible Improvements

The optimal tuning problem should not be avoided, because it can be shown that efforts devoted to optimal tuning can bring spectacular results [3].

The tuning difficulties outlined above actually initiated the development of the digital version of PID controller, which has independent parameters. It was shown in reference 4 that as sampling frequency increases the overall performance of a digital PID controller improves. In the limit it approaches the performance of a continuous controller. This means continuous PID controller would be superior but for its difficulties in optimal tuning.

It was also proved by M. Athans and K.T. Parker [5, 11], that proper choice of cost functionals for the general tracking problems, and application of optimal linear regulator theory to the optimal tuning problem indeed yield a PID type of controller as the solution.

The above arguments with respect to continuous systems and optimality provide sufficient grounds to warrant taking a second look at continuous PID controllers.

A.M. Lopez in his Ph.D. dissertation [6] had indicated the shortcomings of the quarter decay ratio as a performance criterion, especially if applied to higher order plants. He also indicated the desirability of using the integral of error as a performance index. He used a steepest descent computer program to search for optimal

settings for plants with dead time delay (using the integral of
error as performance criterion and assuming an ideal algorithm with
no lag and independent parameters).

A question arises as to whether the ideal algorithm can be
closely approximated. (In real controllers, no lag derivative
action can not be achieved because of noise). If a close approx-
imation can be achieved, one can use the results provided by Lopez
as the optimal settings for a system with integral of error as the
performance criterion. Assuredly this three fold improvement
(better performance criterion, independent parameters and computer
derived results) will bring about spectacular results when compared
to the previous trial and error situation.

In both pneumatic and electronic controllers with purely
passive networks, the parameter interrelating situation is unavoid-
able [3]. This problem can be solved by using active networks.
With the advent of integrated circuits, independence of parameters
can be easily achieved. Also, due to the negligible D.C. drift of
integrated circuits, one can avoid complicated D.C. to A.C. and A.C.
to D.C. conversions as was necessary in conventional electronic
controllers [7, 8]. A certain amount of lag must exist in the
derivative action. Otherwise the gain at high frequencies will be
intolerably large. However, the objective in this thesis project was
not to build a completely ideal controller, but rather to develop
as close an approximation to it as possible. A.M. Lopez's ideal PID
algorithm will be shown in Chapter IV. PID stands for proportional,
integral and derivative.

The Objective

The primary objective in this thesis, therefore, is to design a continuous PID controller with an algorithm closely approximating the ideal one cited by Lopez, such that all the tuning graphs developed by Lopez will be directly applicable.

Other features that will be incorporated in the controller are: integral inhibiting action, direct and indirect action, manual control, bumpless transfer, digital and analog set point adjustment. All these are included to make the controller more versatile and suitable for industrial usage.

Chapter II

Theoretical Background

The conventional PID controller is based on the simple idea of negative feedback. It is well known that the linear regulator theory requires only state variable feedback [9]. In essence, the plant output is fed back and compared with the set point (input). The difference between them, the error signal, will be manipulated in a certain fashion to generate the control action. In turn the control action will force the plant output to move in a direction such as to reduce and eventually eliminate the error signal. Therefore, the sole purpose of the controller is to provide the desired manipulation of the error signal. The position of a controller in a control loop is shown in figure 2-1.
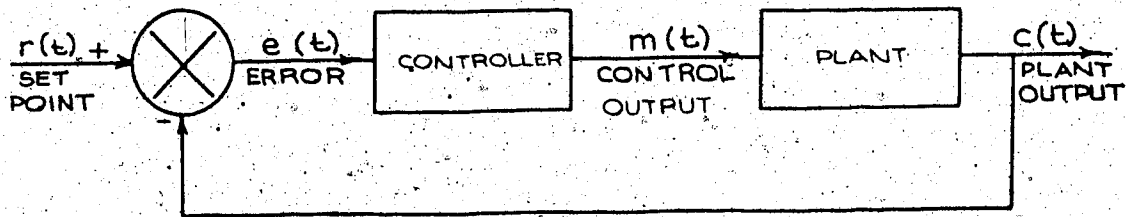
Figure 2-1 The position of the controller in a control loop.

Proportional Action (P action)

The simplest way to manipulate the error signal is to multiply it by a gain K_c as the following:

$$m(t) = K_c e(t) \qquad\qquad (2\text{-}1)$$

$$M(S) = K_c E(S)$$

where $m(t)$ is the control action

$e(t)$ is the error signal

K_c is a gain constant

and S is the Laplace operator. (assuming all initial conditions are zero)

The proportional action is shown in figure 2-2.
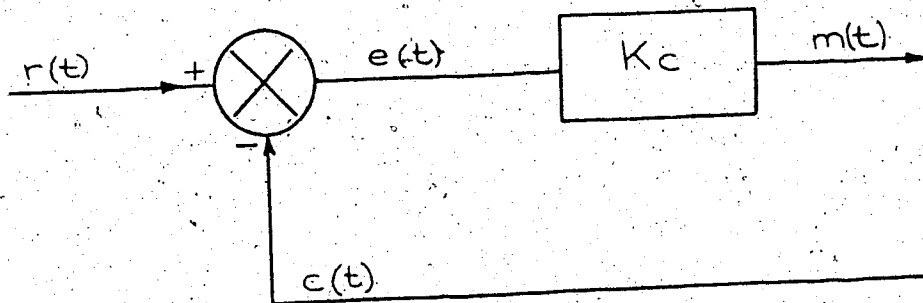
Figure 2-2 The proportional action in a control loop.

From Figure 2-2 it is obvious that the control action $m(t)$ is directly proportional to gain K_c and error signal $e(t)$. A higher value of $m(t)$ will reduce the error faster. However, for a "proportional only" controller there will always be some steady state error (offset), otherwise the control action $m(t)$ would be zero. Although higher gain will produce a smaller offset, it might also lead to a reduced degree of stability in the control loop.

Proportional Plus Integral Action (PI action)

The integral action is primarily introduced to cancel offset. By definition it is the action which integrates the error signal. As

error persists the integrated value will grow with time, and
eventually will be large enough to eliminate offset completely.
The formulation of PI action is:

$$m(t) = K_c\, e(t) + \frac{K_c}{T_1} \int e(t)\, dt$$

$$M(S) = K_c E(S) + \frac{K_c E(S)}{T_1 S}$$

$$= K_c (1 + \frac{1}{T_1 S}) E(S) \qquad\qquad (2\text{-}2)$$

where T_1 is the integral time constant. Or in block diagram form in
figure 2-3.
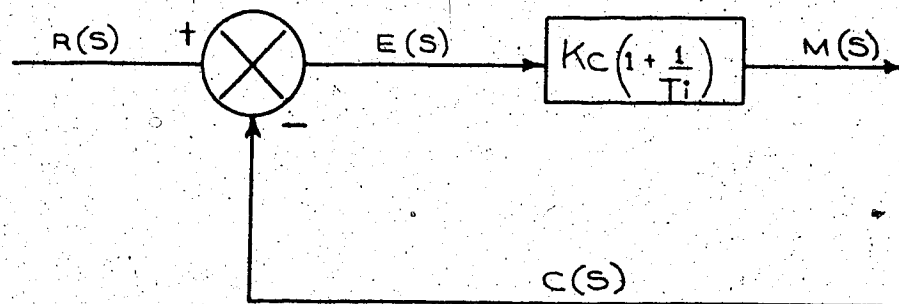
Figure 2-3 PI action in a control loop.

Note that if e(t) equals a constant and $t=T_1$ in equation (2-2), the
integral part will be equal to the proportional part. Therefore, the
integral time constant T_1 is the time needed to produce an integral
action equal to the proportional action. This situation is depicted
in figure 2-4.
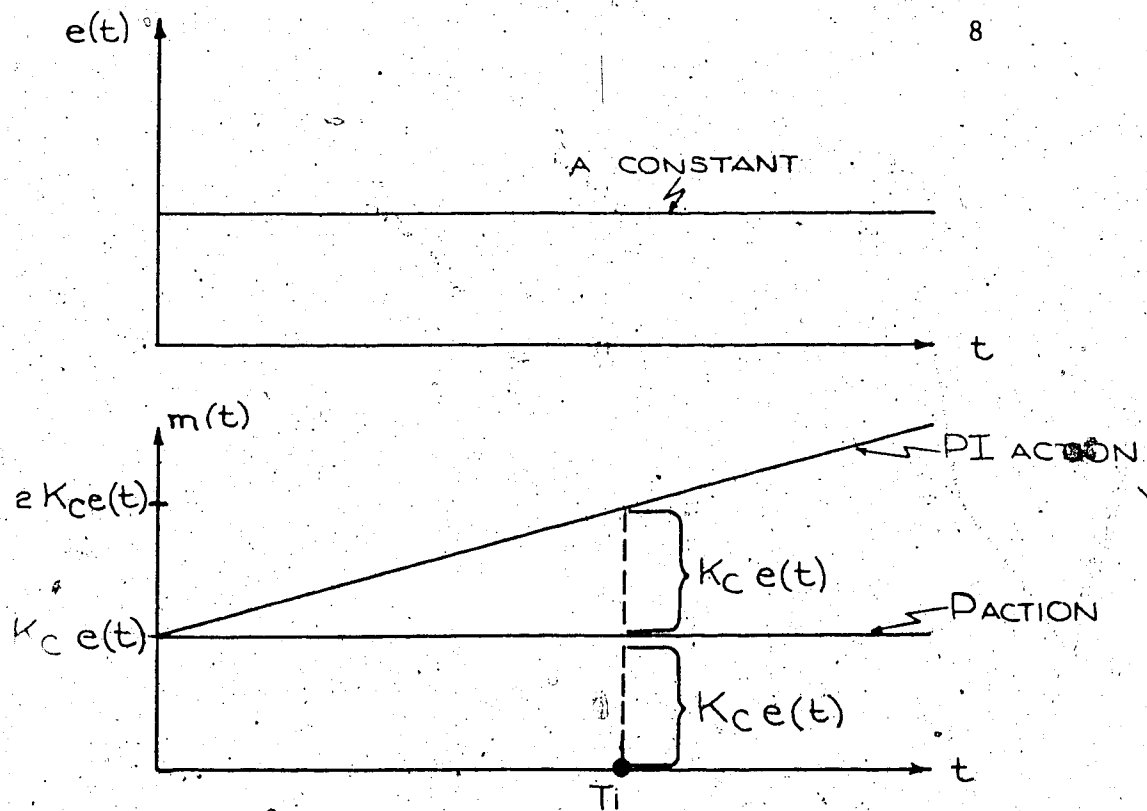
Figure 2-4 The relationship between integral time constant

T_i and control action.

At the very instant when disturbances or load changes of a process occur, the integral action is very small, because the time elapsed is still very short. At this early time the major action is the proportional action. Later the integral action takes over and forces the error to diminish and eventually vanish as time goes on. As the error approaches zero so does the proportional action. However, if the values of $1/T_i$ is too large the integrator will charge up too much and cause the output response to overshoot the set point. Only after overshoot has actually occurred (the error signal will change sign) will the integrator start to discharge. Actually, too much integral action will decrease the stability of the loop.

The frequency response of PI action is shown in figure 2-5.

GAIN

INTEGRAL ACTION

-6db/OCTAVE/SLOPE

K_C

ω RADIANS/SEC

$\frac{1}{Ti}$
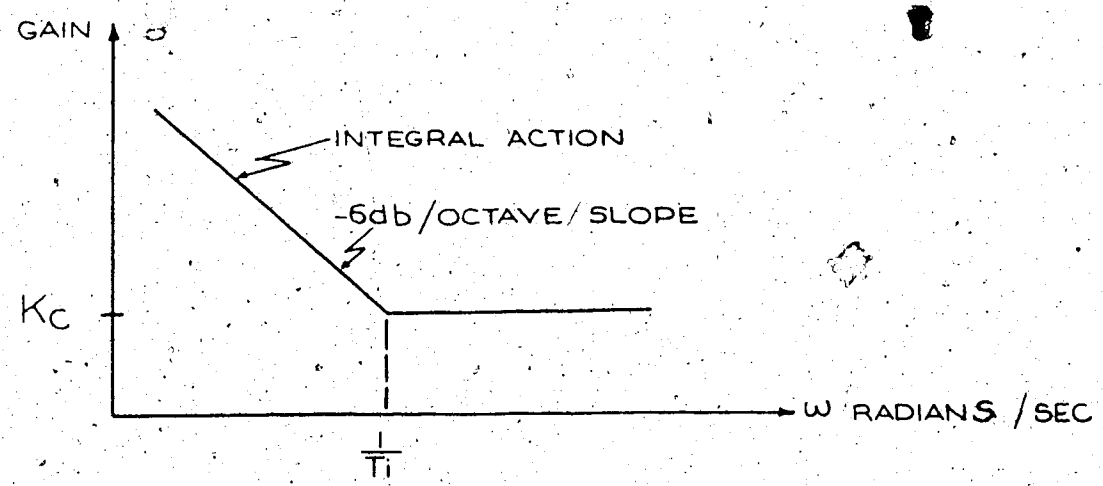
Figure 2-5 The frequency response plot of PI action.

Note that at higher frequencies proportional action predominates. This is in accord with the previous analysis; because the initial transient of the response consists mainly of higher frequency components. On the other hand, as steady state is approached the output contains primarily very low frequency components and hence mainly the integral action is of importance.

Proportional Plus Derivative Action (PD action)

Derivative action is needed whenever substantial time lags exist in the control loop. This action is proportional to the rate of change of error signal, and hence is predictive in nature. The PD action can be described as:

$$m(t) = K_c e(t) + K_c T_d \frac{de(t)}{dt}$$

$$M(S) = K_c E(S) + K_c T_d S E(S)$$

$$= K_c (1 + T_d S) E(S) \qquad (2-3)$$

where T_d is the derivative time constant. Its block diagram form
is shown in figure 2-6.
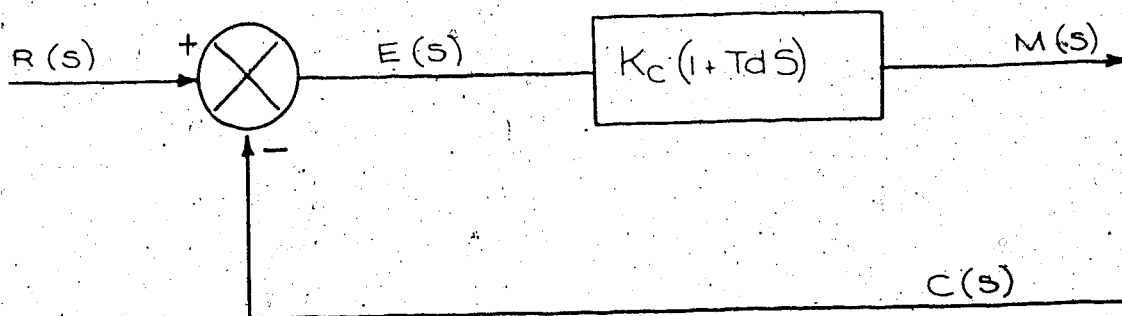
Figure 2-6 PD action in a control loop.

At the very instant when a disturbance occurs, the
derivative action is in the same direction as the proportional action
and therefore fulfills its anticipatory function. After the initial
period the derivative action will become opposite in sign with
respect to the proportional action. This, in effect reduces the control
output, slows down the process and therefore increases the stability
of the control loop. This situation is shown in figure 2-7.

$c(t)$

$r(t)$

t

$K_c\, e(t)$

t

$T_d\, \dfrac{de(t)}{dt}$

t
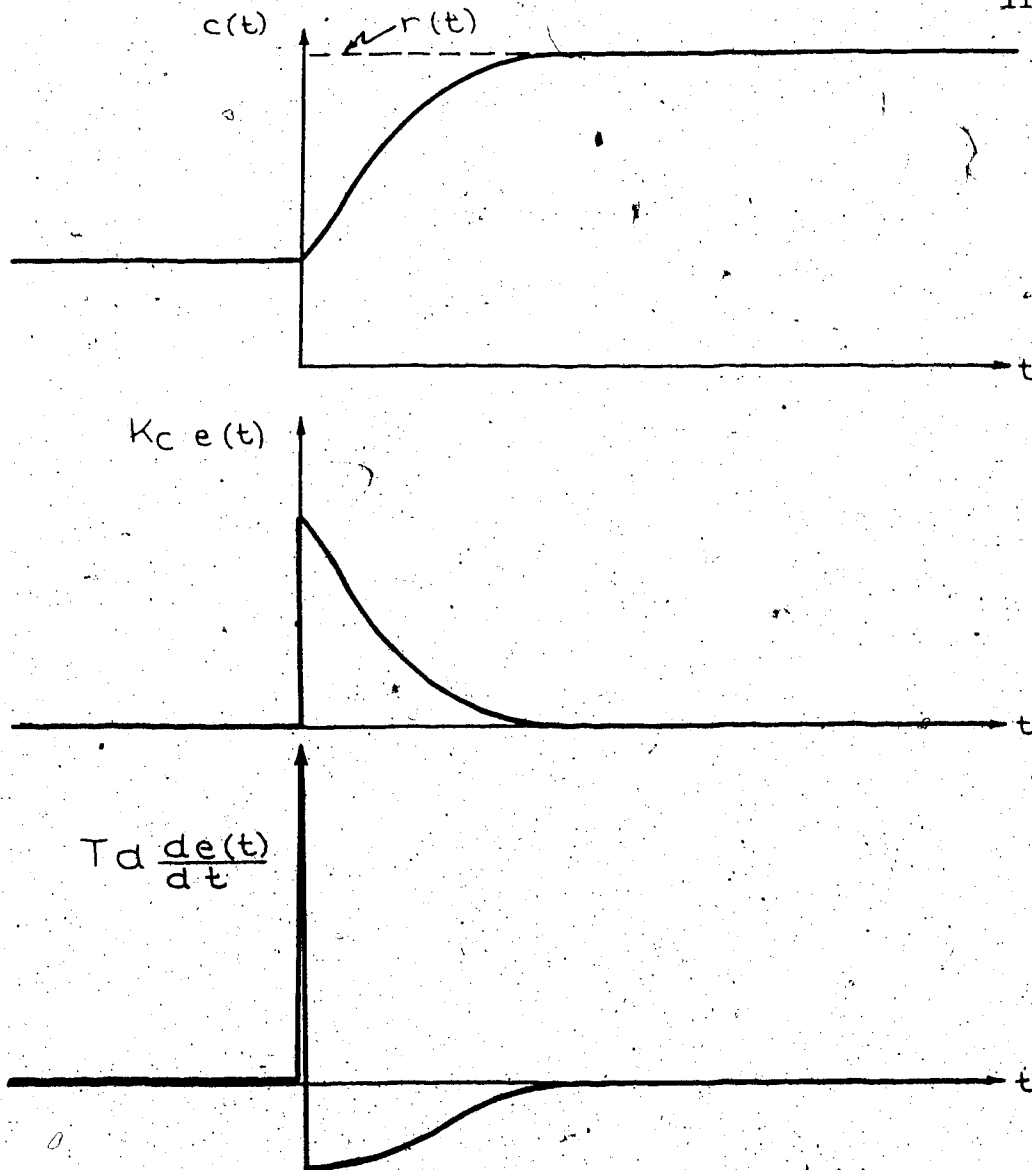
Figure 2-7 The variation of $c(t)$, $K_c e(t)$ and $T_d\ \dfrac{de(t)}{dt}$ during a

sudden change of set point.

Usually, when derivative action exists, the proportional

gain K_c can be increased because of the increased stability. Under

steady state the derivative action is zero . The above description

can also be derived from the frequency response plot of PD action

as shown in figure 2-8.

GAIN

DERIVATIVE ACTION
+6 dB / OCTAVE

K_c

ω RADIANS / SEC

T_d
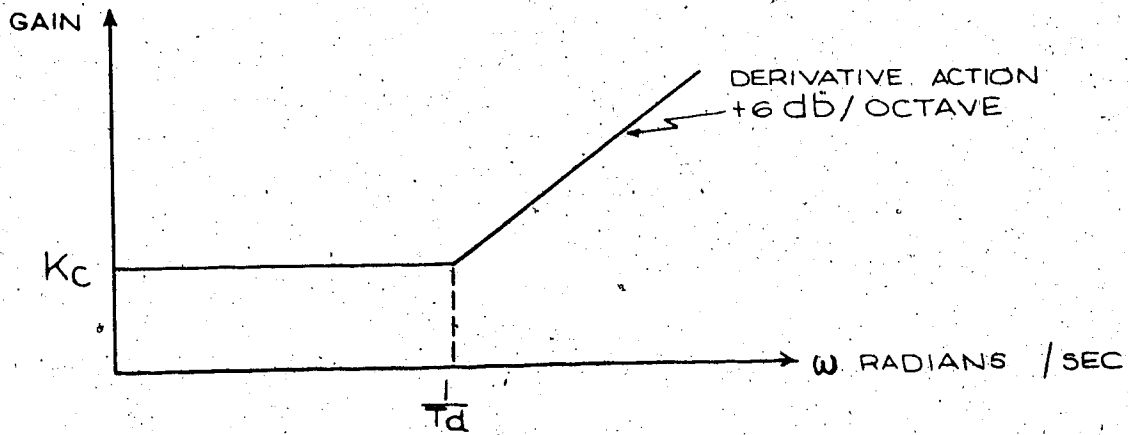
Figure 2-8 The frequency response plot of PD action

If $e(t) = A \cdot t$, a ramp function (A is a constant), the control

action will be :

$$m(t) = K_c e(t) + K_c T_d \cdot \frac{d\ e(t)}{dt}$$

$$= K_c \cdot A \cdot t + K_c \cdot T_d \cdot A \qquad (2-4)$$

The derivative part of control action is equal to $K_c \cdot T_d \cdot A$. When

$t = T_d$,

$$m(t_d) = K_c \cdot T_d \cdot A + K_c \cdot T_d \cdot A \qquad (2-5)$$

That is to say, when $t = T_d$, the proportional part will be equal to

the derivative part as shown graphically in figure 2-9.
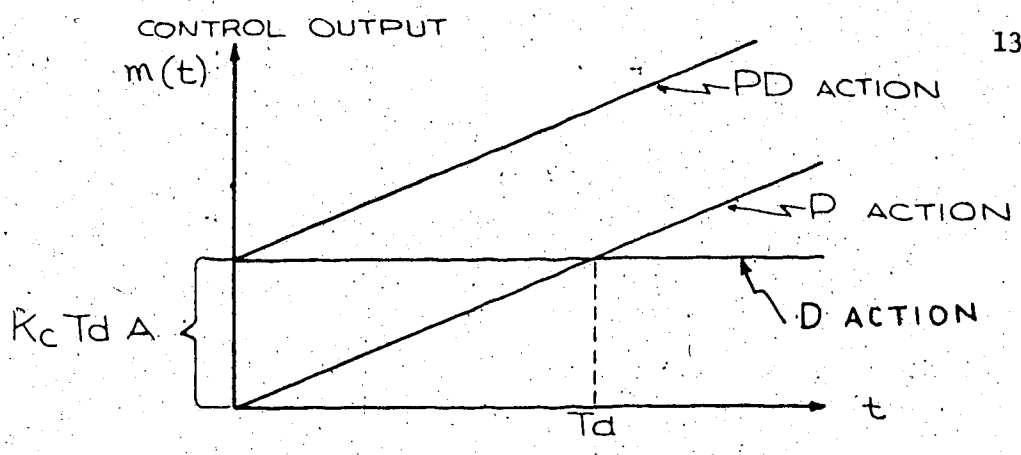
Figure 2-9 The relationship between derivative time

constant T_d and PD action

It should be clear from figure 2-9 that the derivative action is T_d units of time ahead of the proportional action.

Proportional Plus Integral Plus Derivative Action (PID action)

The formulation of the three mode controller is:

$$m(t) = K_c \cdot e(t) + \frac{K_c}{T_i} \int e(t)\, dt + K_c T_d \frac{de(t)}{dt}$$

$$M(S) = K_c(1 + \frac{1}{T_i S} + T_d S)\, E(S) \qquad\qquad (2\text{-}6)$$

The block diagram representation of equation (2-6) is shown in figure 2-10.
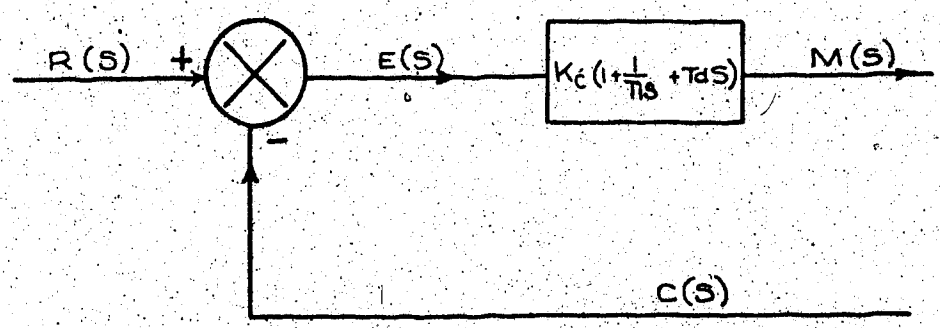
Figure 2-10 Block diagram of a PID (three mode) controller

If e(t) is again a ramp function the control action will be as shown
in figure 2-11.
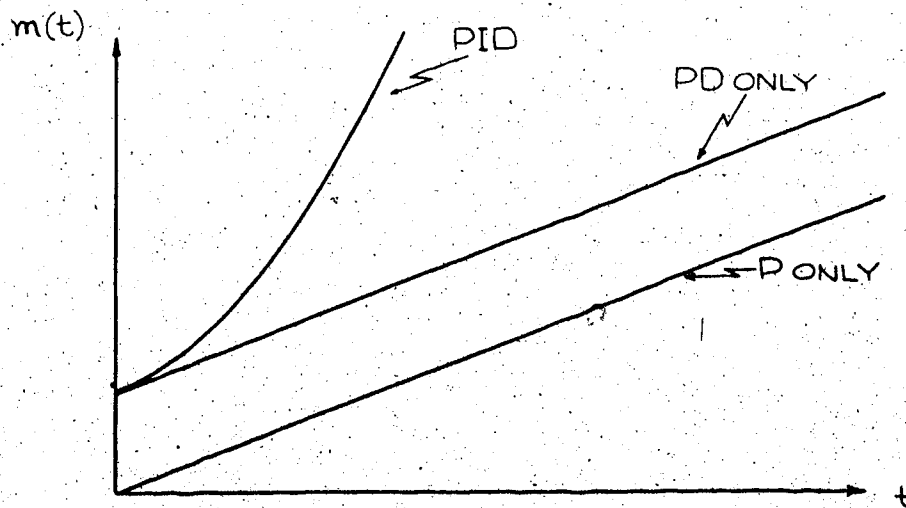
Figure 2-11 Three mode controller action with ramp input

The frequency response of the three mode controller is shown in
figure 2-12. ω_1 and ω_2 in Figure 2-12 are derived from equation 2-6.
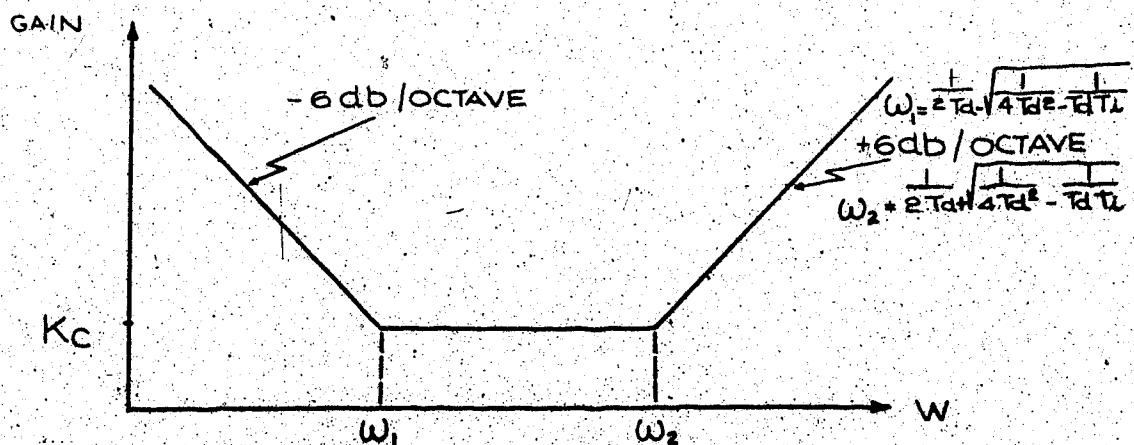
Figure 2-12 Frequency response of a PID controller

In figure 2-12 the high frequency end exhibits a positive slope.

This positive slope represents the effective derivative action and is

intended to take care of errors with primarily higher frequency

components. Similarly the effective integral action is represented

by negative slope at the low frequency end and will deal with steady

state errors which consist essentially of low frequency components.

The manipulation of T_d and T_i will shift the two corner frequencies

of the response horizontally, while a change in K_c value will only

shift the whole curve up and down.

Generally the integral action will decrease stability, reduce

offset to zero and will increase the period of any possible ringing.

The derivative action will increase stability and decrease the period

of ringing. Therefore, when derivative action exists one can use

higher values of K_c and $1/T_i$. Unfortunately, the derivative action

is also very sensitive to noise.

References 1, 2 and 10 give detailed discussion on this subject.

Modern Point of View

In the past, the application of optimal linear regulator

theory to industrial control problems led to PD type of linear feedback

systems. As recently as 1972 M. Athans [5] showed that, in choosing

cost functionals, consideration has to be given to three factors.

These factors are: the cancelling of steady state error, the boundedness

of control output and the independence of control output from nominal

plant parameters. The resultant control algorithm for a first order

plant is a PID instead of a PD combination. K.T. Parker [11], later

in the same year, expanded Athan's method to cover the general problem
of tracking m variables with a nth – order system. For example, the
following control loop will result for a second order plant (figure
2-13).
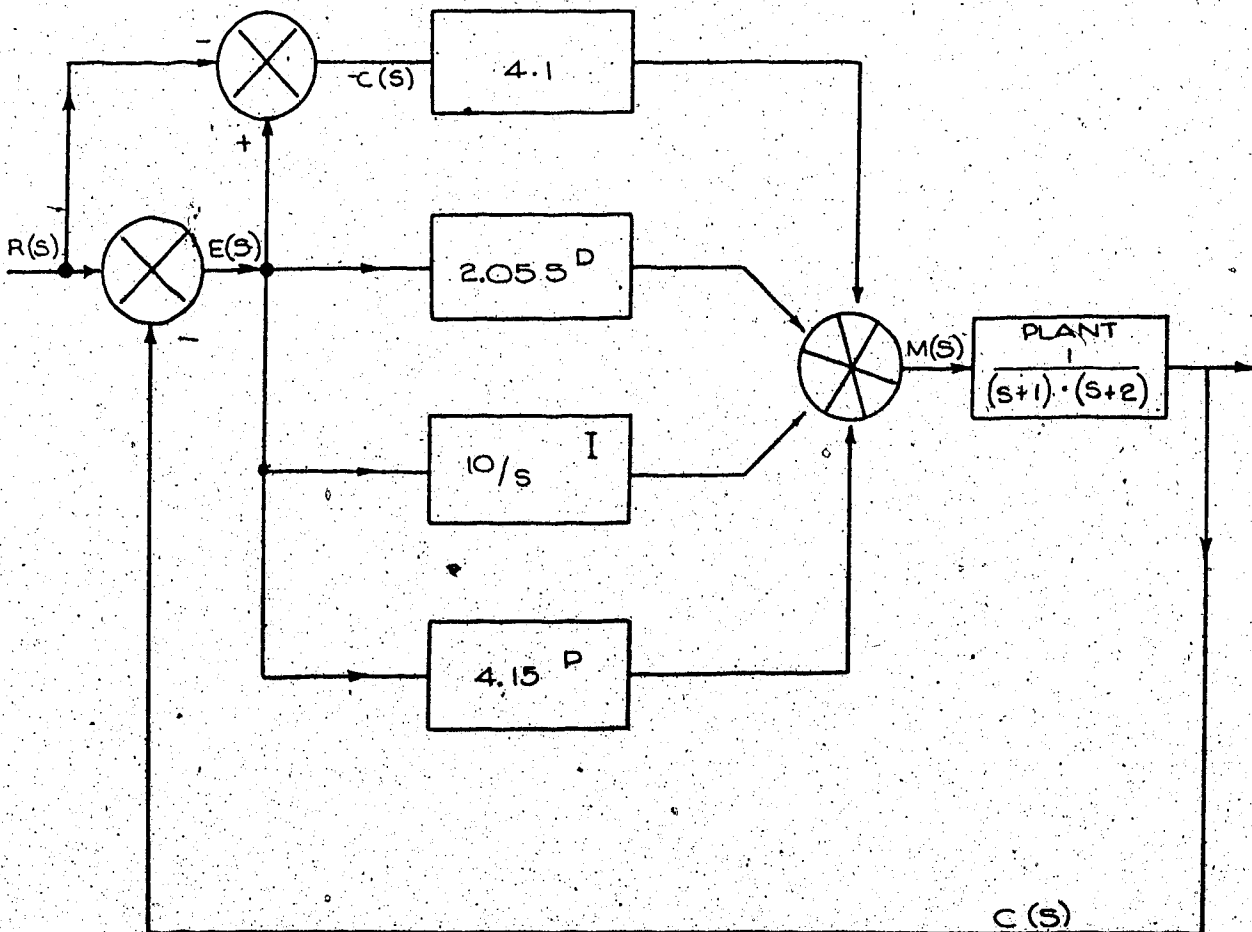
Figure 2-13 The optimal PID combination for the second order plant

$$\frac{1}{(S+1)(S+2)}$$

The above argument shows that, at least for linear systems,
the optimal form of controller has to contain all three modes of

action. Therefore, the works of Athans and Parker can serve as a solid mathematical basis for three mode controlling which was implemented long ago by intuition and experience.

In this thesis, however, it is not intended to design an optimal controller in the strictest sense because great effort is required merely to find a specific PID combination for a particular plant. Instead, to be more general, a fixed format PID controller with independently variable parameters will be developed. Such a controller, with easily adjustable parameters may then be applied to a wide variety of plants.

Integral Inhibiting Action (Reset Inhibiting) [12,13]

By using integral action, the offset inherent in proportional only control will be eliminated. However, when PI action is applied to processes requiring either start up, shut down, large changes in control point or major load changes, large overshoots are generally present during the transient, because of a condition known as integral wind-up. In critical processes such as batch-sintering, batch brazing, diffusion, crystal growing etc., overshoot may not be tolerated because it can affect the quality of the product. Therefore many critical processes using conventional controllers are started manually to avoid overshoot.

At the beginning of a sudden change, the error signal is large. The integral action will integrate this large error signal. As time goes on it probably will saturate the integrator. Consequently

the controller output will be at its maximum or minimum values.
This situation is called integral wind-up. The integral action will
get out of saturation only when the error signal changes sign i.e. the
controlled variable cross the set point (overshoot). Once overshoot
occurs, the integrator will start to discharge from the value it
stored up during the initial moments. It might take some time to
discharge and eventually bring the controlled variable back towards
the set point.

One scheme devised to remedy this situation is to use
derivative action. Consider the responses in figure 2-14:
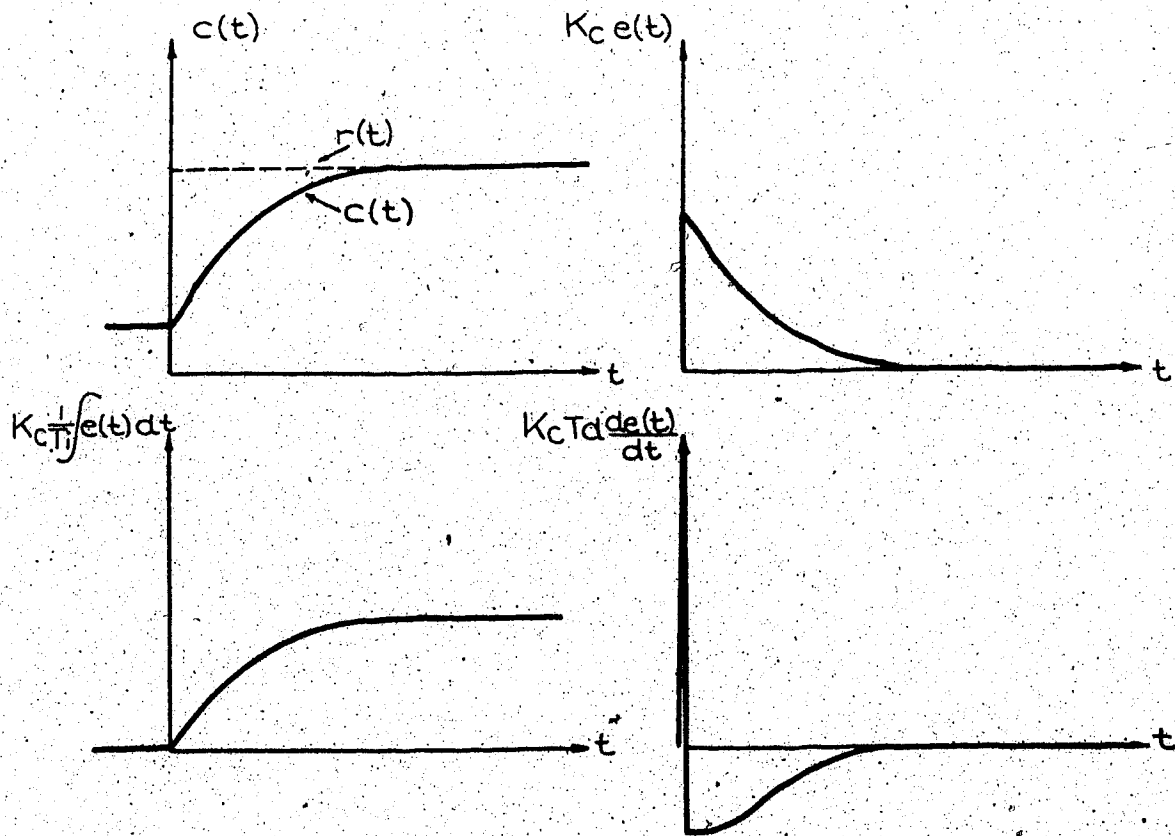
Figure 2-14 The various responses to a set point change

Except in the initial instant, the derivative action is in opposite direction to both P and I actions. Therefore the D action can cancel part of the I action. As a result, the overshoot will be reduced to some extent. Nevertheless, this method is not adequate to solve the problem, especially when the steady state controlled variable is only a fraction of the maximum controller output. (i.e. the integrator has a great deal of range to charge up to a large value)

The reset inhibiting scheme to be used in the proposed design is derived from the following reasoning: (1) Both integral and derivative action are aimed primarily at on-line control where integral action can eliminate offset and derivative action yields quick response to disturbances. (2) In a practical controller there will always be a limit to the range of output (output bounded). Initially the error is so large that proportional action alone would probably demand maximum or minimum controller output. Therefore, the reset action can actually be shut off initially.

To decide the proper moment and amount at which to re-introduce integral action, the following study of figure 2-15 is required. In figure 2-15, the error signal at point A will cause the proportional action to be either 70% or 62% of the maximum output, depending on the gain setting K_c. So long as error exists, P action will be different from its steady state value. The value of P action will depend on both the size of error and the P action gain setting. If the I action is to assist the P action, it should be in the same direction as
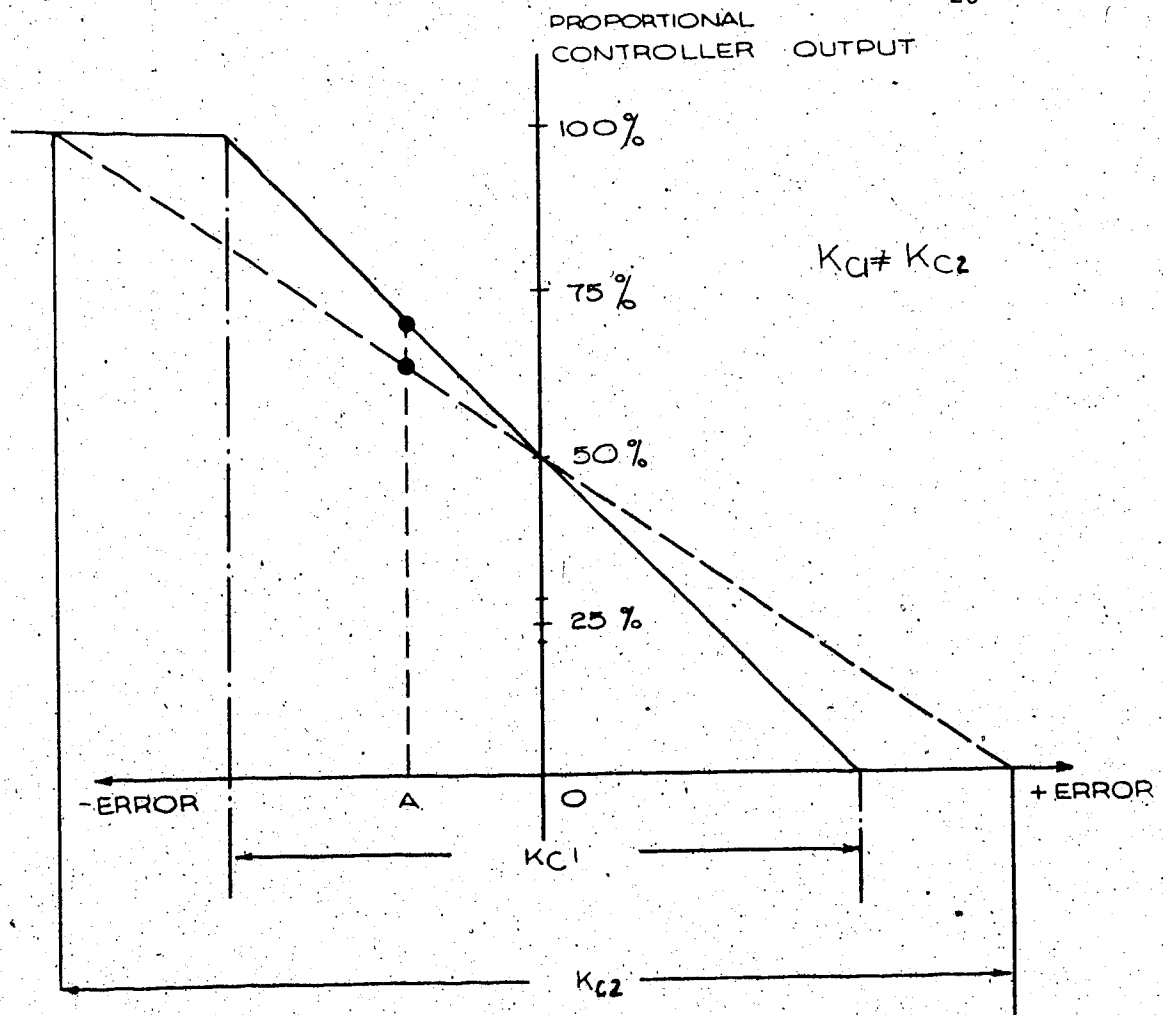
Figure 2-15 The proportional action versus error signal with
different gain K_c as parameter

P action. In the extreme, when P and I action combined give out

the maximum or minimum value of output, the response will be the

fastest. Therefore, it is desirable that the proportional and integral

action combined have the *capability* of producing output extremes.

For example, if the error requires the P action to produce 75% output,

the I action should be *capable* of contributing the remaining 25% of

the output range in the same direction. During steady state the P

action becomes zero. Hence the integral action *alone* should be *capable*

of giving the output extremes. It should be realized that reset

wind-up is no longer of concern because the reset action is initially
inhibited.

To conclude: whenever the error signal is within the
proportional band (and therefore the P action is within the output
range) the I action will be allowed to attain such a value that the
combined P and I action equal 100% of output range. This can be
achieved by constantly monitoring the sum of P and I action. Whenever
the sum exceeds the output limit, the integrator will be completely
discharged, in other words, inhibited. With this arrangement, the
integrator becomes self regulating. It adjusts its own operating
range to precisely that amount needed to produce output extremes.
Whenever the extremes are exceeded, it inhibits its own operation.

Besides the elimination of the reset wind-up problem, other
benefits   this scheme are:

(be no start-up problam, and

(2   vative action is free to carry out its original

Chapter III

The Design of a Near Ideal PID Controller

With the design objective and its theoretical background

already laid out in Chapter I and II, the design work itself may now

be discussed.

System Description

For any real device, physical limitations are unavoidable.

Hence, an understanding of the operational limits of the controller

and the control loop is needed. In figure 3-1, a particular control

loop and its signal operating ranges are shown.

r(t) (1 to 5V) e(t) (-4V to 4V) CONTROLLER PROPER m(t) (10 to 50MA) TRANS DUCER PHYSICAL VARIATIONS PLANT c(t)

c(t) (1-5V)

I.V.C. c(t) (10 to 50MA) V.I.C. SENSOR c(t) (1 to 5V)
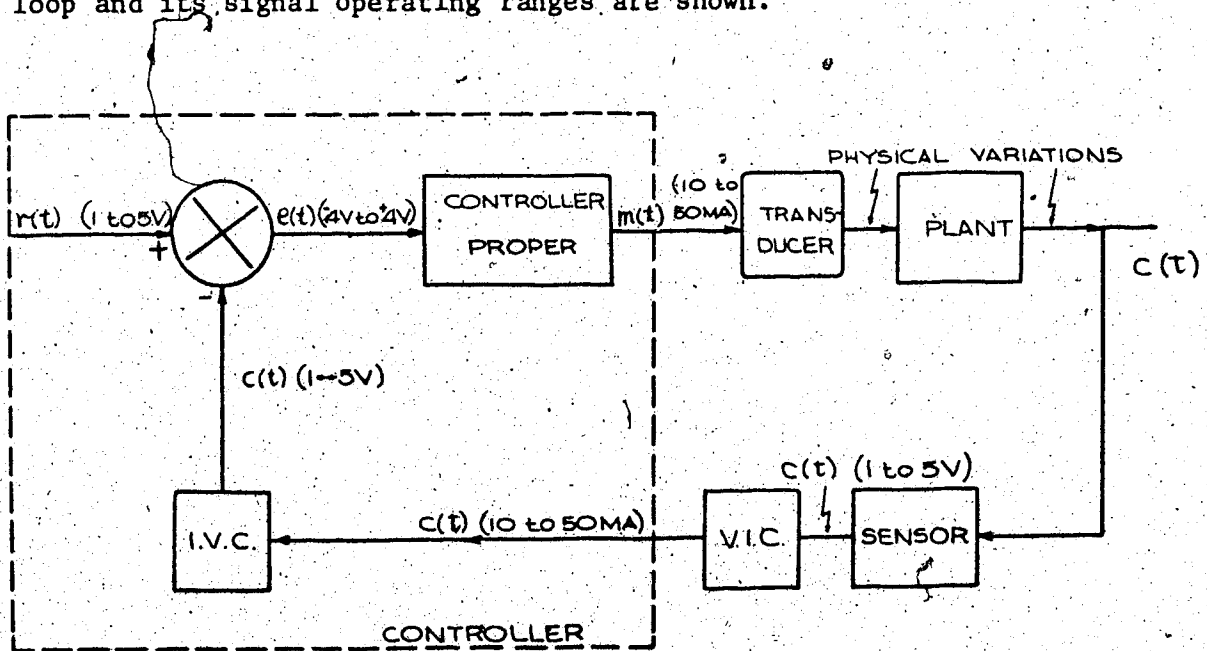
CONTROLLER

Figure 3-1 A particular control loop and its signal operating

ranges

The distance between a controller and the controlled plant could be

quite large. In order to prevent the electrical signal from being

affected by the distance, the controller output port is designed to be a current source. Actually the controller internal signal of 1 to 5 volt is converted into 10 to 50 mA current. This is because the majority of industrial transducers operate in the 10 to 50 mA range.

The sensor within the plant will provide the voltage representation of the controlled variable. This voltage output $c(t)$ will be subsequently transformed into 10 to 50 mA range of current The reason for the transformation is again the possible long distance between controller and plant. Upon arrival at the controller, the output $c(t)$ (in current form) will be converted back into a 1 to 5 volt range of voltage. The set point voltage is also in the range of 1 to 5 volt [14,15].

The proposed PID controller will have the following ranges for its parameters:

Proportional gain K_c $0 \leq K_c \leq 20$

Integral time T_i $0 \leq \frac{1}{T_i} \leq 10$ repeats/min

Derivative time T_d $0 \leq T_d \leq 10$ minutes

As will be shown in Chapter IV, these parameter ranges are adequate for most industrial requirements.

Power Supply

Since integrated circuits will be used in the controller and a larger signal swing is desirable, ± 15 volt is used as the power supply voltage. A + 40 volt supply is also needed for the output

current drive. The + 40 volt supply was selected for convenience in this proposed design. If necessary a 90 volt supply can be used to allow series connection of transducers.

It is presently quite common to rack-mount controllers. Hence, it is convenient to have one set of external power supplies to provide power for several controllers and their accessories. In this proposed design, only external power supplies will be used. The required ± 15 volt and + 40 volt supplies are drawn from standard laboratory power supplies. The auxilliary ± 6 volt and ± 3 volt supplies for logic circuits are derived from the ± 15 volt supplies by voltage regulators and voltage divider circuits. The complete circuit details for the power supplies are shown in figure 3-18.

Manual and digital set point adjustments

The manual set point voltage can be easily generated as shown in figure 3-2.
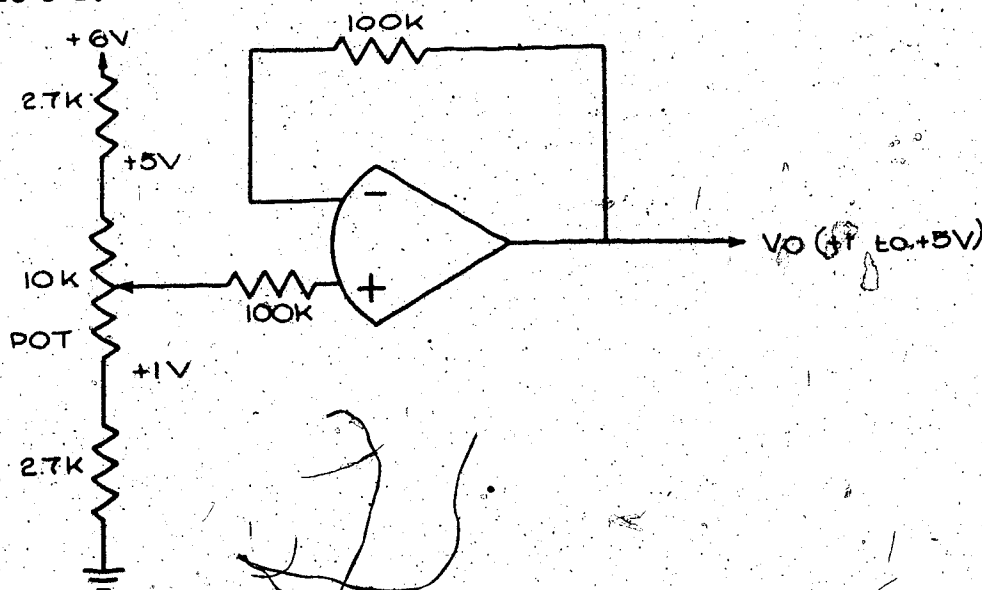
Figure 3-2 The generation of manual set point variations

The + 1 to + 5 voltage range is derived from the potentiometer
and fed into the positive input of the operational amplifier. The
op-amp here serves as a buffer and a voltage source.

The digital set point adjustment was designed into a part-
icular format. This particular design is intended only to demonstrate
the possibility of digital computer control. Other forms of digital
set point adjustment are possible.

For this particular design, the digital set point range of
1 to 5 volt is divided into one hundred evenly spaced steps, such
that each step equals 40 mV. [(5-1)volt/100 = 40 mV]. The command
signal, asking for any quantized value between + 1 to + 5 volts, is
coded in binary format. To represent 100_{10} in binary, one needs at
least seven bits. For example, the binary 1100100 equals the decimal
100 and will represent a + 5 volt output (+ 1 volt + 40 mV X 100).

The devices chosen to convert binary codes into voltages are
a Fairchild's μA722 10 bit current source and an op-amp as shown in
figure 3-3. The resistors marked as R_E in figure 3-3 are selected,
such that each successive transistor in the μA722 device will deliver
twice as much current as the previous one. By applying a binary 1
to any logic gate in the μA722 device, the gate will be closed and
the transistor below that gate will draw an integral number of current
units from the following op-amp. As specified in the μA722
specification sheets, the maximum current when all bits are on,
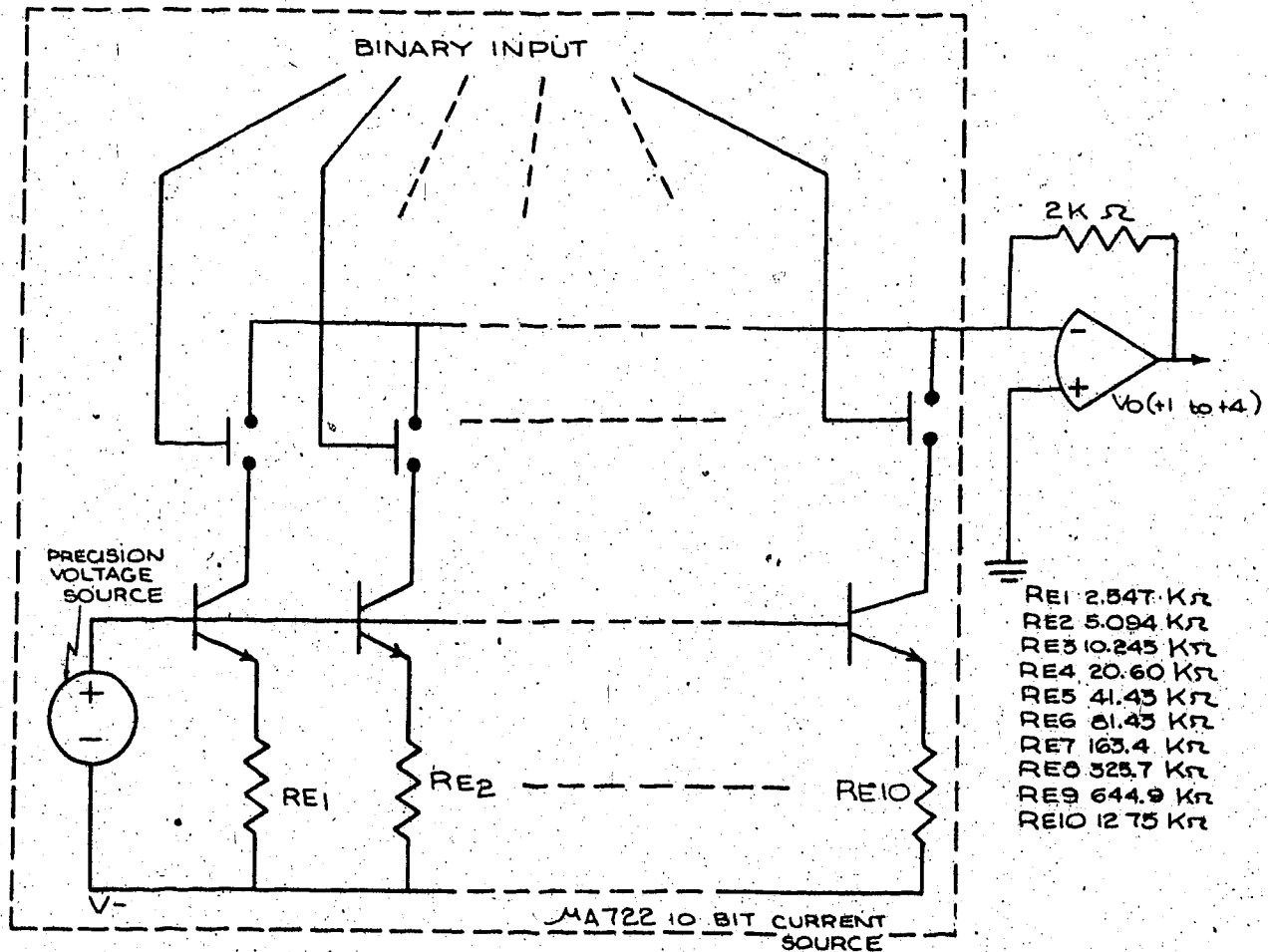
Figure 3-3 Using µA722 and an op-amp to convert a

binary code into a voltage

is 2560 µA. Taking the current through the least significant bit

transistor as one unit, the maximum current when all bits are on,

corresponds to 1023 units $(N = \sum_{n=0}^{9} 2^n = 1023)$. Therefore, each unit

equals 2.5 µA (2560 µA/1023 $\approx$ 2.5 µA). Since only seven bits are

needed to represent 100 steps in binary, the seven most significant

bits in the µA722 device were chosen. This way the µA722 will be

able to deliver a heavier output current. The least significant bit

in the µA722 device will now be the 7th bit, which delivers a current

8 times ($2^3 = 8$) the current of the 10th bit. Therefore, the 7th

transistor will draw 20 µA (2.5 µA x 8), which is the new current unit.

For each step to correspond to 40 mV, the 20 µA drawn through the op-

amp should produce 40 mV. Consequently 2KΩ (2KΩ x 20 µA = 40 mV)

was chosen to be the feedback resistor value for the op-amp.

Manipulation of the binary digits is accomplished through

mechanical switches on the front panel. But these mechanical switches

are not directly connected to the gates of the µA722. Instead the

output of each mechanical switch goes to a 'D' type flip-flop. The

'D' type flip-flop has to wait for a read pulse before it transfers

its content to the gates of the µA722. The purpose of the above is

to allow time for manipulation of the mechanical switches, without

changing the previous set point level until the read-in switch is

activated. The read-in switch is a normally open mechanical switch,

which will give a + 3 volt output when pushed on. At the release of

the read-in switch, the trailing edge of the + 3 volt pulse will

trigger a monostable multivibrator, which in turn will produce a one

shot pulse. The leading edge of the one shot pulse will act as the

read pulse to the 'D' type flip-flop.

The width of the one shot pulse is calculated to suit the

particular 'D' type flip flop chosen.

A pedestal of 1 volt is added to the output to elevate the
set point level into the + 1 to + 5 volt range. The complete circuit
is shown in the digital set point section of figure 3-18.

Error Signal Generation

By definition the error signal is the difference between the
set point level and the controlled variable. Assuming that the
feedback signal is in current form, then a conversion to a voltage
signal is needed. After the current to voltage conversion the plant
output and the set point voltage are subtracted from each other by
feeding them into the opposite polarity inputs of a differential
amplifier. Therefore the output of the differential amplifier is
the error signal. The circuit to generate error signal is shown
in figure 3-4.
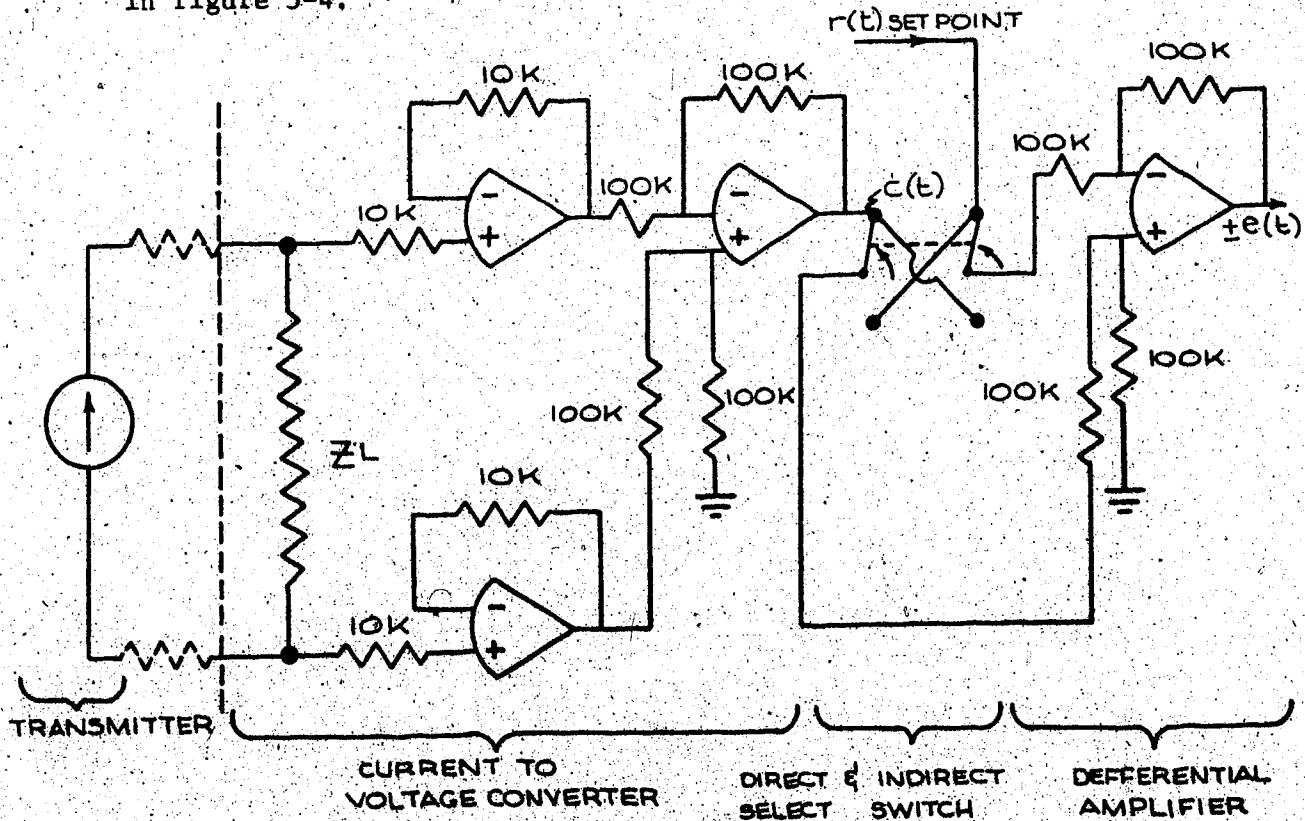
Figure 3-4 The generation of error signal

The double pole double throw switch in figure 3-4 serves the purpose of generating either + e(t) or - e(t). This switch therefore enables one to select direct or indirect action.

The Controller Proper

The ideal PID algorithm in mathematical formulation is:

$$\frac{M(S)}{E(S)} = K_c \left(1 + \frac{1}{T_i S} + T_d S\right)$$ (3-1)

The block diagram form is shown in figure 3-5:
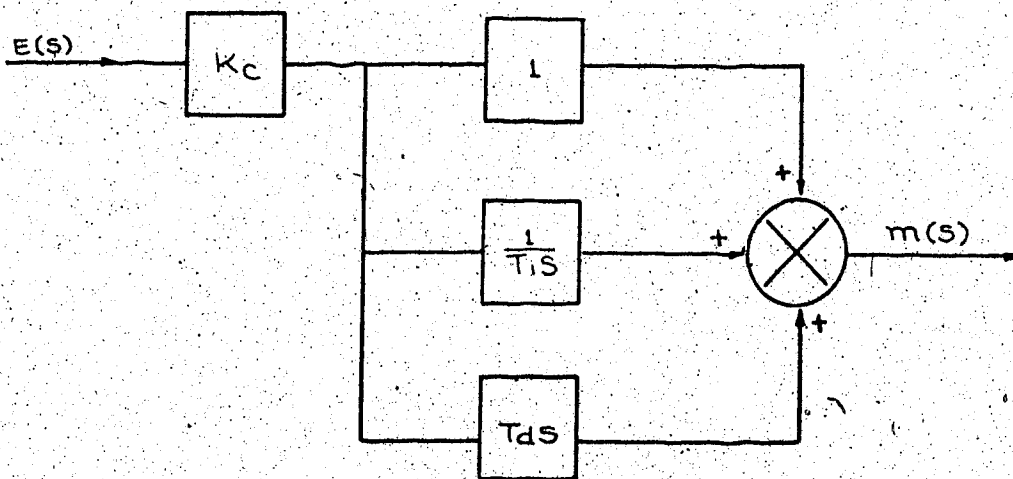
Figure 3-5 The block diagram of an ideal

PID controller

The signals from the three branches in figure 3-5 may, at times, cancel each other partly. This situation can be visualized in figure 3-6 where the signs of the signals are considered.

In the arrangement as shown in figure 3-5, whenever a signal in any of the three branches exceeds the output range of the op-amps, true representation of the wanted control action will be lost. If gain K_c is
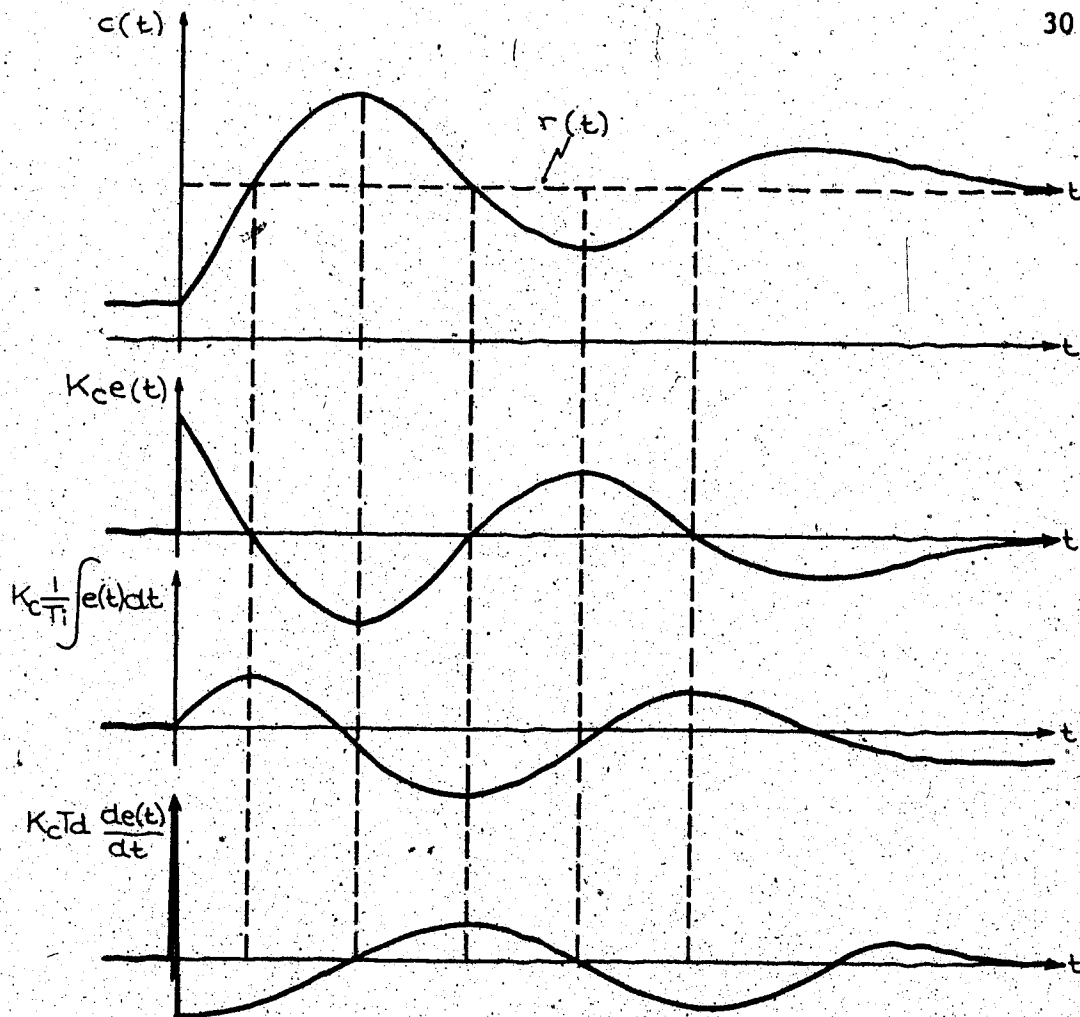
Figure 3-6 Control action of different modes.

positioned at the summing point instead of positioned before the

three branches, the signals within the three branches will be

considerably smaller (being only $e(t)/T_i$, $T_d e(t)$ and $1 \times e(t)$). With

this arrangment, the output from the three branches will cancel each

other partly, before being multiplied by the gain K_c. This arrangement

will reduce the chances of saturation.

However, the signal input to each branch must not be too small

either, for noise considerations. The gain K_c therefore is split

into three parts i.e.

$$K_c = \alpha \times K_c' \times K_c'' \qquad (3-2)$$

where $0 \le \alpha \le 1$, $K_c' = 2$, $K_c'' = 10$

As mentioned in the section entitled "System description" in this chapter the gain K_c is limited to 20 in this controller. With α being represented by a potentiometer, K_c' and K_c'' are set to 2 and 10 respectively. Hence the gain K_c can be varied by the potentiometer between values of zero and twenty. The format of the proportional gain is therefore decided and is shown in figure 3-7.
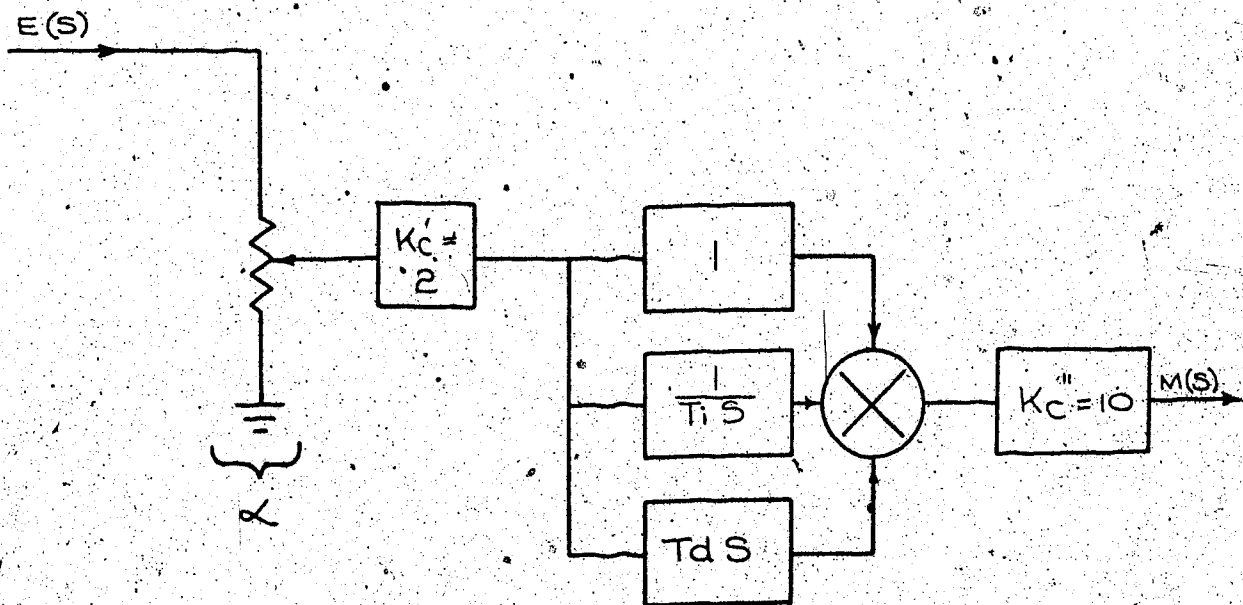
Figure 3-7 The gain K_c is split into α, K_c' and K_c''
to reduce the chane of saturation

The design of an active integrator is relatively easy compared to the design of a differentiator. In the latter, filtering of higher frequencies is absolutely necessary. A true differentiator can never be used because of its ever increasing gain for higher frequency components of noise and disturbances. Therefore, a close approximation rather than the ideal algorithm is all that can be achieved.

The circuit adopted is a passive lead network which, when combined with the branch of $\frac{1}{T_1 S}$, will be very close to the ideal algorithm. This circuit is shown in figure 3-8.
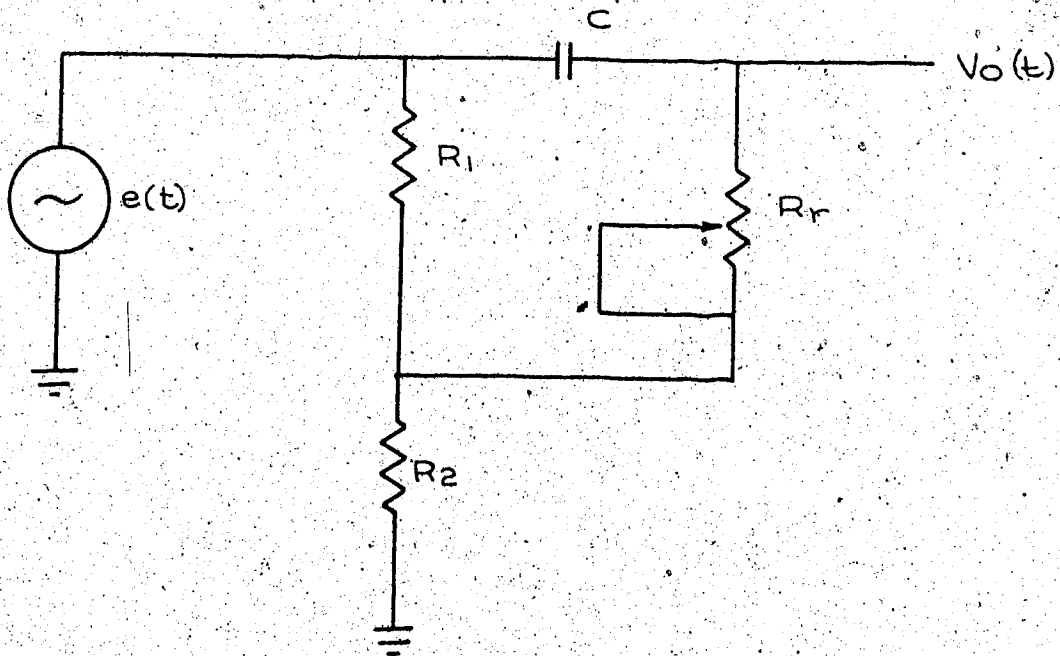
Figure 3-8 The passive lead network

The transfer function of the circuit in figure 3-8 is:

$$\frac{V_o(S)}{E(S)} = \frac{SC[R_r(R_1+R_2) + R_1R_2] + R_2}{R_1+R_2+SC[R_r(R_1+R_2) + R_1R_2]} \tag{3-3}$$

The value of R_1 and R_2, as later sections will show, are in the range of a few hundred ohms while R_r is in the mega ohm range. Hence:

$$\frac{V_o(S)}{E(S)} \approx \frac{SC[R_r(R_1+R_2)] + R_2}{SC[R_r(R_1+R_2)] + R_1+R_2}$$

$$= \frac{S \dfrac{CR_r (R_1 + R_2)}{R_2} + 1}{[SCR_r + 1]\left(\dfrac{R_1 + R_2}{R_2}\right)} \qquad (3\text{-}4)$$

Let $T_d = \dfrac{CR_r(R_1+R_2)}{R_2}$ and $T_d' = cR_r = T_d \dfrac{R_2}{R_1+R_2}$ Then:

$$\frac{V_o(S)}{E(S)} = \frac{T_dS + 1}{(T_d'S+1)\left(\dfrac{R_1+R_2}{R_2}\right)}$$

$$= \frac{T_dS + 1}{(T_d'S+1)\dfrac{T_d}{T_d'}} \qquad (3\text{-}5)$$

Note that the ratio of T_d' over T_d is a constant. The frequency response plot of equation (3-5), as given in figure 3-9, shows that $\frac{1}{T_d}$ and $\frac{1}{T_d'}$ are the corner frequencies corresponding to the zero and pole location respectively. On the logarithmic abscissa, the two corner frequencies will be maintained at a fixed distance and hence a fixed gain difference, no matter in what position they appear along the abscissa. In this manner, whenever the position of the zero $(\frac{1}{T_d})$ is changed, the new position of the pole is also determined and any possibility of excessive gain at high frequencies is excluded.
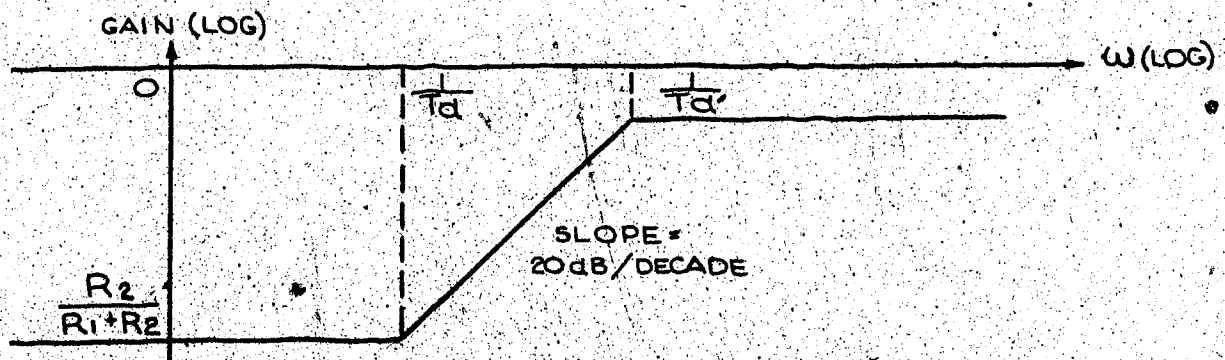
Figure 3-9 The frequency response of equation (3-5)

The values of the lead network were chosen to be:

$$R_1 = 900\Omega$$

$$R_2 = 100\Omega$$

$$c = 7\mu f$$

$$R_r = 0.86 \times M \text{ Meg}\Omega \text{ where } 0 \leq M \leq 10 \qquad (3-6)$$

Substituting equation (3-6) into (3-5) :

$$\frac{V_o(S)}{E(S)} = \frac{T_d S + 1}{(T_d'S+1)(\frac{R_1+R_2}{R_2})}$$

$$= \frac{1 + 60 \text{ MS}}{(1 + 6 \text{ MS}) \times 10} \qquad (3-7)$$

In equation (3-7) when T_d equals 60M seconds, T_d' will be 6M seconds, in other words $T_d' = T_d/10$. As M varies between zero and ten, the derivative time constant T_d varies between zero and 600 seconds. With this set-up, $\frac{1}{T_d'}$ will always remain one decade of frequency away from $\frac{1}{T_d}$, with a high frequency gain of 20 dB above the low frequency gain. As will be shown later, this distance of one decade and a gain different of 20 dB make the approximate algorithm close enough to the ideal one. The approximate algorithm in block diagram form is shown in figure 3-10.
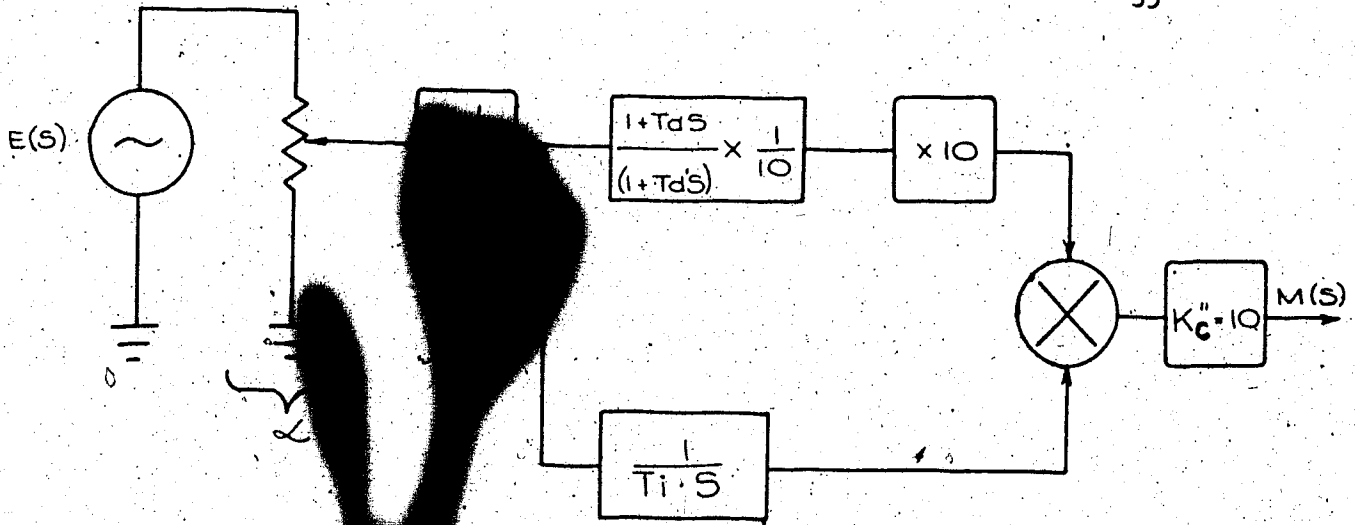
Figure 3-1 the block diagram of the approximate

PID algorithm

The transfer function for the approximation is:

$$\frac{M(S)}{E(S)} = \alpha \; K_c' \; K_c'' \; [\; \frac{1 + T_d S}{1 + T_d' S} + \frac{1}{T_i S} \;]$$

$$= K_c \; [\; \frac{1 + T_d S}{1 + \frac{T_d}{10} S} + \frac{1}{T_i S} \;] \qquad\qquad (3\text{-}8)$$

In most cases the time constant T_d used is of a rather small value
[6]. The value of T_d' which is only one tenth of T_d, can be neglected.
Therefore:

$$\frac{M(S)}{E(S)} = K_c \; [\; \frac{1 + T_d S}{1 + T_d' S} + \frac{1}{T_i S} \;]$$

$$\approx K_c \; [\; 1 + T_d S + \frac{1}{T_i S} \;] \qquad\qquad (3\text{-}9)$$

It is clear from equation (3-9), that the algorithm adopted will give

a fairly independent parameter set as desired. To prove that the approximation is really a good one, the following analysis is carried out. Given the transfer function:

$$\frac{V_o(S)}{E(S)} = K_c \left(\frac{T_d S + 1}{T_d' S + 1} + \frac{1}{T_1 S} \right)$$

$$\text{where } T_d' = \frac{1}{10} T_d \qquad (3\text{-}10)$$

and the input $e(t)$ is a ramp i.e.

$$e(t) = At \quad \text{where } A = \text{constant}$$

$$\text{or} \qquad E(S) = \frac{A}{S^2} \qquad (3\text{-}11)$$

Then:

$$V_o(S) = K_c \left(\frac{T_d S + 1}{T_d' S + 1} + \frac{1}{T_1 S} \right) \frac{A}{S^2}$$

$$= \frac{K_c A T_d S}{(T_d' S + 1) S^2} + \frac{K_c A}{(T_d' S + 1) S^2} + \frac{K_c A}{T_1 S^3} \qquad (3\text{-}12)$$

Taking the inverse Laplace transform:

$$v_o(t) = K_c At + K_c A T_d \left(1 - e^{-\frac{t}{T_d'}} \right) - K_c A T_d' \left(1 - e^{-\frac{t}{T_d'}} \right)$$

$$+ \frac{1}{T_1} K_c A \frac{t^2}{2}$$

$$= K_c At + \frac{1}{T_1} K_c \frac{At^2}{2} + K_c AT_d (1 - \frac{1}{10})(1 - e^{-\frac{t}{T_d'}})$$

$$= K_c(At) + \frac{K_c}{T_1} \cdot \frac{t}{2} \cdot (AT) + K_c T_d \cdot \frac{9}{10} (1 - e^{-\frac{10t}{t_d}}) \cdot (A)$$

$$(3-13)$$

Equation (3-13) can be split into 3 parts:

the P action is: $v_p(t) = K_c (At)$

the I action is: $v_I(t) = \frac{K_c}{T_1} (\frac{At^2}{2})$

and the D action is: $v_D(t) = K_c T_d \cdot [0.9A(1 - e^{-\frac{10t}{t_d}})]$

Obviously, the P and I action in equation (3-13) are identical to the ideal P and I action. Only the D action in equation (3-13) shows the effect of approximation. The ideal D action for a ramp input would be:

$$v_D(t) = K_c T_d \frac{d\,e(t)}{dt}$$

$$= K_c T_d \frac{d}{dt} At \qquad\qquad (3-14)$$

$$= K_c \cdot T_d \cdot A$$

To compare the ideal and the approximate D action, both of them are plotted in figure 3-11.

OUTPUT OF D ACTION

IDEAL D ACTION

RAMP INPUT x K_c = P ACTION

AK_cTd

$0.9\,AK_cTd$

THE APPROXIMATED D ACTION

0.636 x 0.9 x AK_cTd

Td' = $\frac{1}{10}\,Td$

Td

t
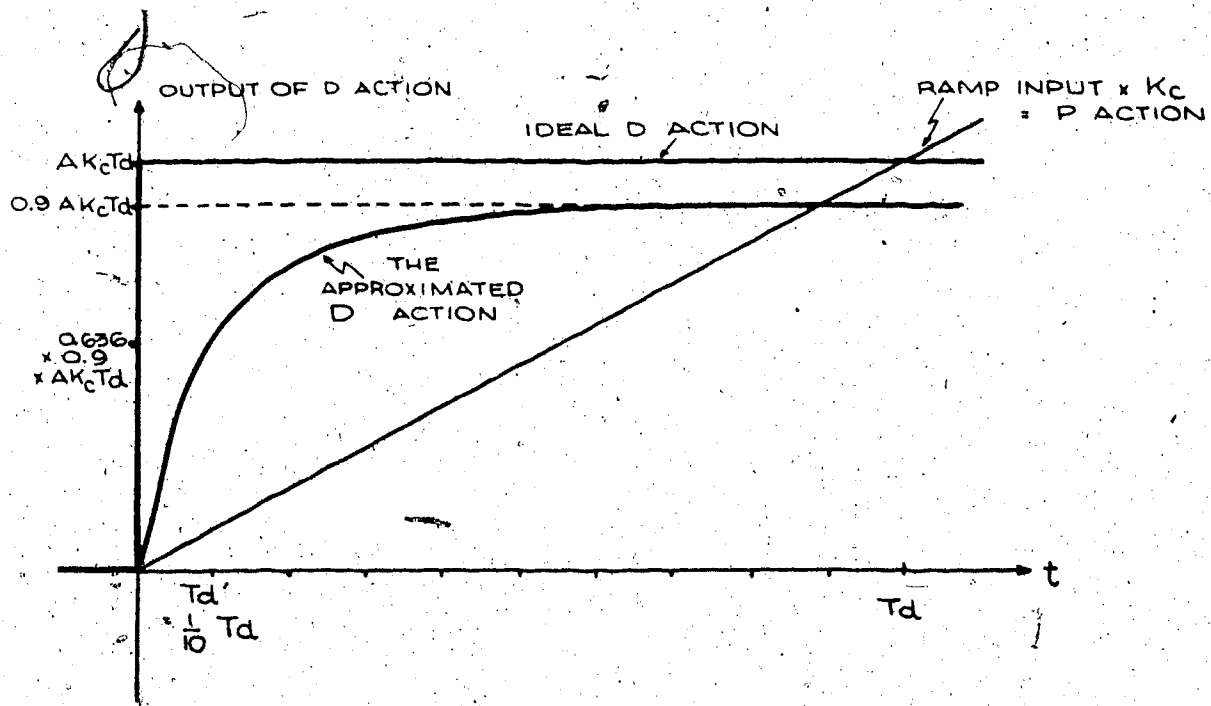
Figure 3-11 Comparison of the ideal and

the approximate D action under a ramp input

Figure 3-11 illustrates that at a time equal to $T_d/10$ the D action

has reached 63% of its final value, and also the final value equals

90% of the ideal value.

Hence it becomes obvious that the algorithm adopted is a

sufficiently close approximation.

The integrator circuit is straightforward as shown in figure

3-12. The output from the integrator circuit of figure 3-12 is:

$$v_I(t) = \alpha\,\frac{1}{cR}\int e(t)\,dt$$

$$= \frac{1}{T_i}\int e(t)\,dt \qquad\qquad (3\text{-}15)$$
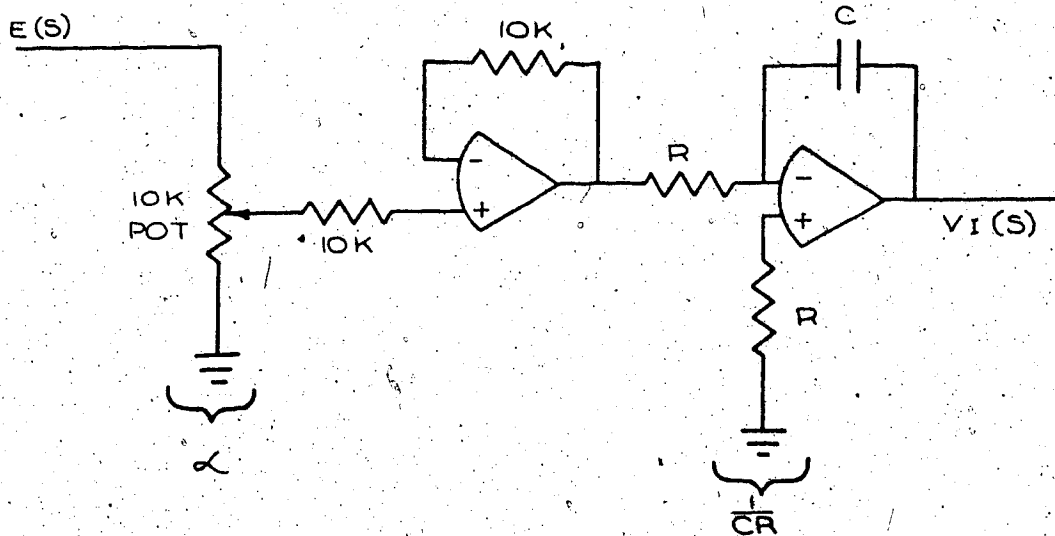
Figure 3-12 The integrator circuit

where $T_i = \dfrac{cR}{\alpha}$ and $0 \le \alpha \le 1$

Varying of integral time T_i is accomplished by means of a potentiometer.

The op-amp chosen for integration must be selected with care to have

low drift and input offset [16].

The complete circuit for the PID controller proper is shown

in figure 3-13. With regard to figure 3-13, the following points

of interest should be mentioned. The value of M is designed to be

adjustable in 20 steps. The first 10 steps vary M between 0.1 to 1,

and the next 10 steps vary M from 1 to 10. The potentiometer at the

summer is provided for padding the output to the range of 1 to 5

volt. The zener diode acts as a voltage limiter. The switches

around the integrator are there for the purpose of reset inhibition.

Output current source and filtering

The control voltage m'(t) generated by the PID summer will
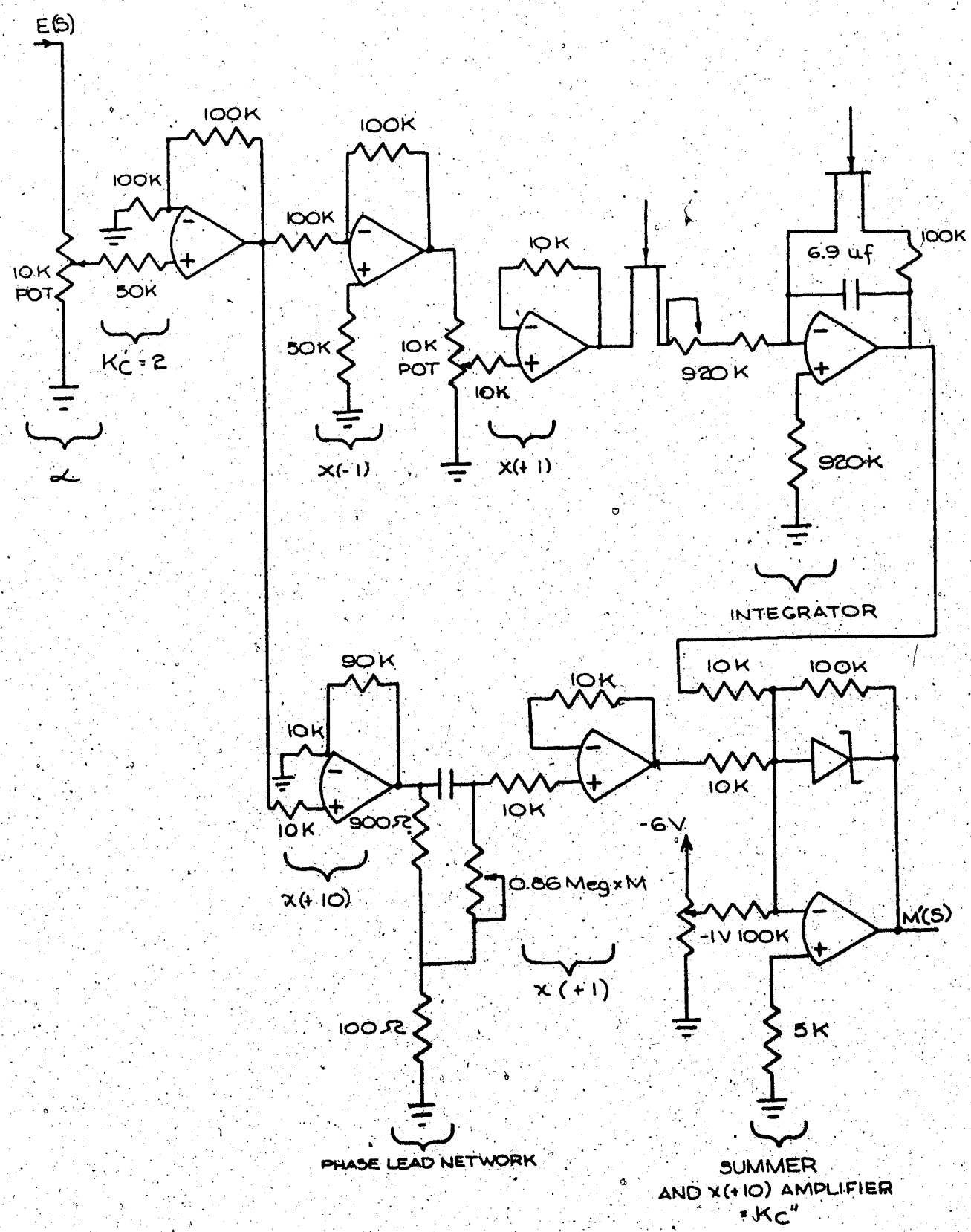
Figure 3-13 The complete circuit of PID controller proper

pass through a low pass filter, so that any frequency component above 10 Hz will be attenuated. Mainly, the controller controls plants with large time constants in the range of minutes [6]. Therefore, frequencies above 10 Hz can be filtered out without affecting the relevant spectral characteristics of the control loop. At the same time noise and higher frequency components of disturbances are also reduced.

The voltage to current conversion is achieved by the combination of an op-amp and a medium power transistor shown in figure 3-14.
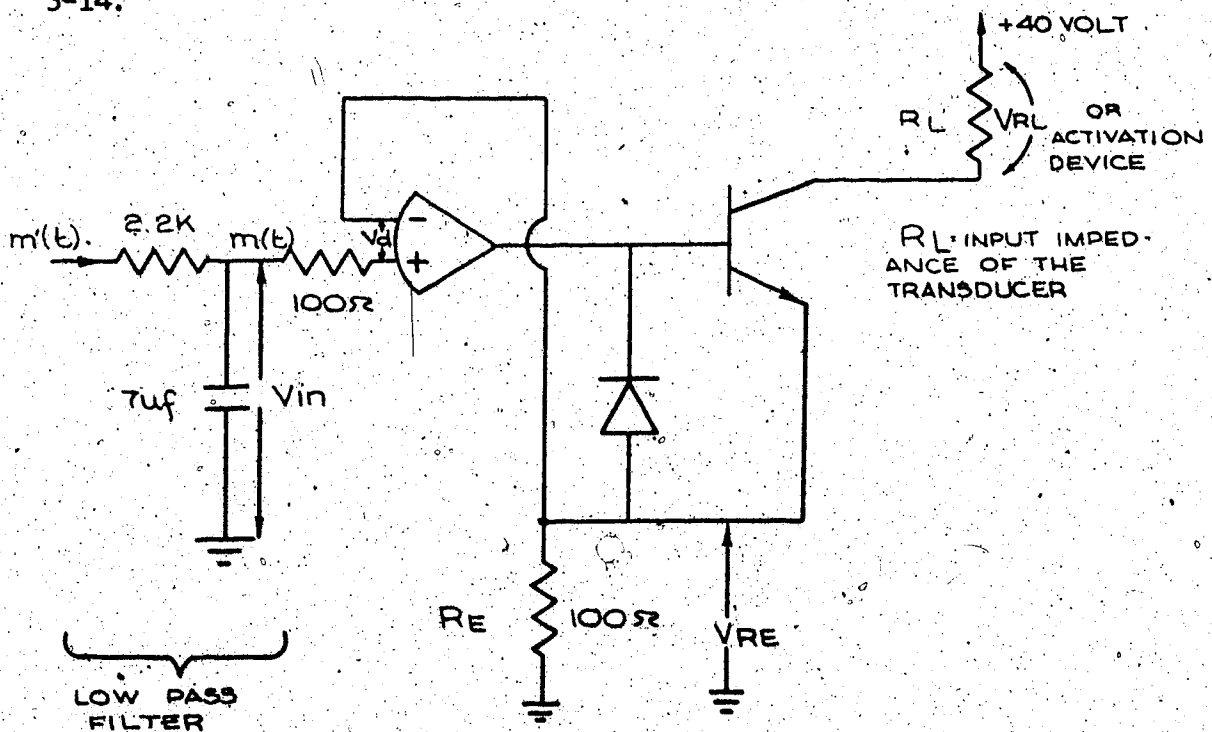
Figure 3-14 The controller-output driving circuit
with low-pass filter

The output of the op-amp directly drives the base of the power transistor. The true purpose is to keep V_{RE} equal to V_{in}, such that the

op-amp differential input voltage V_d will be zero. The value of R_E is chosen to be 100Ω. With 1 volt appearing across R_E, there will be a current of 10 ma passing through it. When $V_{in} = V_E = +5$ volt, the maximum output, there will be 50 mA of current passing through R_E. Since the current through R_E, is I_E $(I_E \approx I_c)$, approximately the same amount of current will be forced through the collector load.

Therefore, the intended purpose to convert output voltage ranging from +1 to +5 volts into a 10 ma to +50 ma range of current has been achieved. If a +40 volt supply is allowed while the output transistor is driven to saturation at 50 ma, the voltage value of V_{RL} will be +35 volts (under the situation $V_{RE} = +5$ volt). In other words, when the output current is at its maximum 50 ma, R_L can be chosen to have a value up to seven times the value of R_E before the transistor saturates. This is desirable, because there is no control over the transducer input impedance i.e. R_L. The best one can do is to set an upper limit for the transducer input impedance. In this case the +40 volt supply sets the upper limit at 700Ω. It should be remembered that this is a current source; therefore the transducer input impedance will not affect the current output.

Note that the output from the summer is actually from -0.6 volt + 6.5 volt instead of the specified +1 to +5 volt range. This is dictated by the limiting diodes. When $V_E = V_{in} = -0.6$ volt, the output of the op-amp becomes -15 volt in order to force enough reverse current through the reverse biased base-emitter junction. Understandably, this kind of operation will eventually damage the output circuit.

The remedy is to use a diode as a path by-passing the emitter-base junction when negative voltage appears across R_E. This diode is also shown in figure 3-14.

Reset Inhibiting

The purpose of reset inhibiting was mentioned in Chapter II. A realization of it was also described. The method used was simply to monitor the output of the PID summer. Whenever the sum exceeds either of the limits (+5 volt or +1 volt) the integrator will be inhibited.

First of all a direction detector is needed to indicate in which direction the controlled variable is moving. If it is rising towards maximum output, the PID summer output will be compared with +5 volt. Otherwise the summer output will be compared with +1 volt. After the direction detector a set of special comparators is needed to check if either of the limits is exceeded. And finally, a set of solid state switches to carry out the inhibit or non-inhibit commands is required.

For the direction detector, the circuit discussed in Appendix I is chosen [16]. The input signal e_i for it will be the negative error signal, $-e(t)$, in the controller. Since $-e(t) = c(t) - R(t)$, where $R(t)$ is the fixed set point level, it is obvious that $-e(t)$ can represent the controlled output $c(t)$ for the purpose of direction detection. Note that the input $e(t)$ is a signal that varies around the zero volt level. Hence the circuit in Appendix I will have $e_{ref}=0$.

The circuit of the direction detector is shown in figure 3-15.

Whenever a major disturbance occurs, reset wind-up is possible. At the same time, the error signal will be large enough to cause a change of state in the direction detector. On the other hand, whenever the controlled variable approaches steady state, the error signal becomes very small. The threshold level in the circuit is designed so as to disallow the error signal under effectively steady state conditions to cause any change of state in the direction detector. It should be remembered that the integrator should never be inhibited under line-out (steady state) conditions. Moreover, noise of amplitudes smaller than the threshold level will not cause unwanted changes of state.

The same level detector with hysteresis is used as the input stage of the signal comparators. Only this time e_{ref} does not equal zero but equals either +5 or +1 volt. Suppose e_{ref} equals +5 volts, and $|V_L|$ = 6 volt, then:

$$e_0 = \pm V_L \left(\frac{R_3 + R_4}{R_4} \right) + e_{ref}$$

$$\approx \pm V_L + e_{ref} \quad \text{where } R_4 >> R_3$$

or $\quad e_0 = + 11$ volt or -1 volt $\qquad\qquad$ (3-16)

The asymmetrical values of e_0 are intended to act as the command signals for subsequent logic circuits. The logic circuits chosen are the RCA CD4016 COS-MOS switches. They are biased in such a manner that a ±3 volt control signal is required. To obtain this ±3 volt it was decided to pass the asymmetrical output e_0 through a gain 10
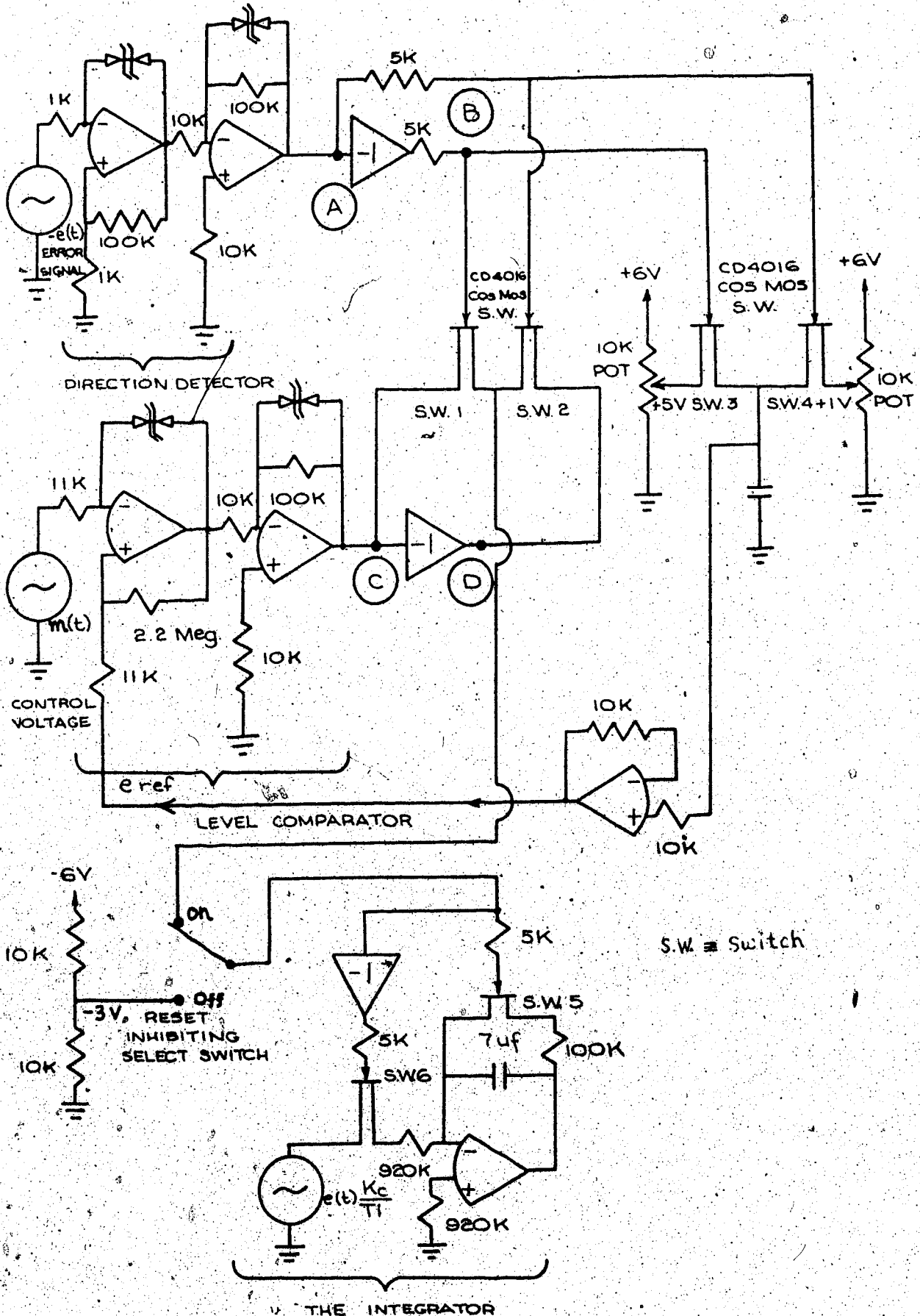
Figure 3-15 The reset inhibiting circuit

amplifier with a voltage limiter as mentioned in Appendix I. The complete comparator as well as the reset inhibiting circuit are shown in figure 3-15. The operation of the reset inhibiting circuit in figure 3-15 is roughly described in the following: Suppose there is a sudden positive step change in set point, and if it is assumed that the reset inhibiting is operating, there should be no overshoot in the controlled variable. The controlled signal, the error and set point changes are shown in figure 3-16.
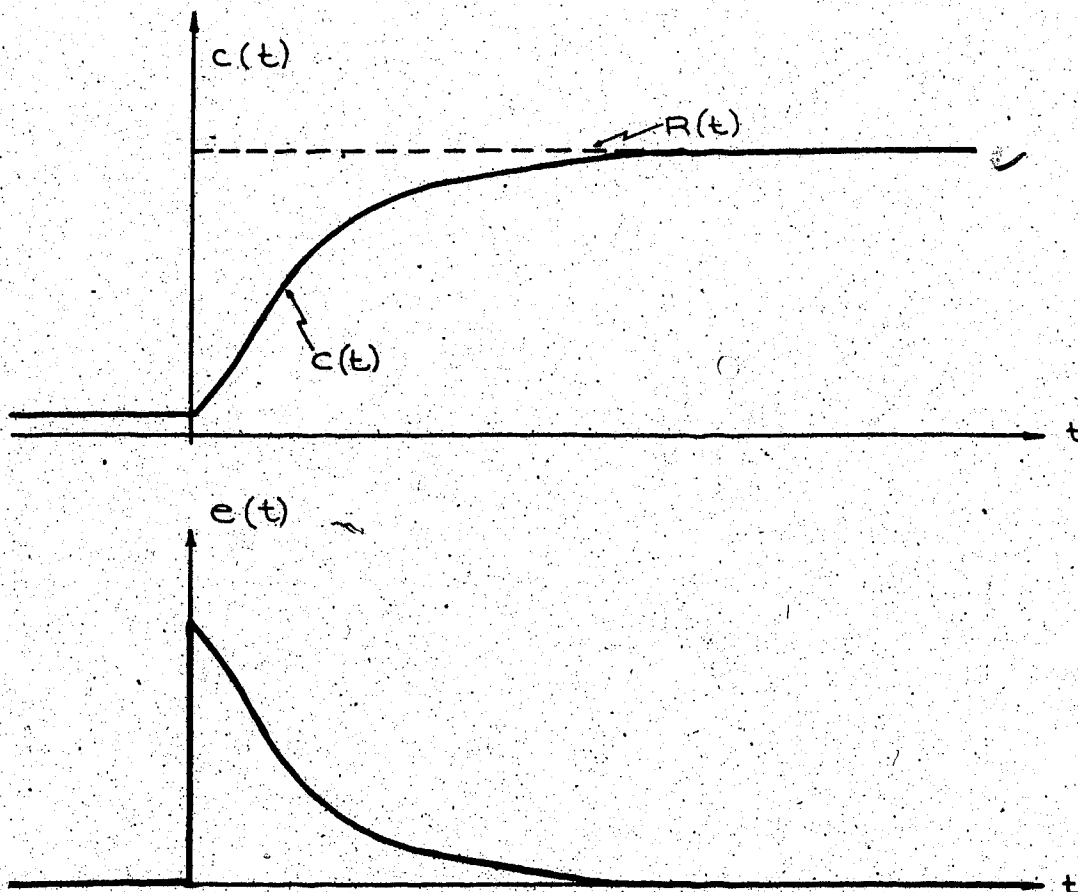
Figure 3-16 The response of c(t) and e(t)

under set point change and reset inhibiting

The error signal in figure 3-16 is going positive. The positive error will cause point A and point B of figure 3-15 to become - 3 volt and +3 volt respectively. The values of voltage at points A and B will be maintained until an oppositely directed change of e(t) occurs. If the expected reset inhibiting action is going to take place, the error signal will not overshoot but will approach the new set point from one side only. Hence there will be no change of sign in e(t) and no change of state in the direction detector unless another disturbance should take place. At this very instant in time the voltage values at points A and B will cause switches 1 and 3 to close and switches 2 and 4 to open. The closing of switch 3 allows +5 volts to appear as e_{ref} at the positive end of the level comparator. At any moment when m(t), the control output, exceeds +5 volts, point c will become +3 volts and point D -3 volts. Recalling that the direction detector is still forcing switch 1 closed and switch 2 open, only +3 volt from point c will be allowed to pass through switch 1. The result is that switch 5 in the integrator circuit will be closed and switch 6 will be open. Thus the integrator is inhibited.

Once m(t) falls back below +5 volts, point c will reverse its sign to become -3 volts. Yet switch 1 is still closed. Therefore, -3 volts will pass through it and reactivate the integrator.

When the error signal goes negative, switch 2 and 4 will be closed, making +1 volt the e_{ref} at the input of the level comparator. This time, only signals from point D can pass through switch 2 and control the integrator. Only when m(t) drops below +1 volt, will the

integrator be inhibited.

There are three sets of mechanical switches involved with the integrator. They are:

1) Reset inhibiting select switch.

2) Reset on-off switch.

3) Manual or automatic select switch.

These switches together with the integrator are shown in figure 3-17.
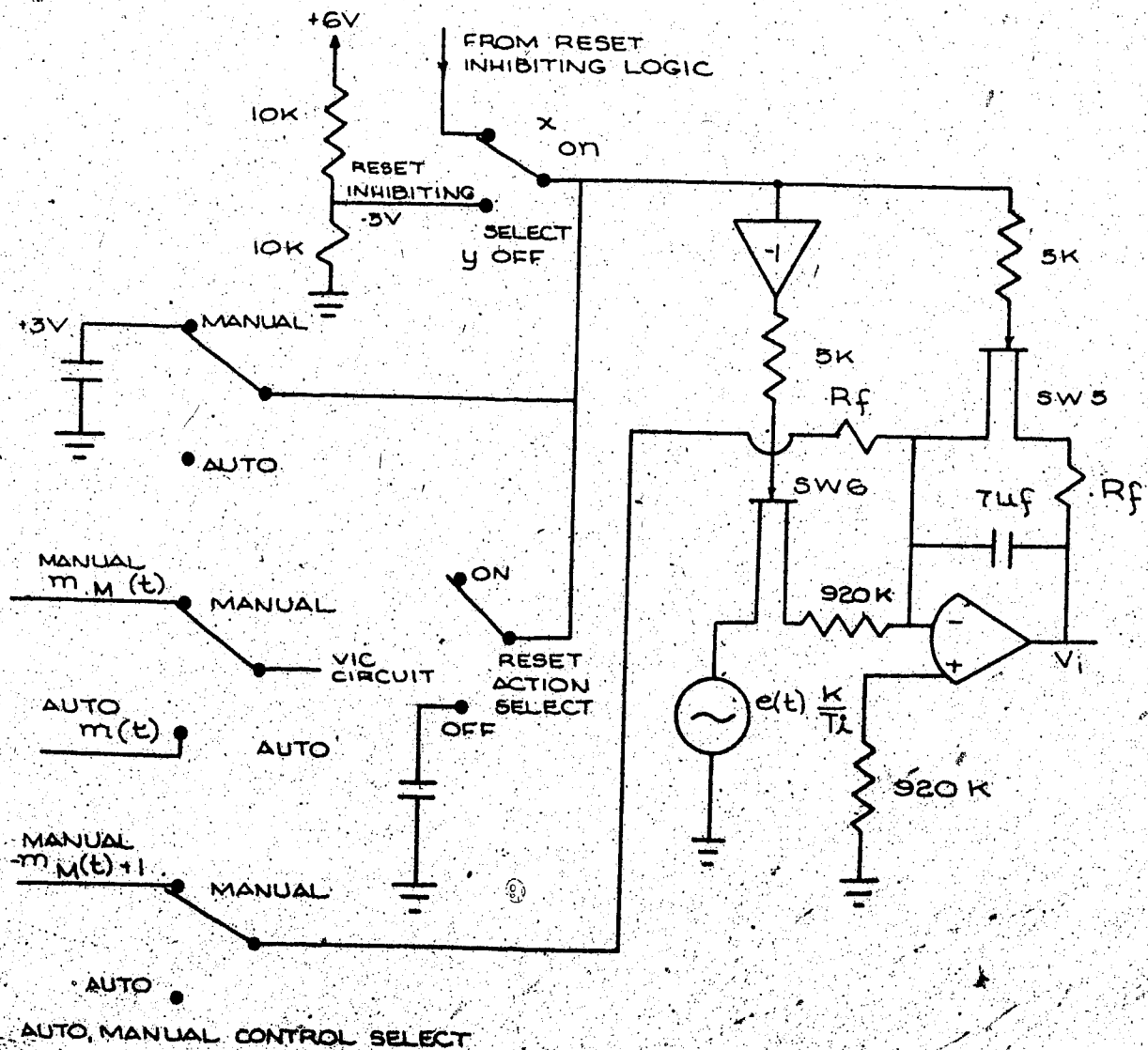
Figure 3-17 Mechanical switches involved with the integrator circuit

When the reset inhibiting select switch is in the on

position, the integrator is under the control of the reset inhibiting

logic. When it is in the off position, a fixed -3 volts level or

voltage appears and allows the integrator to function freely.

There are occasions when reset action must be cancelled

completely, such as in the case of pure PD operation. The rest on-

off switch serves this purpose.

The purpose of connecting the triple ganged auto manual select

switch to the integrator is to provide bumpless transfer operation.

When set in the manual position as shown in figure 3-17, the first

of the triple ganged switches will provide +3 volt level to disable

the integrator and at the same time turn the integrator into a gain

1 inverter. The second switch will provide $-m_M(t) + 1$ volt to the in-

put of the integrator. Hence the positive manual control output minus

one volt will appear at the output of the integrator.

When switched back to automatic control, the integrator will

be reactivated but with the initial value $m_M(t) - 1$ volt stored in it. If

set point equals c(t) during the manual steady state, the automatic

control output m(t) will be equal to the previous manual control

output $m_M(t)$. Thus no bump will occur during the transition.

Note that all these mechanical switch outputs are tied to

the same point. However, the +3 volts for the auto-manual switch

and reset on-off switch are both derived from a voltage source, while

the -3 volts for the reset inhibiting select switch comes from a

voltage ░░░░░░░░░░ er +3 volt and -3 volt occur at the same time,

the +3 volt will always over-ride the -3 volts. In other words, whenever the reset action is at the off position (gives +3 volts) or when manual control is selected (+3 volts also), the integrator ceases to be an integrator, regardless of the state of the other switches.

Accessories

A set of accessories on the front panel is required to select or indicate the proper functions. They are:

1) Digital or manual set point select switch

2) Manual set point knob

3) Digital set-point switch set

4) Automatic or manual control select switch

5) Manual control knob

6) Direct or indirect action select switch

7) Reset inhibiting select switch

8) Reset on-off switch

9) Meter reading select switch, selects to show a) set point
   b) plant output, c) automatic control output, d) manual control
   output, e) zero check

10) Digital set point read in switch

11) Power on off switches for ±15 volt and +40 volt supply

12) Indicating lights for ±15 and + 40 volt supply

13) Current output connector: a female plug for cable connection
    at the back of the device

14) Voltage output connector: a female plug for monitoring purposes

at the back of the device

15) Input connector: a female plug for cable connection to receive

feedback from the plant output

16) Safety fuses: to limit power consumption from ±15 volts and +40 volt

supply

17) P.I.D. parameter indicating dials

The present circuit lay-out is purely for convenience reasons.

The controller can be easily modified to a smaller size for industrial

uses. The complete circuit, and the appearance of the device is shown

in the following diagrams:

FIG 3·18·α POWER SUPPLY CIRCUIT.
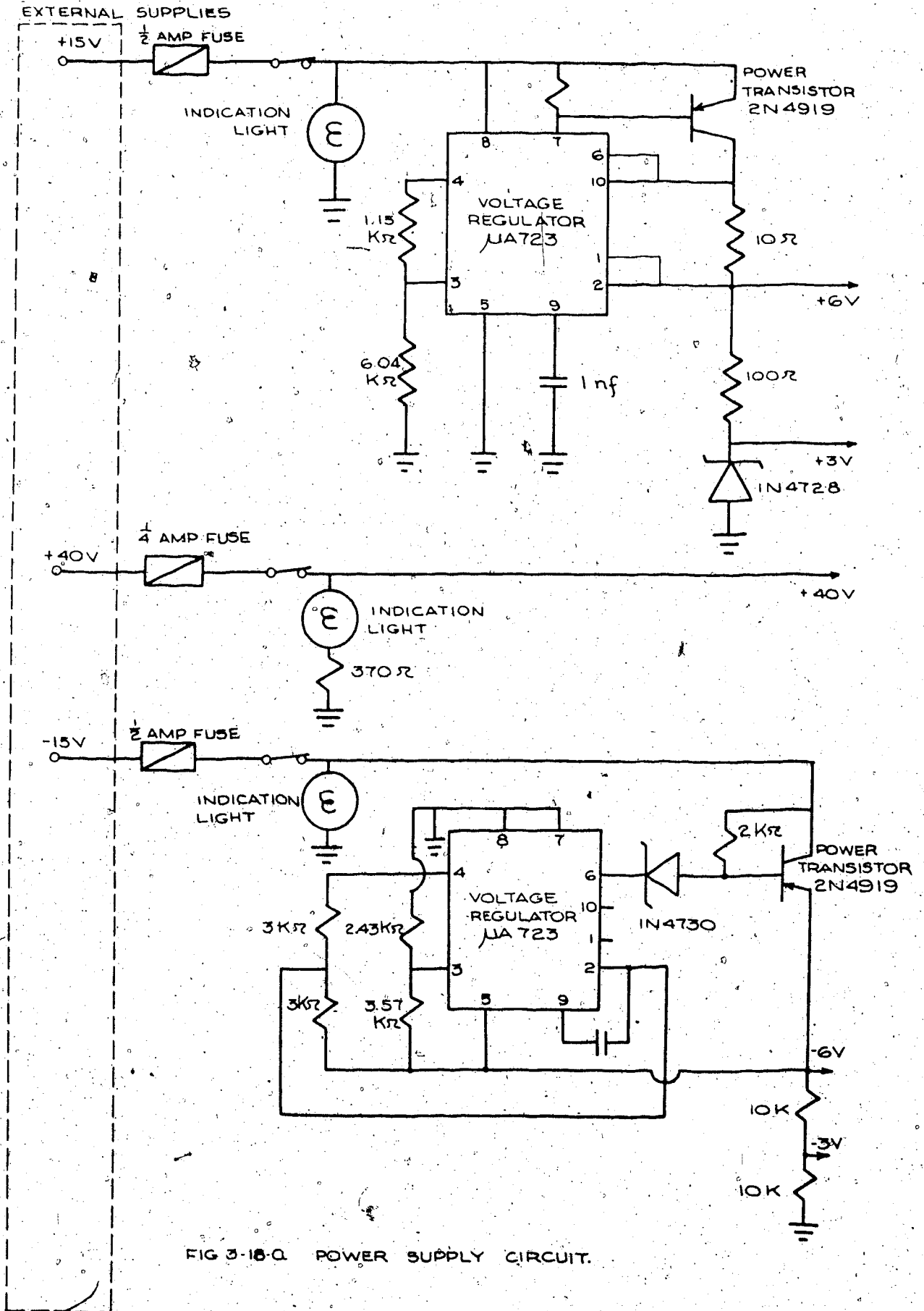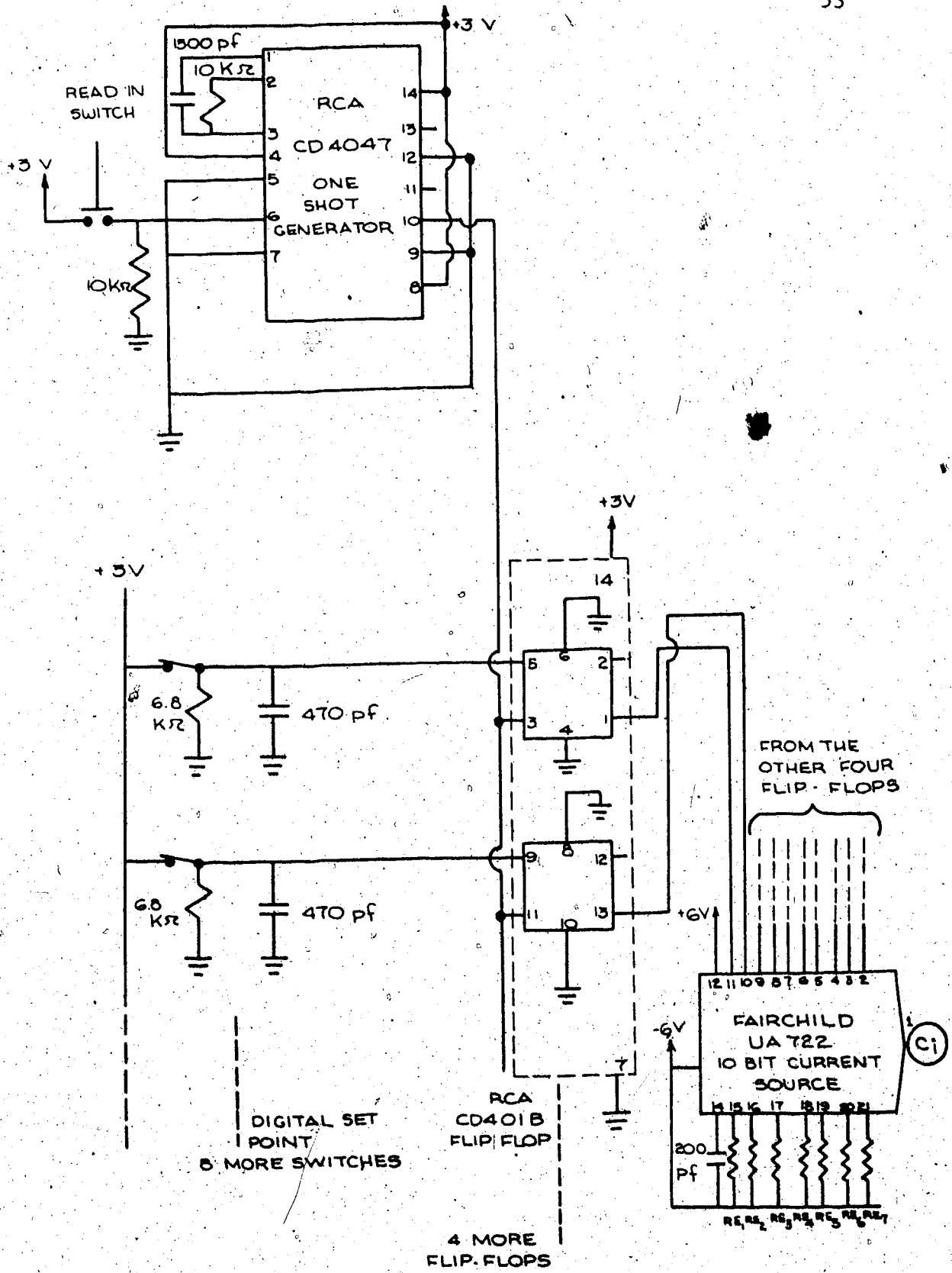
FIG 3-18b. DIGITAL SET POINT GENERATION.

FIG. 18C   THE CIRCUIT OF THE CONTROLLER PROPER.
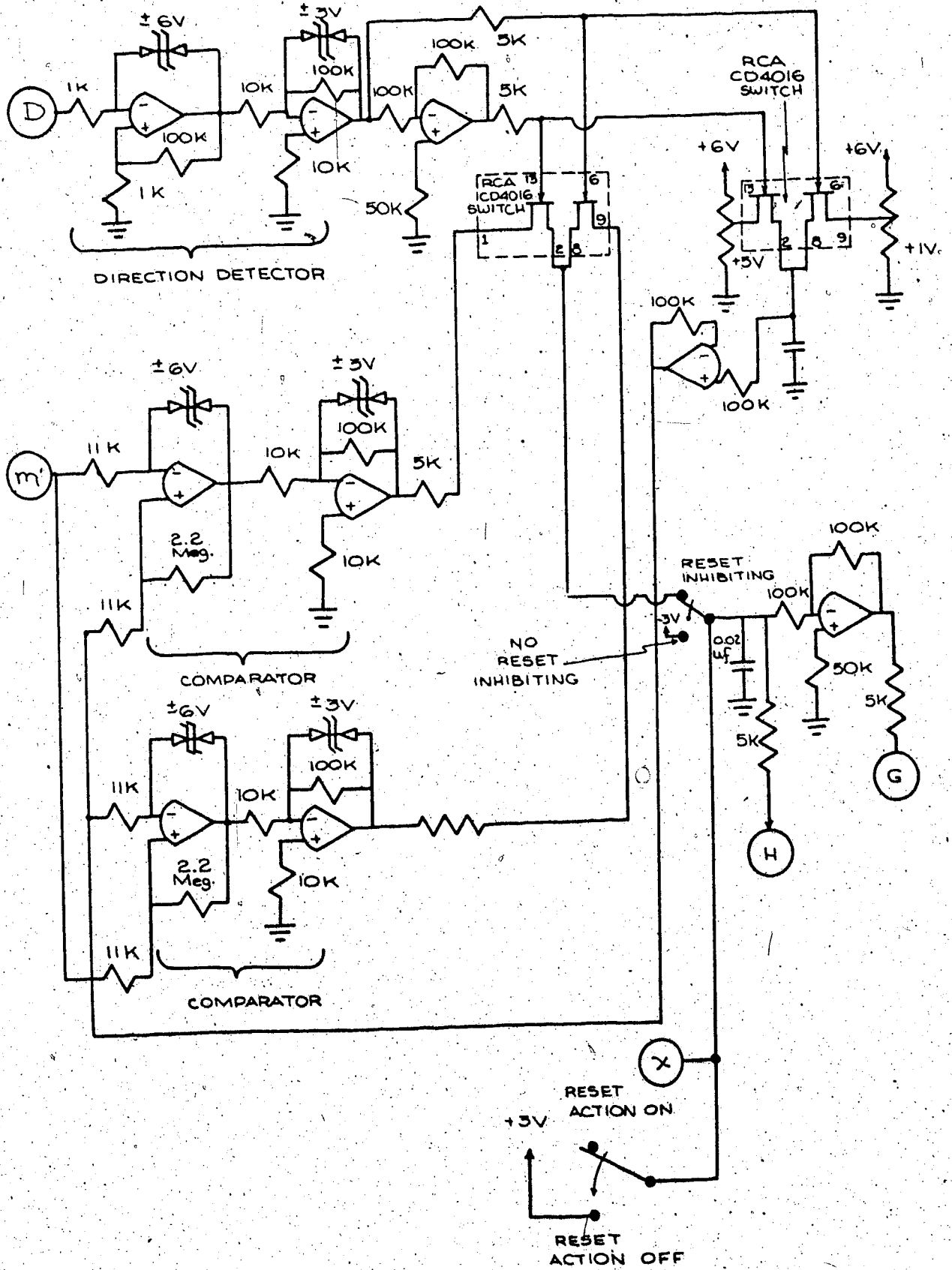
FIG 3·18·D RESET INHIBITING CIRCUIT.
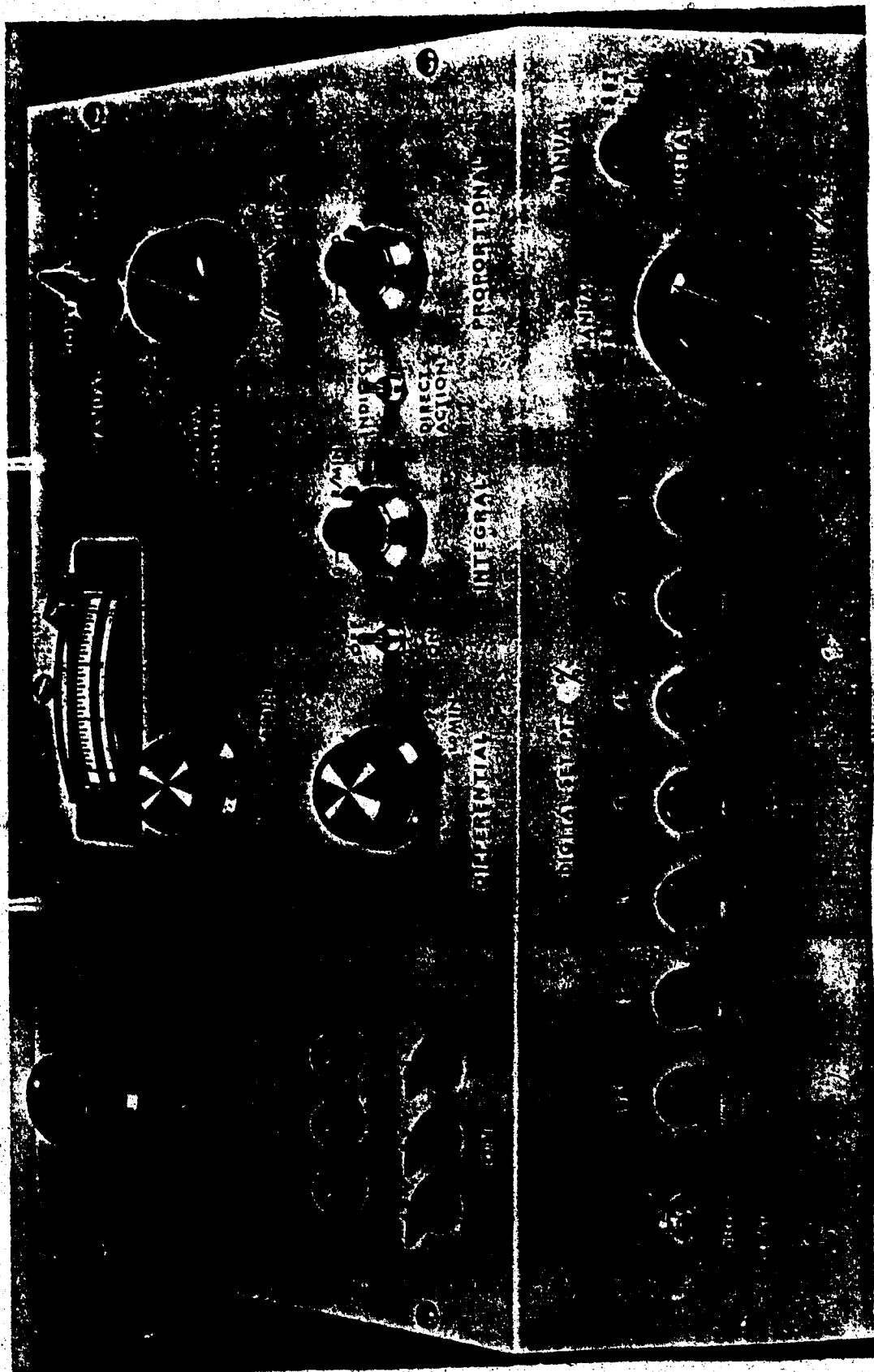
Figure 3-19 The Appearance of the near ideal P.I.D. controller

Chapter IV

The Tuning of an Ideal Controller

The existing tuning techniques are numerous. They are the product of different definitions of process and performance criteria [17, 18]. To name a few: there are Zeigler-Nichol's closed-loop and open-loop methods, Cohen-Coon's method, Harriot's method, three constraints method and integral of error methods. The co-existence of these methods proves two things: (1) control systems with nonlinear elements are difficult to understand [19]; (2) optimal tuning brings marked improvement in process control, and hence the effort to search for it is justified [3].

A controller is not designed for the controlling of random noise, but rather for set point changes, disturbances and load changes [20]. The solving of a tuning problem usually starts from the proper characterization of the process itself and the choosing of a sound performance criterion. The object is to find a controller setting which will produce the desired performance for a particular plant.

The characterization of a plant [19]

The characterization of a plant falls into the category of open loop method. In contrast to open loop method, the closed loop method seeks to characterize the entire control loop. In practice it became obvious that the open loop is superior. Because the open loop method needs to upset the plant only once, while in the closed loop method the necessary information must be acquired through a number of upsets of the entire control loop. In many cases the closed

loop method is not only cumbersome, but also intolerable. The

open loop method requires information to be extracted from the process

reaction curve. A process reaction curve can be produced in the

following manner.

1) Place the controller on manual operation and allow

the system to reach steady state.

2) With the control still in manual operation, impose a

step change at the output of the controller.

3) Record the response of the process output.

A typical process reaction curve is shown in figure 4-1.
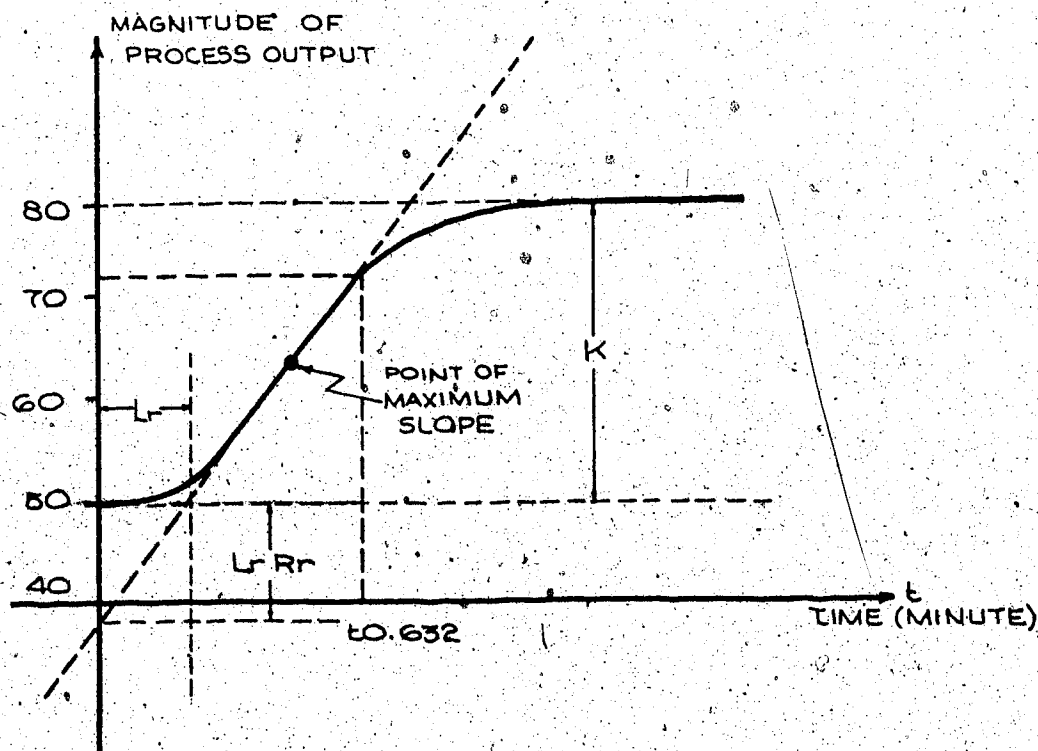
Figure 4-1 A process reaction curve

Different methods are available to approximate a process represented by the process reaction curve in figure 4-1. The most common approximation is a pure time delay plus a first order lag. One reason for the popularity of this approximation is that a real time delay of any duration can only be represented by a pure time delay. There is no other simple adequate approximation. A higher order lag plus pure time delay is also possible, but not necessary. The pure time delay plus first order lag approximation is easy to obtain and sufficiently accurate for most purposes. The approximated process transfer function is:

$$G(S) = \frac{K e^{-\theta_o S}}{\tau S + 1} \qquad (4-1)$$

where $\theta_o = L_r$ dead time delay

$\tau = t\ 0.632 - \theta_o$ time constant of a 1st order

                                      system

The parameters K, θ_o and τ can all be obtained from the process reaction curve as shown in figure 4-1. In figure 4-2 the reaction curve of a second order plant with dead time delay, and its approximation by a first order lag plus dead time delay are shown. Figure 4-2 reveals the closeness of the approximation to the true process reaction curve.

For plants with an underdamped reaction curve, the first order lag plus dead time delay approximation is not suitable. Instead, a second order lag plus dead time delay model should be used. Note

Figure 4-2 The reaction curve of a 2nd order plant

plus dead time delay and its approximation

that this model can actually represent both underdamped and over-damped processes. This higher order approximation requires three parameters to be extracted from the process reaction curve instead of two parameters as in the previous model. This extra bit of information insures a better approximation and as a result better controller tuning.

The transfer function of the second order lag plus dead time delay model is:

$$G(S) = \frac{K e^{-\theta_o S}}{\frac{S^2}{\omega_n^2} + \frac{2\xi}{\omega_n} S + 1} \qquad (4-2)$$

There are a number of methods to extract θ_o, ω_n, ξ and K from the

process reaction curve. Meyer's [21] method published in 1967 can

be applied to both underdamp and overdamp systems with dead time

delay. Meyer's method is good in the sense that the ease to apply

is comparable to that of the first order model.

The second order lag plus dead time method is a better approx-

imation for higher order systems. However, in most cases the first

order lag plus dead time delay approximation is sufficiently adequate.

Unless a higher accuracy is needed or in the case of an underdamped

reaction curve, the second order lag plus dead time model is seldom

used.

Choosing the performance criterion

Most of the time the process under control is at steady

state. Starting up, or set point changes are rare to encounter.

Under the on-line control situation the most frequent happenings

are load changes and disturbances. Hence the majority of control

tunings are tuned for better performance under disturbance and load

changes. The answer to what comprises the best performance, may

well be a subjective one. Most of the older tuning techniques were

based on the so called quarter decay ratio as the performance criterion.

The idea behind it is that, if the difference between each successive

peak and the steady state value is one-fourth of the previous

difference, the output will settle down very quickly. This situation

is depicted in figure 4-3.

However, the situation in figure 4-3 is only true for a pure
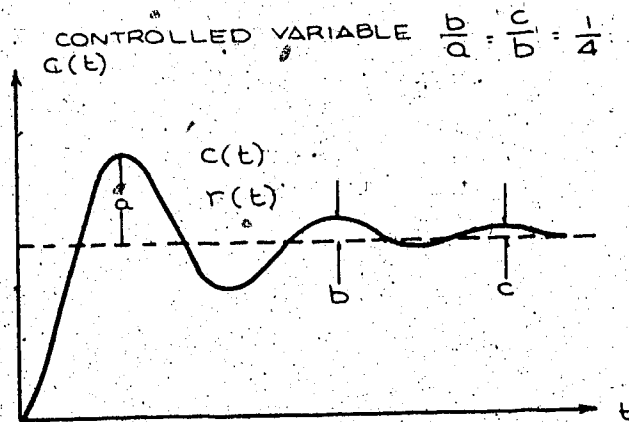
Figure 4-3 A response with a quarter decay characteristic

second order system. In any other system, there is no guarantee

that this decay ratio will hold true through all subsequent peaks.

There is another problem with quarter decay ratio as a performance

criterion. In a multi-parameter controller such as PI or PID

controller, there are infinite combinations of parameters to produce

a quarter decay response. It was based on this fact that arbitrary

constraints were imposed on the original Zeigler-Nichol's open loop

tuning method. It became known as the three constraints method [18].

The fallacy with quarter decay ratio is that, it relies upon a few

points from the response curve to determine the goodness of a control.

So is any other similar method bound to fail (e.g. frequency response

method, also relies on a few points).

The ideal performance criterion should be a single figure that accounts for, not only a few points, but the entire closed loop response. Originally, the purpose of a feedback control system was to minimize the output error as a function of time after some upset has been introduced. Both the magnitude of error and the time over which the error is present, should contribute to the definition of the optimal control. Accordingly it is logical to propose a figure of merit to characterize the entire time response of the system as:

$$\phi = \int_0^\infty F[e(t),t]dt \qquad (4-3)$$

where F is a function of error and time. By integrating F with respect to time, a single number will be obtained, characteristic of the entire time response of the system. The criterion of performance: ϕ should have the property of being zero only if the error is zero at all times. This is clearly impossible after a disturbance has been introduced. However, the smaller the value of ϕ is the better the performance of the system. Optimum performance can therefore be defined as that time response which gives the minimum value of ϕ. Since the time response of a particular system is a function of the controller settings, the criterion of performance ϕ is also a function of the controller settings. The problem of minimizing ϕ can be mathematically formulated as:

$$\phi = \phi(K_c, T_i, T_d) \tag{4-4}$$

$$\frac{\partial \phi}{\partial K_c} = 0 \tag{4-5}$$

$$\frac{\partial \phi}{\partial T_i} = 0 \tag{4-6}$$

$$\frac{\partial \phi}{\partial T_d} = 0 \tag{4-7}$$

where K_c, T_i, and T_d are the controller parameters for gain, integral time, and derivative time respectively. The simultaneous solution of equations (4-5) to (4-7) is the necessary condition to yield a controller setting which will cause an optimum performance. It is obvious then, that the use of a single figure of merit to characterize the system response results in a unique combination of parameters as the optimum setting. A number of possible definitions of ϕ is listed below:

$$\phi_{ITE} = \int_0^\infty t\,e\,dt = ITE \text{ integral of error x time} \tag{4-8}$$

$$\phi_{ISE} = \int_0^\infty e^2 dt = ISE \text{ integral of error squared} \tag{4-9}$$

$$\phi_{IAE} = \int_0^\infty |e|\,dt = IAE \text{ integral of absolute error} \tag{4-10}$$

$$\phi_{ITAE} = \int_0^\infty t|e|\,dt = ITAE \text{ integral of absolute error x time} \tag{4-11}$$

$$\phi_{ITSE} = \int_0^\infty te^2 dt = ITSE \text{ integral of error square x time} \tag{4-12}$$

Some of the above listed criteria are applied to a linear second order system:

$$G(S) = \frac{1}{S^2 + 2\xi S + 1} \qquad (4-13)$$

with a step function as the input variation. The resultant Φ value versus system parameter variation is plotted in figure 4-4[22].
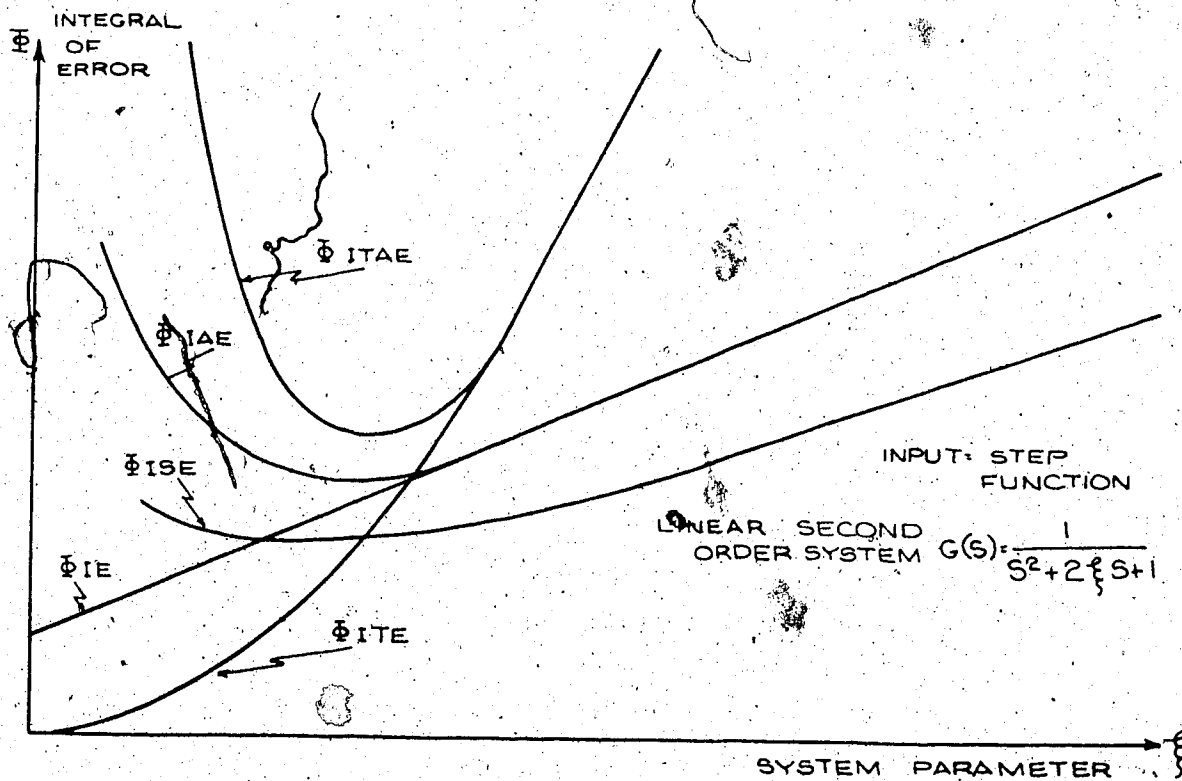

Figure 4-4 Integrals of error versus

system parameter variation

From figure 4-4, it is clear that Φ_{ITAE}, Φ_{IAE} and Φ_{ISE} are the curves that have selectivity. Among the three, the performance criterion

Φ_{ITAE} is the most selective one. When apply all different ϕ's to higher order systems, Φ_{ITAE} still maintains its selective character while the other Φ's wane into non-selective curves [22]. Hence, it can be concluded that Φ_{ITAE} is superior to the others, for both low and high order systems. In practice the most often used criteria are: ISE, IAE and ITAE.

The ISE criterion (integral of error squared) is relatively insensitive to small errors, while large errors contribute heavily to the value of the integral. The use of ISE as a criterion will result in responses with small overshoots. However, long line-out time appears because small error occurring late in time do not contribute much to the error integral.

The IAE criterion (integral of absolute error) is more sensitive to smaller errors but less to large errors than in the case of ISE. Often the result of using this criterion is intermediate to those of ISE and ITAE criteria.

The ITAE criterion (integral of absolute error weighted by time) is insensitive to the initial unavoidable errors, but it penalizes heavily those error that occur late in time. Consequently, optimum response as defined by ITAE has the characteristic of short total response time and larger overshoots.

Among these three criteria (ISE, IAE, ITAE), if sensitivity is not an issue, then it is left for the individual engineer to choose. The particularity of the system, or even personal taste can play a role in the choosing.

Tuning relationship based on integrals of error criteria

With the process model properly defined and the performance criterion chosen, the focus should now be brought to the control loop itself. In figure 4-5, a simple control loop is shown with its controller blocks, process block and its inputs.
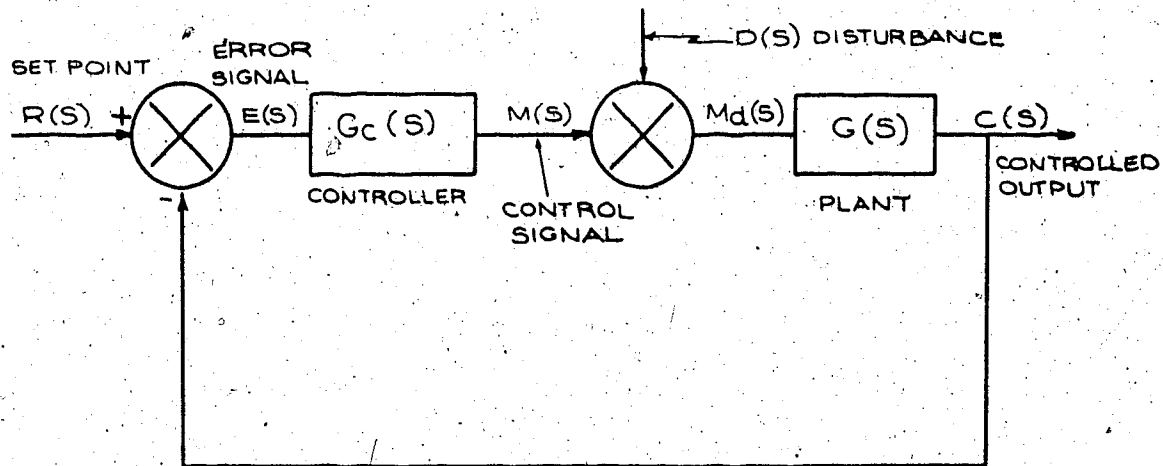
Figure 4-5 A simple feedback control loop

The process block includes the dynamics of the measurement devices and that of the valves. Two input signals are shown, a change in set point r(t) and a disturbance signal d(t).

The transfer function for the control element is assumed to be represented by either:

$$G_c(S) = K_c \qquad \text{P control} \qquad (4-14)$$

$$\text{or} \qquad G_c(S) = K_c(1 + \frac{1}{T_i S}) \qquad \text{PI control} \qquad (4-15)$$

$$\text{or} \qquad G_c(S) = K_c(1 + \frac{1}{T_i S} + T_d S) \qquad \text{PID control} \qquad (4-16)$$

Equations (4-14) to (4-16) represent the ideal controller algorithms,

with no lag in P or D modes and no interaction between all three modes. However, as was pointed out in Chapter III, these ideal algorithms can be very closely approximated by the controller proposed in this thesis. Hence, it can be claimed that any tuning relationship developed for an ideal controller, should also fit for this controller. This point will be shown to be true later in Chapter V.

Assuming the process is a first order lag with dead time delay, and a PID controller is used, the response to a disturbance can be written as:

$$c(S) = \frac{K S e^{-\theta_o S}}{\tau S^2 + S + KK_c e^{-\theta_o S}(T_d S^2 + S + \frac{1}{T_1})} D(S) \qquad (4-17)$$

If the disturbance is a unit step, then

$$D(S) = \frac{1}{S} \qquad (4-18)$$

and

$$c(S) = \frac{K e^{-\theta_o S}}{\tau S^2 + S + KK_c e^{-\theta_o S}(T_d S^2 + S + \frac{1}{T_1})} \qquad (4-19)$$

Making the transformation $\mu = \tau S$, the following equation results:

$$c(\frac{\mu}{\tau}) = \frac{\tau \cdot K e^{-\frac{\theta_o}{\tau}\mu}}{\mu^2 + \mu + KK_c e^{-\frac{\theta_o}{\tau}\mu}(\frac{T_d}{\tau}\mu^2 + \mu + \frac{\tau}{T_1})} \qquad (4-20)$$

The above transformation is equivalent to introducing a dimensionless time t^o defined by:

$$t^o = \frac{t}{\tau} \tag{4-21}$$

Expressing equation (4-20) in time domain:

$$c(t^o) = K \, X(t^o) \tag{4-22}$$

where

$$X(t^o) = \mathcal{L}^{-1} \left[\frac{\tau \cdot e^{-\frac{\theta_o}{\tau}\mu}}{\mu^2 + \mu + KK_c e^{-\frac{\theta_o}{\tau}\mu} \left(\frac{T_d}{\tau}\mu^2 + \mu + \frac{\tau}{T_1}\right)} \right] \tag{4-23}$$

Equation (4-23) indicates that the dynamic characteristic of the time response is a function of the dimensionless parameters: $\frac{\theta_o}{\tau}$, KK_c, $\frac{\tau}{T_1}$ and $\frac{T_d}{\tau}$. Of these parameters, only $\frac{\theta_o}{\tau}$ contains pure plant characteristics. The other parameters each contains a controller setting, and thus can be manipulated to obtain an optimal response.

For a unit step disturbance, the error signal is given by:

$$e(t) = - c(t) \tag{4-24}$$

Combining equations (4-24), (4-21), (4-22), (4-9) and using ISE as performance criteria, the result is:

$$\phi_{ISE} = K^2 \times \int_o^\infty [X(t^o)]^2 dt^o \tag{4-25}$$

The analytical calculation of the function $X(t^o)$ involves the inverse transformation of equation (4-23). However, the presence of dead time in a control loop makes the analytical calculation of the inverse transformation extremely difficult. It seems reasonable then to consider numerical techniques to evaluate ISE in equation (4-25). In order to minimize the ϕ_{ISE} in equation (4-25), the optimum controller settings K_c, T_1 and T_d' have to be found. The multi-parameter optimization problem was solved by the use of a modified steepest ascent method known as optimum gradient. This optimization technique has been extensively discussed by Bekey [23].

Using integrals of error as performance criteria A.M. Lopez set up a control loop simulation and a three dimensional optimization program on an IBM 7040 digital computer. The result was a set of tuning relationship graphs and equations. Those tuning graphs and equations that are related to this thesis are listed in Appendix III.

With the understanding that the designed controller should be a very close approximation to the ideal algorithm, A.M. Lopez's tuning graphs and equations should also be directly applicable to the controller designed. These graphs and equations will surely enable one to determine the optimum settings rapidly. They also eliminate the numerous trials necessary in the older tunning techniques.

For more information on tuning please see references 24, 25 and 26.

Chapter V

Results and Conclusions

In order to test the designed controller, the complete

control loop must be set up. The plant itself with dead time delay

were simulated by a hybrid system, consisting of a PDP8 digital

computer, a EAI TR-48 analog computer and a REDCOR 610 linkage system.
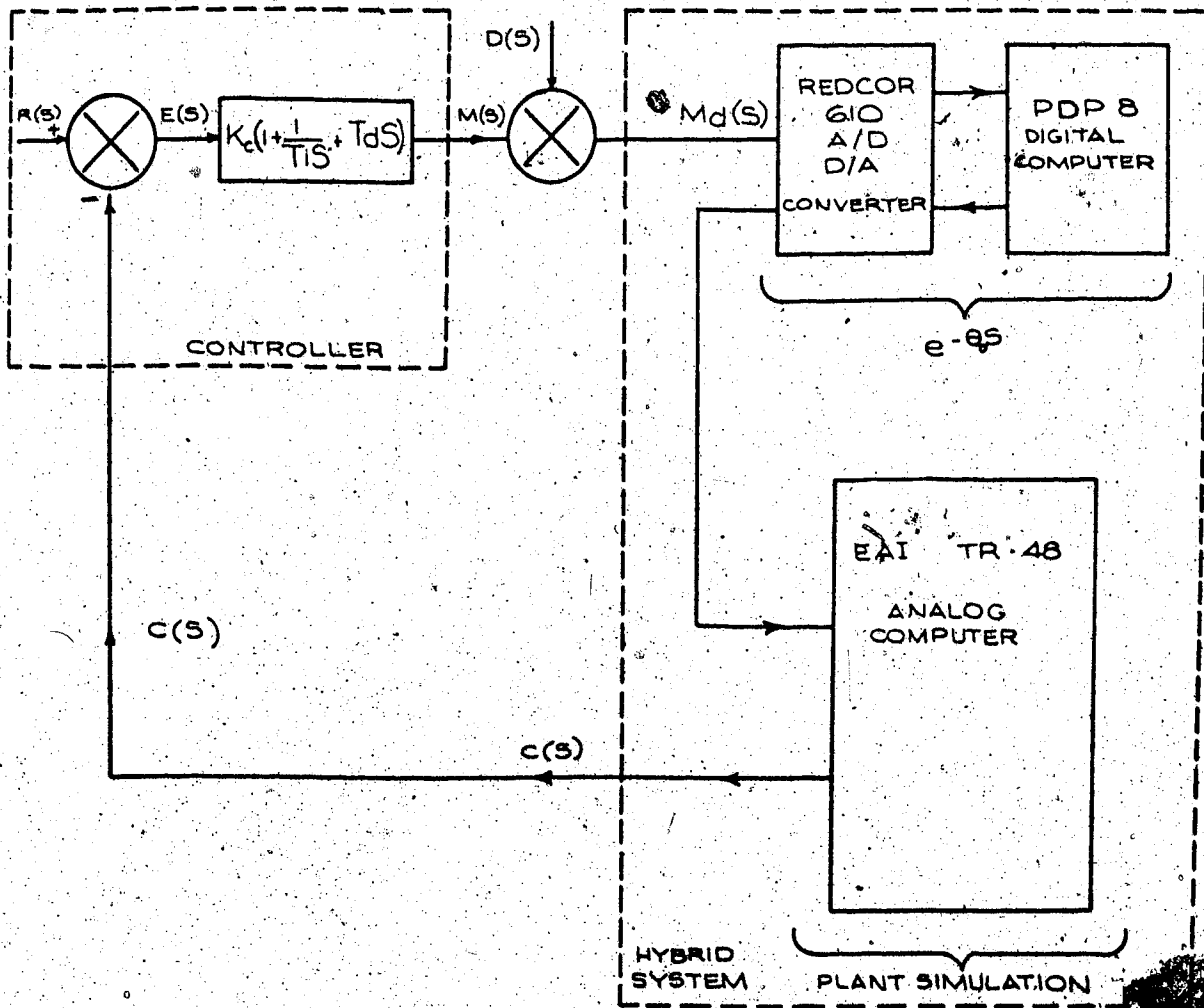
A detailed diagram is shown in figure 5-1.

Figure 5-1 The complete control loop with the plant and dead time

simulated by a hybrid system

From figure 5-1 it is clear that the D/A and A/D converter together with the digital computer functions as a dead time generator, while the analog computer simulates the plant proper. The control signal plus disturbance:

$$M_d(S) = M(S) + D(S) \tag{5-1}$$

is sampled by an A/D converter at a certain rate. This rate is determined to be : $\frac{3072}{\theta_o}$ times/sec (Appendix A II). Considerations have been given to the capability of the hybrid system and the desirability of higher rate of sampling.

The sampled analog signal is converted into binary code and stored in a specified memory area of the digital computer. After θ_o units of time, this binary code will be brought out and converted back to an analog signal. The reconverted analog signal will then be sent to the simulated plant in the analog computer. The detailed explanation, flow chart and program are listed in Appendix A II.

The following plant models were used during the test of the designed controller:

$$G_1(S) = \frac{K e^{-\theta_o S}}{\tau S + 1} \tag{5-2}$$

and

$$G_2(S) = \frac{K e^{-\theta_o S}}{\frac{S^2}{\omega_n^2} + \frac{2\xi S}{\omega_n} + 1} \tag{5-3}$$

For all practical purposes, these two models can represent most of the processes. Plants without dead time delay are not considered here in order to shorten this presentation. Furthermore, only PID controlling form will be used.

The original objective of the proposed controller is to build a near ideal PID controller, so that A.M. Lopez's optimum tuning chart can be utilized. Whether this design objective is achieved or not can be shown by comparing the results obtained from different tunings. In all subsequent tests, the IAE performance criterion is used.

First order plant with dead time delay

The chosen plant parameters for $G_1(S) = \dfrac{K e^{-\theta_o}}{\tau S + 1}$ are:

$$K = 1$$

and

$$\tau = 2.1 \text{ min} = 126 \text{ sec}$$

Three arbitrary $\dfrac{\theta_o}{\tau}$ values were chosen to test the designed controller. They are : $\dfrac{\theta_o}{\tau} = 0.2$, 0.5 and 0.8. Using $\tau = 126$ sec, $\dfrac{\theta_o}{\tau} = 0.2$ means $\theta_o = 25.2$ sec, $\dfrac{\theta_o}{\tau} = 0.5$ means $\theta_o = 63$ sec, and $\dfrac{\theta_o}{\tau} = 0.8$ means $\theta_o = 100.8$ sec. For each of the $\dfrac{\theta_o}{\tau}$ values, Figure AII-I contains the optimum P, I, D settings. They shall be designated as K_{co}, T_{io}, and T_{do}. The controller will then be tuned according to these optimum values. Set point r(t) will be held constant at 2.5 volts, a mid point value of the output span. Then the control loop will be allowed to come to steady state. When steady state arrives, a disturbance of 1 volt

magnitude (a substantial one) will be imposed onto the control out-
put. The control loop is upsetted and the output response will be
recorded. This response should be the optimum one.

Then each of the three parameters will take turns to vary
above and below the optimum values while the other two parameters
remain at their respective optimum values. Therefore, a total of
six variations will be obtained. Each of these variations should
bring an inferior response to the supposedly optimum response.

The test was carried out and the results are listed in
Figure 5-2 to 5-10.

Second order plant with dead time delay

In the transfer function $G_2(S) = \dfrac{K e^{-\theta_o S}}{\dfrac{S^2}{\omega_n^2} + \dfrac{2\xi S}{\omega_n} + 1}$, K and

ω_n are chosen to be:

$K = 1$

and

$\omega_n = 0.1$

Two arbitrary values of $\theta_o \omega_n$ were chosen. They are: $\theta_o \omega_n = 1.1$ and
$\theta_o \omega_n = 4.0$. The damping ratio ξ is allowed to be either 1 or 0.5 to
represent overdamp or underdamp systems. Therefore, four different
sets of plant characteristics are available. Optimum PID settings for
them can be obtained from figure AIII - 2 to AIII - 10.

The controller was tuned according to the optimum settings
and its deviations. The supposedly optimum and non-optimum responses
were recorded in figure 5-11 to 5-22.

PLANT := $\dfrac{K_c e^{-\theta_0 s}}{\tau s + 1}$

PERFORMANCE CRITERION: IAE

A1O TUNING = K_{co}, T_{io}, T_{do}

A1a TUNING = $\frac{3}{2} K_{co}$, $\dfrac{T_{io}}{1}$, T_{do}

A1b TUNING = $\frac{1}{2} K_{co}$, $\dfrac{1}{T_{io}}$, T_{do}
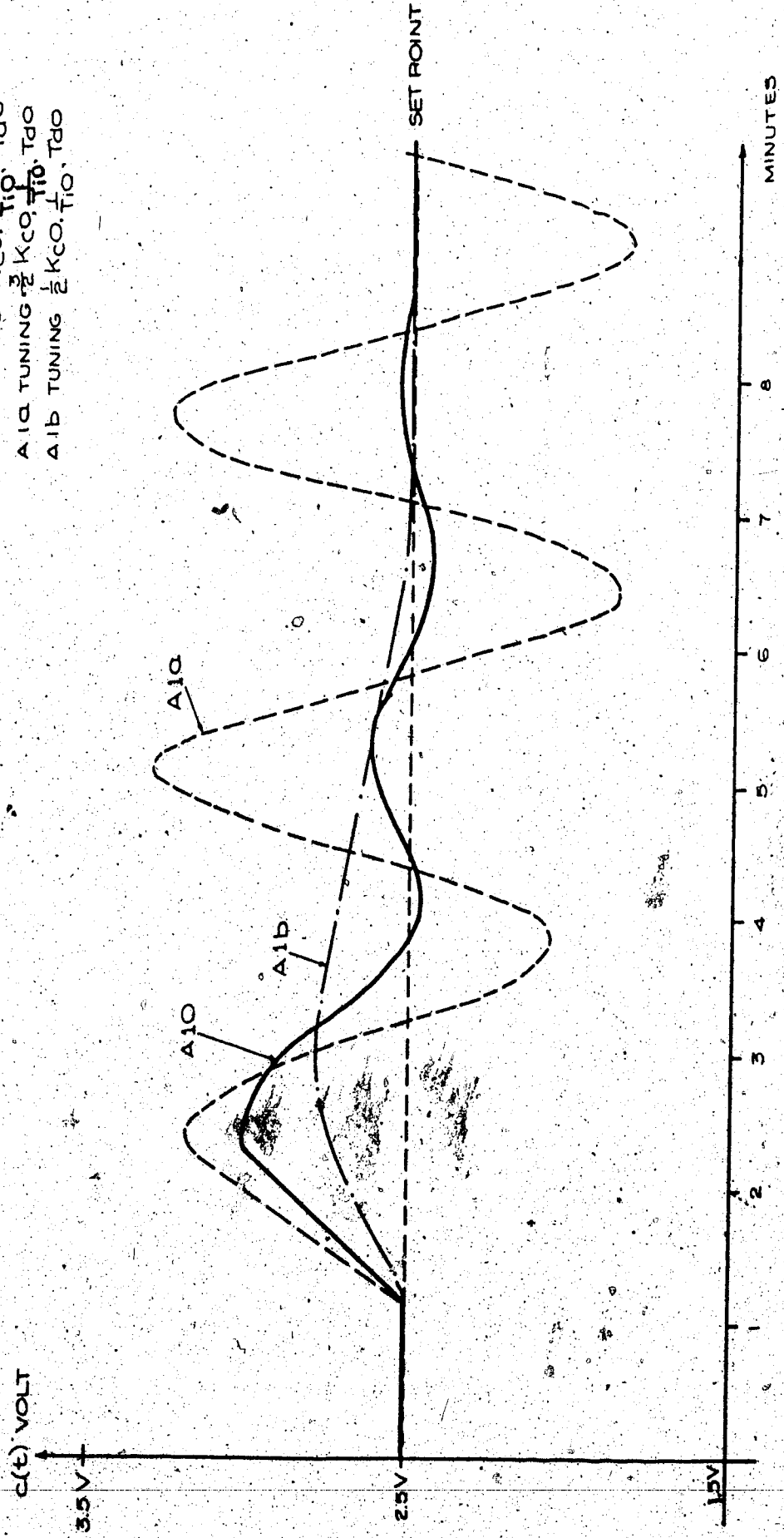
SET POINT
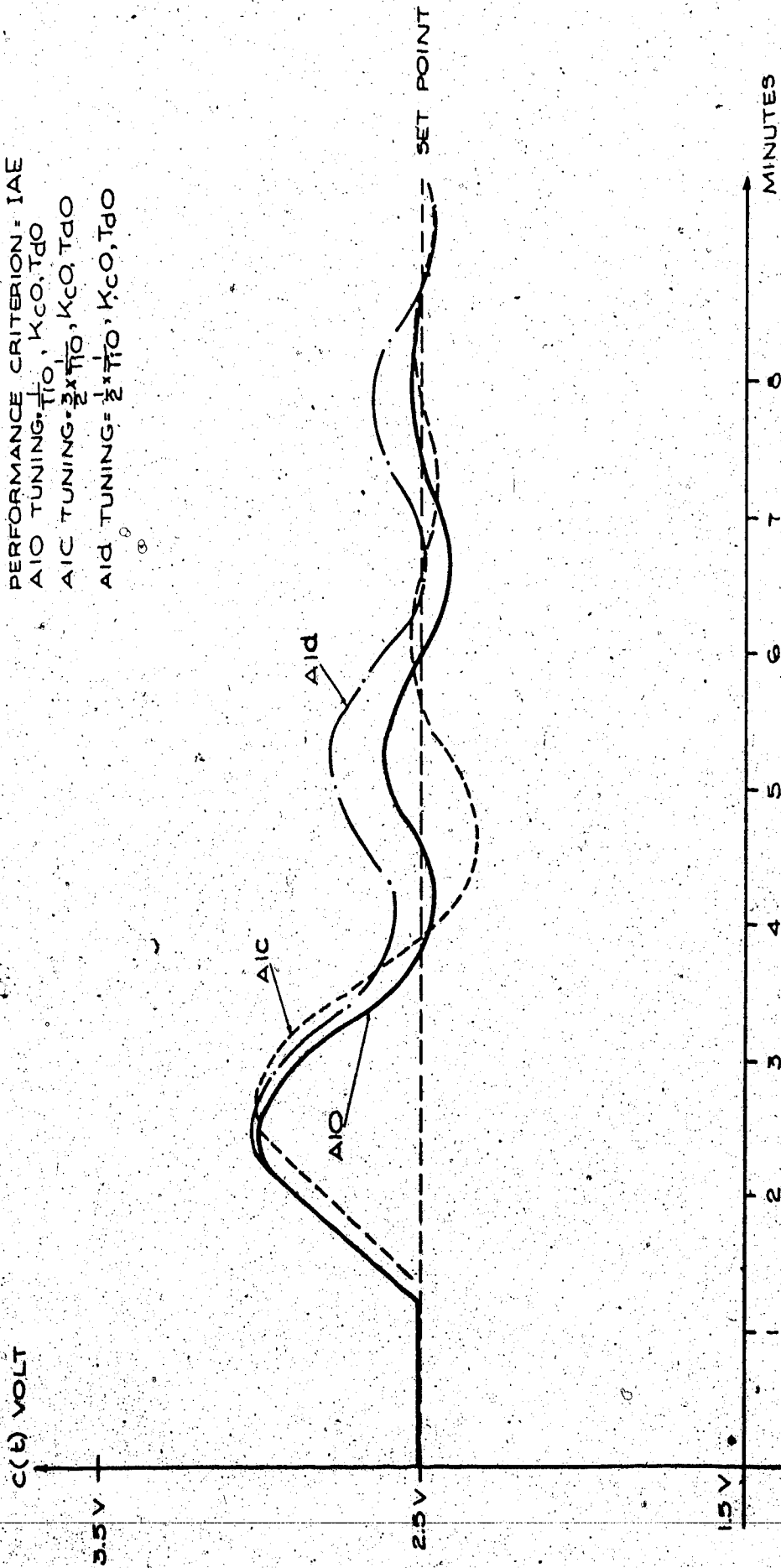
A1a

A1b

A1O

c(t) VOLT

3.5V

2.5V

1.5V

MINUTES

FIG 5·2· COMPARISON OF OPTIMUM TUNING AND ITS DEVIATIONS IN GAIN K_c FOR A FIRST ORDER PLANT WITH $\theta_0/\tau = 0.2$.

PLANT $\dfrac{Ke^{-\theta_o s}}{\tau s + 1}$

PERFORMANCE CRITERION: IAE

AIo TUNING: $\frac{1}{\tau}$io, K_co, Tdo

AIc TUNING: $\frac{3}{2} \times \frac{1}{\tau}$io, K_co, Tdo

AId TUNING: $\frac{1}{2} \times \frac{1}{\tau}$io, K_co, Tdo

SET POINT

MINUTES

AId

AIc

AIo

C(t) VOLT

3.5 V

2.5 V

1.5 V

FIG. 5-3 COMPARISON OF OPTIMUM TUNING & ITS DEVIATIONS IN T_i FOR A FIRST ORDER PLANT. WITH $\theta_o/\tau = 0.2$.
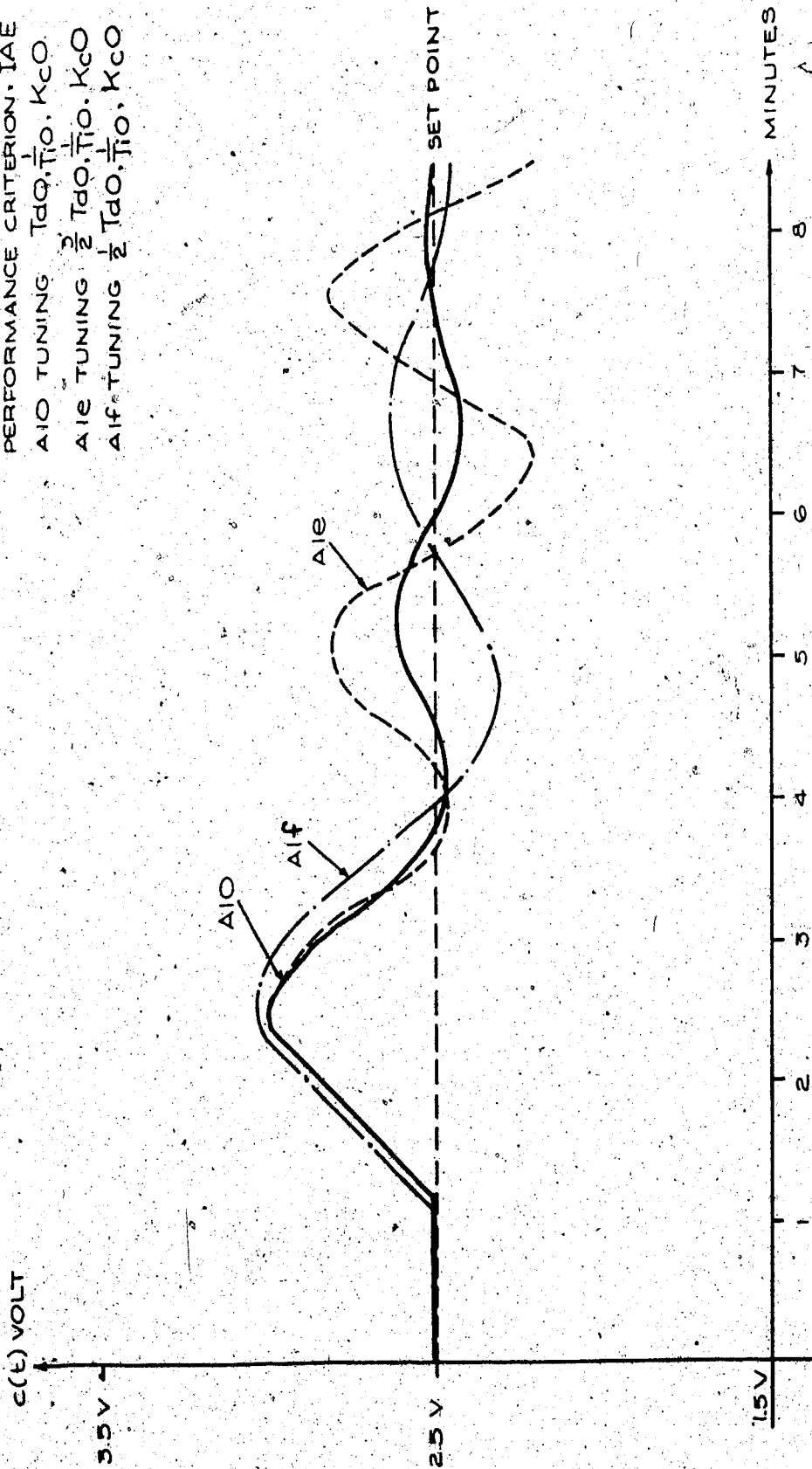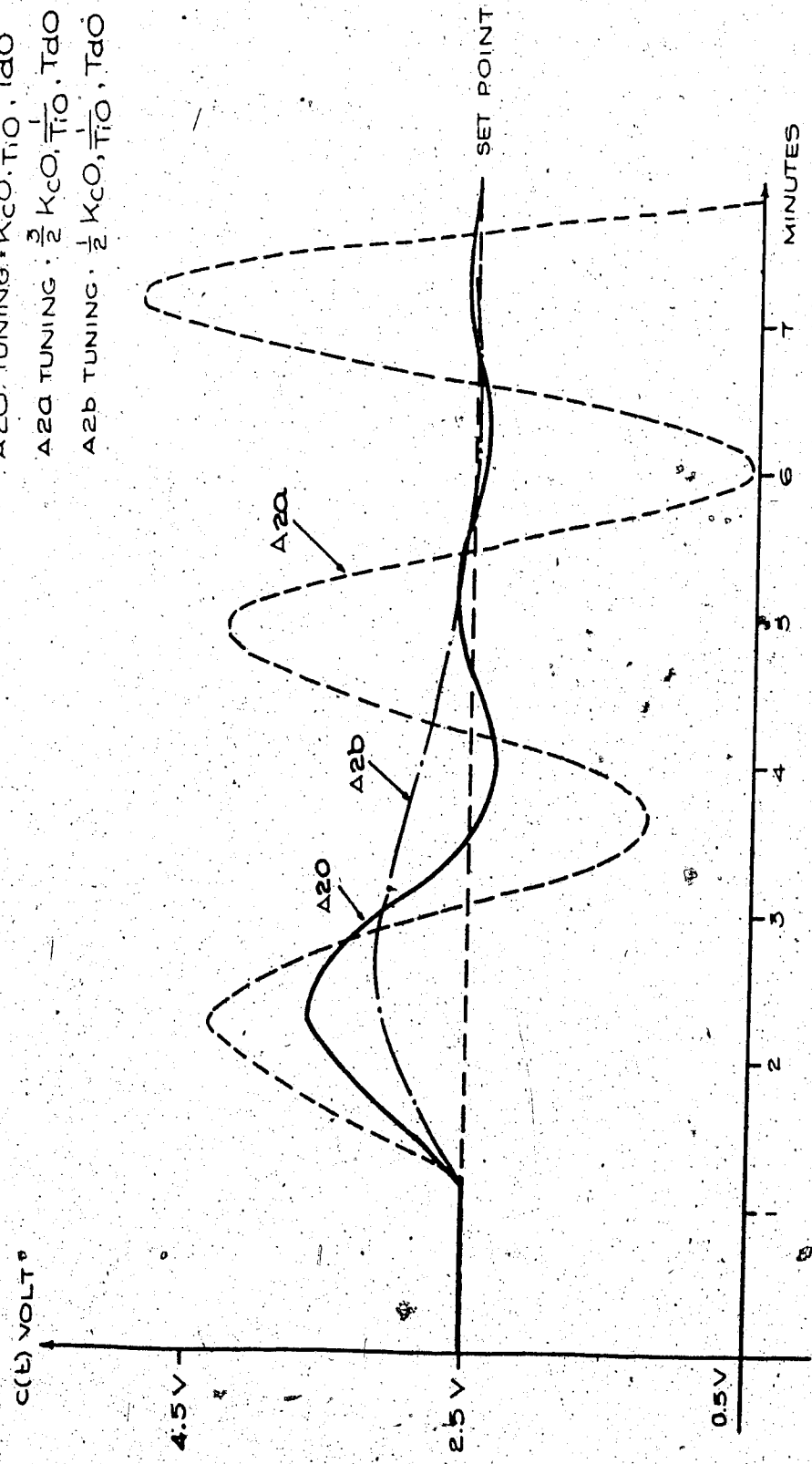
FIG. 5-4. COMPARISON OF OPTIMUM TUNING & ITS DEVIATIONS IN Td. FOR A FIRST ORDER PLANT. WITH $\frac{\theta o}{\tau} = 0.2$.

PLANT : $\dfrac{K_c e^{-\theta_0 S}}{T_S + 1}$

PERFORMANCE CRITERION: IAE

A2O. TUNING : $K_{cO}, \overline{T_{iO}}, T_{dO}$

A2a TUNING : $\dfrac{3}{2} K_{cO}, \overline{T_{iO}}, T_{dO}$

A2b TUNING : $\dfrac{1}{2} K_{cO}, \overline{T_{iO}}, T_{dO}$

SET POINT

MINUTES

A2O

A2b

A2O

C(t) VOLT

4.5 V

2.5 V

0.5 V

FIG 5·5   COMPARISON OF OPTIMUM TUNING & ITS DEVIATION
IN GAIN K_C FOR A FIRST ORDER PLANT WITH $\dfrac{\theta_0}{\tau} = 0.5$

PLANT: $\frac{Ke^{-\theta_0 s}}{\tau s + 1}$

PERFORMANCE CRITERION = IAE

A2o TUNING = $\frac{1}{\tau i o}$, KcO, TdO

A2c TUNING = $\frac{3}{2} \times \frac{1}{\tau i o}$, KcO, TdO

A2d TUNING = $\frac{1}{2} \times \frac{1}{\tau i o}$, KcO, TdO

c(t) VOLT

4.5 V
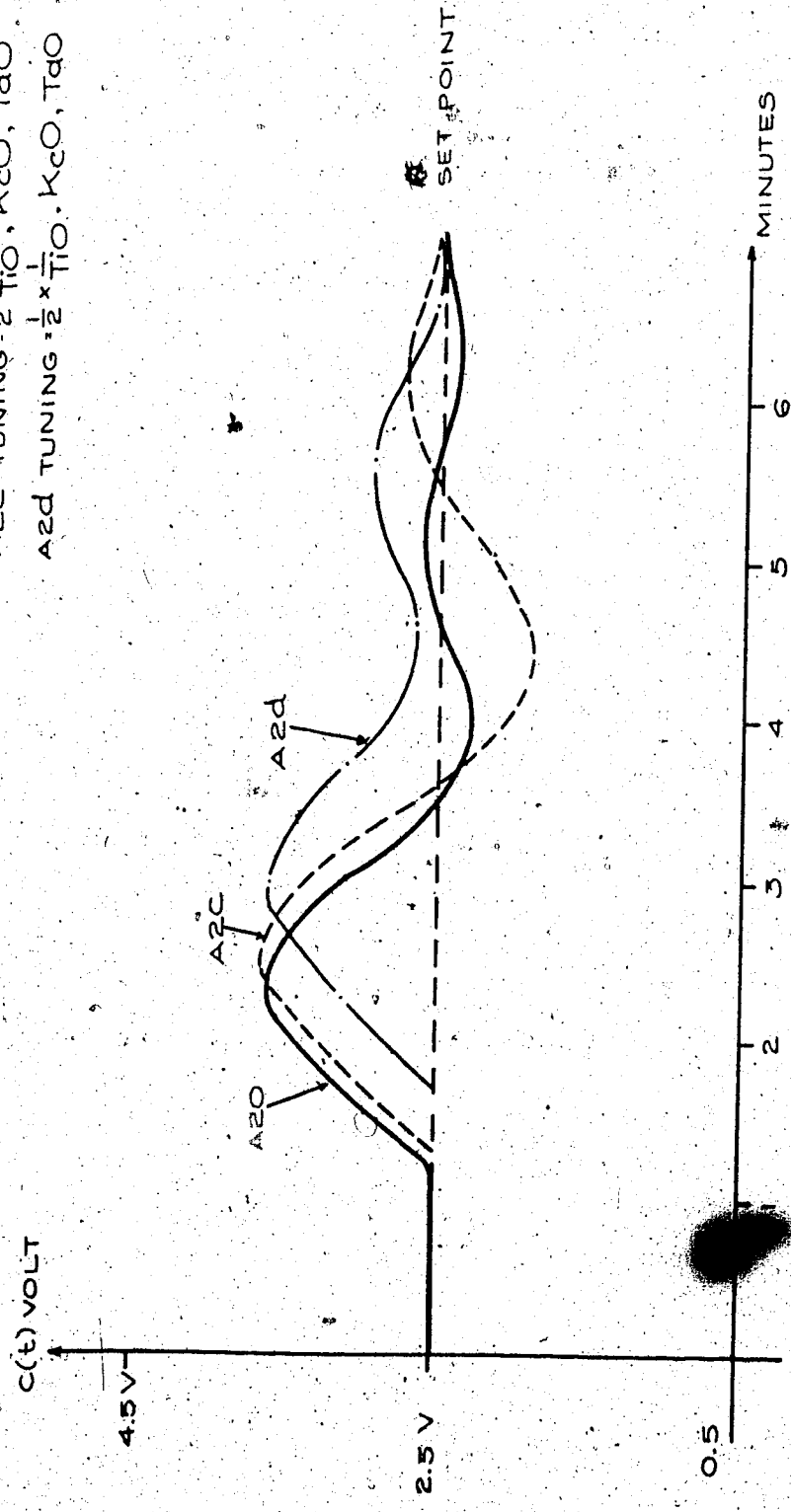
2.5 V

0.5

SET POINT

A2d

A2c

A2o

MINUTES

2   3   4   5   6

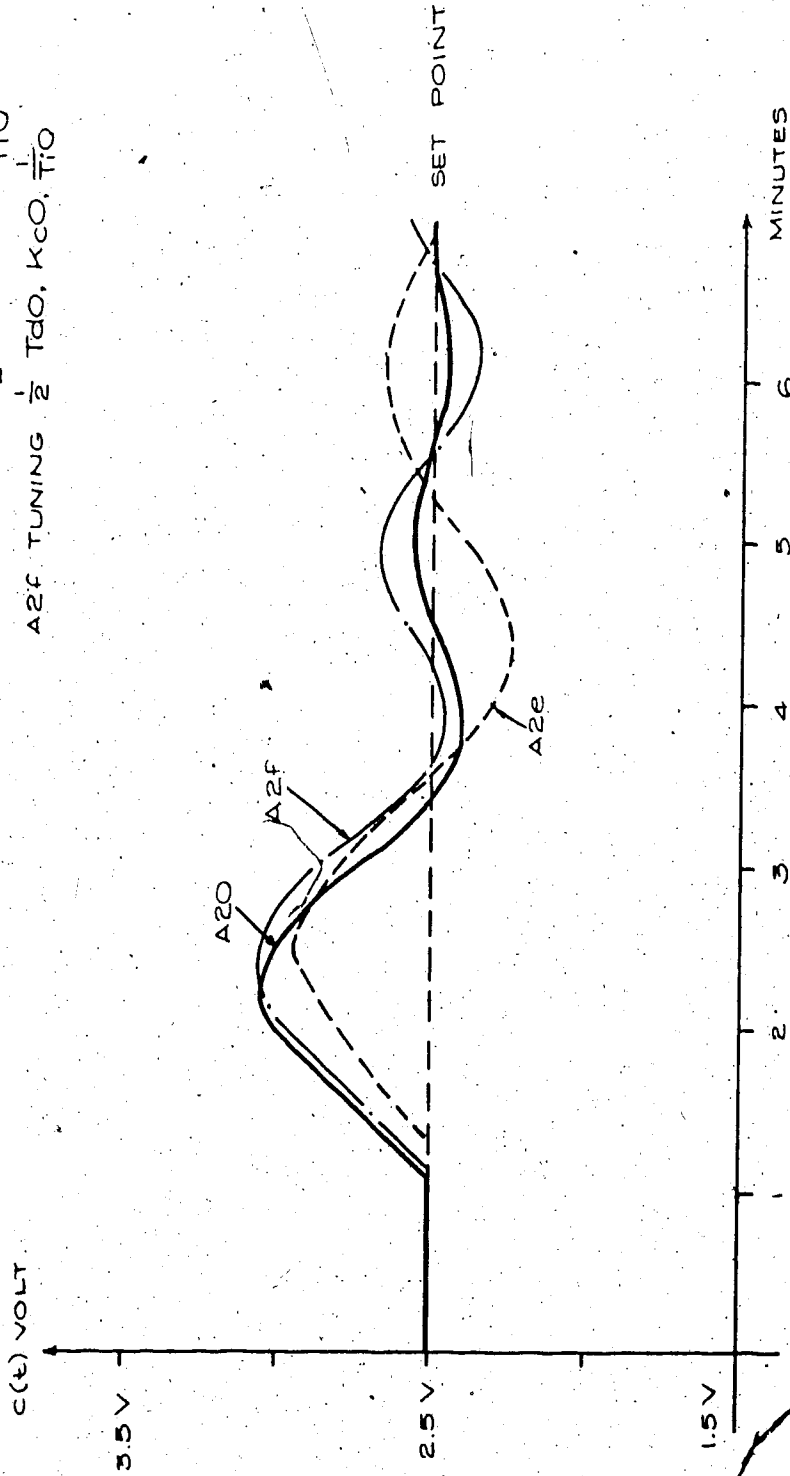FIG. 5·6   COMPARISON OF OPTIMUM TUNING & ITS DEVIATION IN τi FOR A FIRST ORDER PLANT WITH $\theta_0/\tau = 0.5$.

FIG 5-7 COMPARISON OF OPTIMUM TUNING WITH ITS DEVIATIONS IN Td FOR A FIRST ORDER PLANT WITH $\frac{\theta_0}{\tau} = 0.5$.

FIG. 5·8   COMPARISON OF OPTIMUM TUNING WITH ITS DEVIATIONS IN, GAIN K_c FOR A FIRST ORDER PLANT WITH $\frac{\theta_o}{\tau}$, 0·8

PLANT = $\dfrac{Ke^{-\theta_0 S}}{\tau S + 1}$

PERFORMANCE CRITERION = IAE

$\Delta 30$ TUNING $Ti0, Kc0, Td0$

$\Delta 3C$ TUNING $\dfrac{3}{2} \times \dfrac{1}{Ti0}, Kc0, Td0$

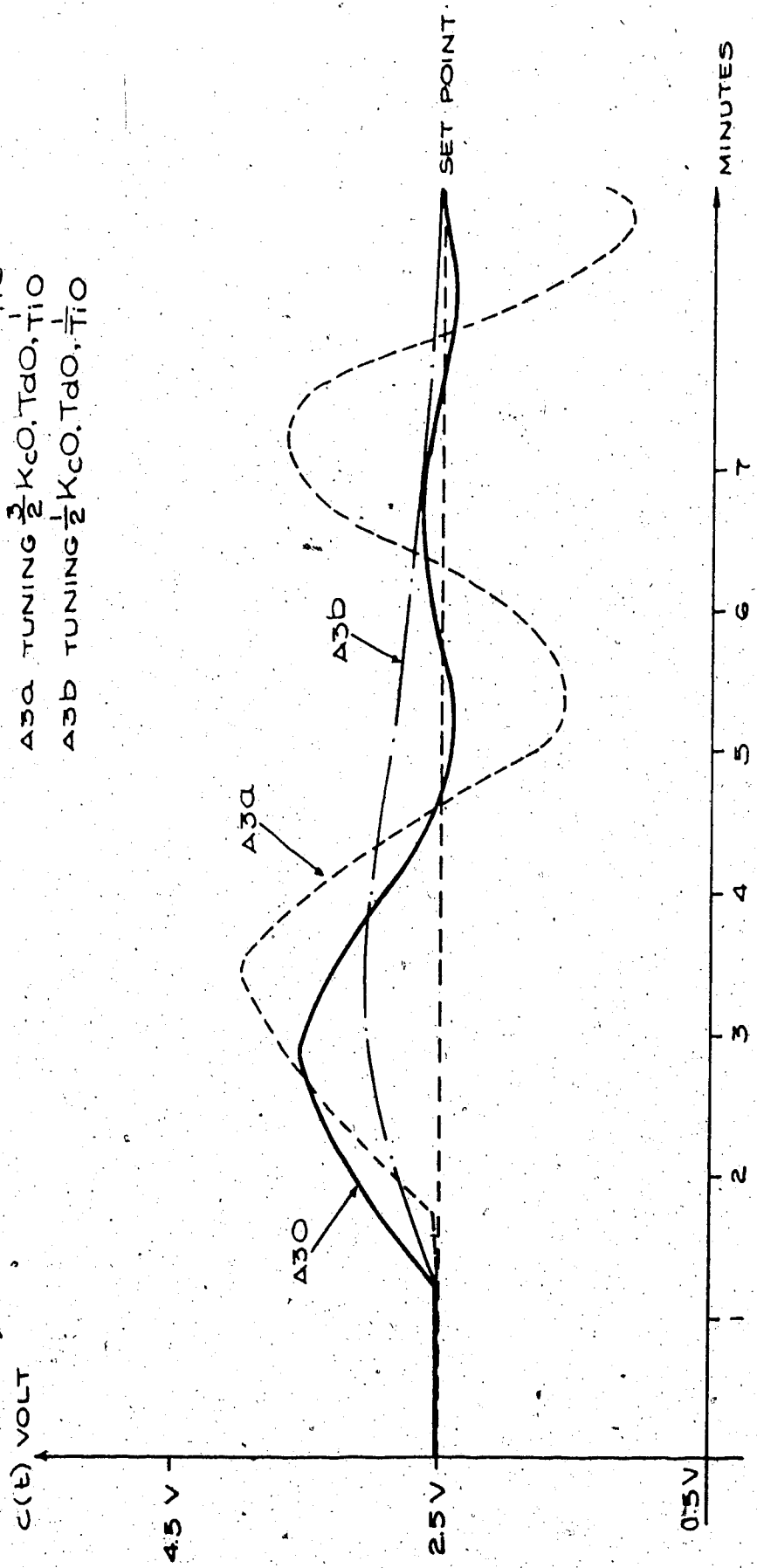$\Delta 3d$ TUNING $\dfrac{1}{2} \times \dfrac{1}{Ti0}, Kc0, Td0$

FIG 5·9   COMPARISON OF OPTIMUM TUNING WITH ITS DEVIATION IN
Ti FOR FIRST ORDER PLANT WITH $\dfrac{\theta_0}{\tau} = 0.8$

PLANT $\dfrac{Ke^{-\theta_0 S}}{Ts+1}$

PERFORMANCE CRITERION : IAE

A3O TUNING = TdO, KcO, $\dfrac{T_iO}{T_iO}$

A3e TUNING = $\dfrac{3}{2}$TdO, KcO, $\dfrac{T_iO}{T_iO}$

A3f TUNING = $\dfrac{1}{2}$TdO, KcO, $\dfrac{T_iO}{T_iO}$
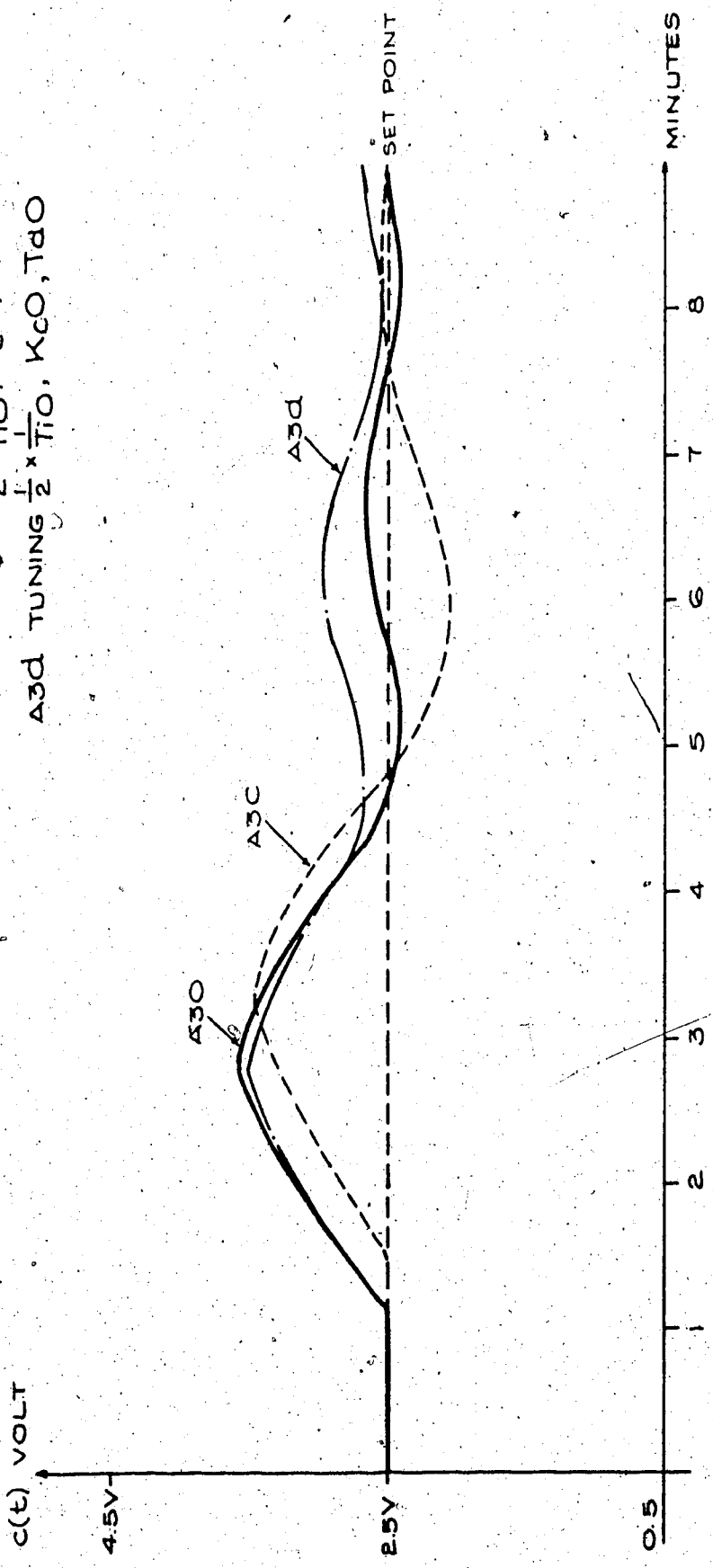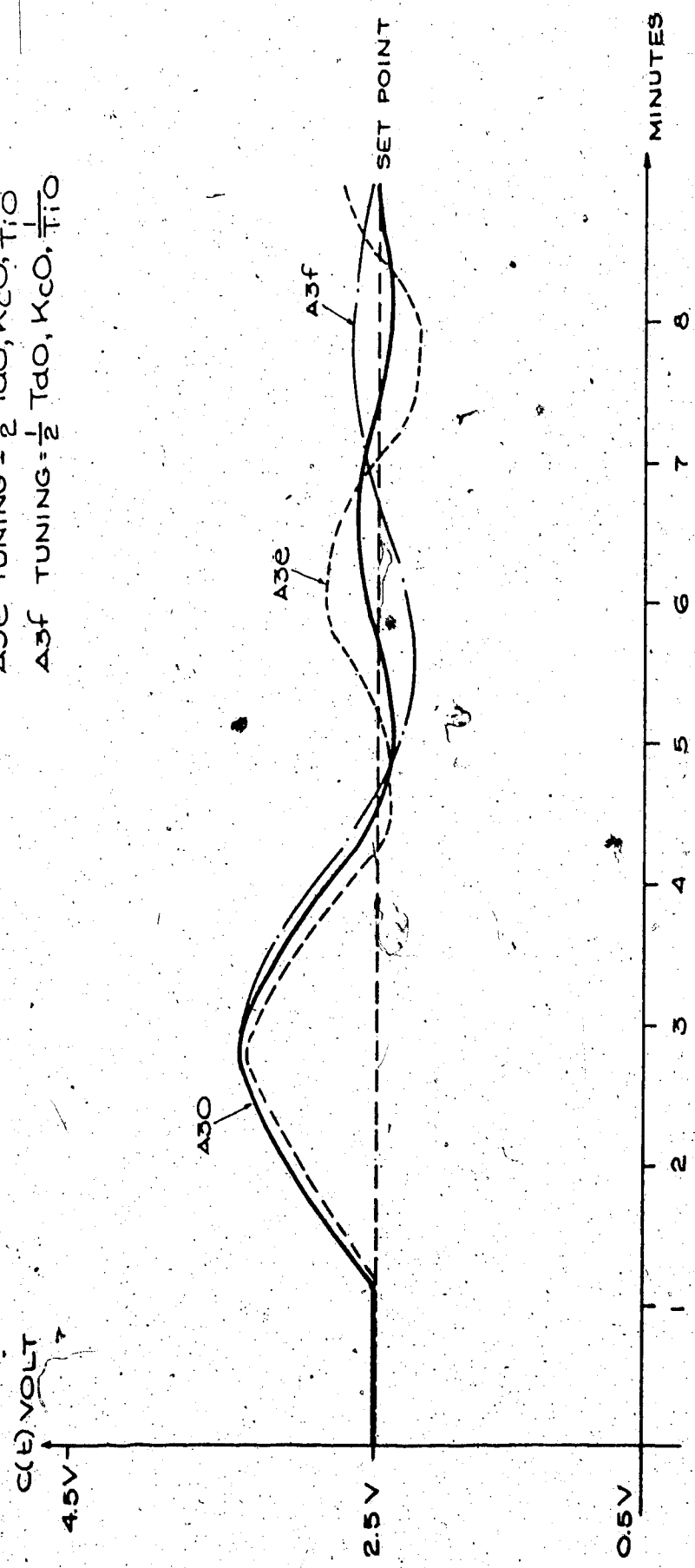
FIG. 5-10   COMPARISON OF OPTIMUM TUNING WITH ITS DEVIATIONS IN

Td FOR A FIRST ORDER PLANT WITH $\dfrac{\theta_0}{T}$, 0.8

PLANT : $\dfrac{Ke^{-\theta_0 S}}{\dfrac{S^2}{\omega_n^2} + \dfrac{2\xi S}{\omega_n} + 1}$

PERFORMANCE CRITERION : IAE

B10 TUNING : $K_{C}O, T_{d}O, \dfrac{1}{T_{i}O}$

B1a TUNING : $\dfrac{3}{2} K_{C}O, T_{d}O, \dfrac{1}{T_{i}O}$

B1b TUNING : $\dfrac{1}{2} K_{C}O, T_{d}O, \dfrac{1}{T_{i}O}$

c(t) VOLT

3.5V

B10

B1a

B1b

2.5V

SET POINT

1.5V

1   2   3   4   MINUTES

FIG 5-11   COMPARISON OF OPTIMUM TUNING WITH ITS
DEVIATIONS IN GAIN Kc FOR A 2ND ORDER
PLANT WITH $\theta_0 \omega_n = 1.1$ AND $\xi = 0.5$

PLANT : $\dfrac{Ke - \theta o S}{\dfrac{S^2}{\omega_n^2} + \dfrac{2\xi S}{\omega_n} + 1}$

PERFORMANCE CRITERION : IAE

BIO TUNING : $\dfrac{1}{TiO}$, KcO, TdO

BIC TUNING : $\dfrac{3}{2} \dfrac{1}{TiO}$, KcO, TdO

BId TUNING : $\dfrac{1}{2} \dfrac{1}{TiO}$, KcO, TdO

$C(t)$ VOLT

3.5V

2.5V

1.5V

BIO

BId

BIC

SET POINT

MINUTES
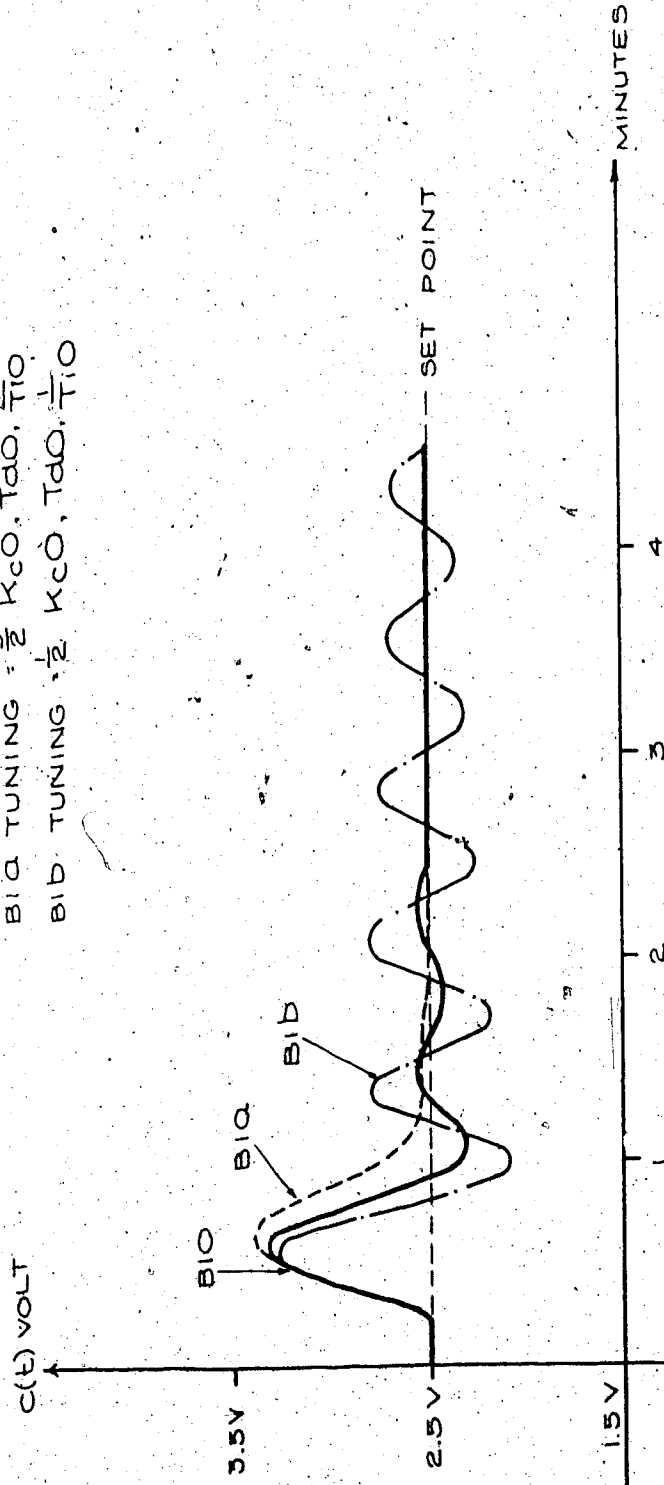
FIG 5-12   COMPARISON OF OPTIMUM TUNING WITH ITS DEVIATIONS IN Ti FOR A 2ND ORDER PLANT WITH $\theta o \omega_n = 1.1$ AND $\xi = 0.5$

PLANT : $\dfrac{Ke^{-\theta_0 S}}{\dfrac{S^2}{\omega_n{}^2} + \dfrac{2\xi S}{\omega_n} + 1}$

PERFORMANCE CRITERION : IAE

BIO TUNING T_dO, K_cO, $\dfrac{1}{T_iO}$

B1e TUNING $\dfrac{3}{2} T_dO$, K_cO, $\dfrac{1}{T_iO}$

B1f TUNING $\dfrac{1}{2} T_dO$, K_cO, $\dfrac{1}{T_iO}$

C(t) VOLT

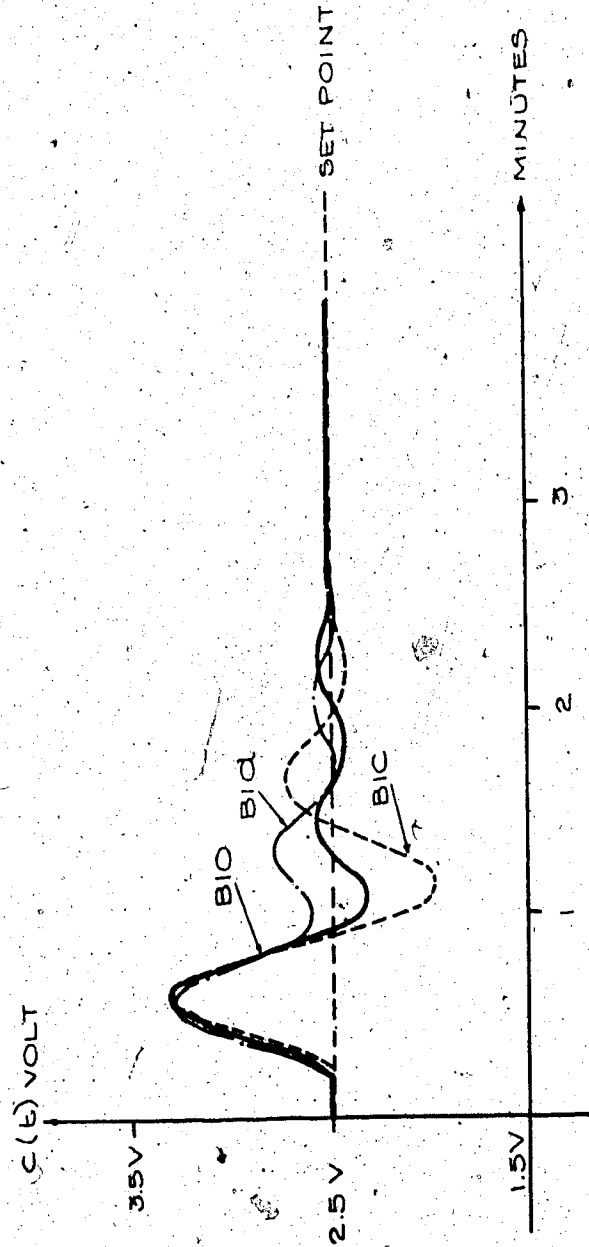3.5V

2.5V

1.5V

SET POINT

B1O

B1e

B1f

MINUTES

3

2

1

FIG 5-13   COMPARISON OF OPTIMUM TUNING WITH ITS
DEVIATIONS IN Td FOR A 2ND ORDER PLANT
WITH $\theta_0 \omega_n = 1.1$ $\xi = 0.5$.

PLANT. $\dfrac{Ke^{-\theta_o s}}{\dfrac{s^2}{\omega_n^2} + \dfrac{2\xi s}{\omega_n} + 1}$

PERFORMANCE, CRITERION = IAE

B2O TUNING = K_cO, T_dO, $\dfrac{1}{T_iO}$

B2a TUNING = $\dfrac{3}{2} \times K_cO$, T_dO, $\dfrac{1}{T_iO}$

B2b TUNING = $\dfrac{1}{2} \times K_cO$, T_dO, $\dfrac{1}{T_iO}$

c(t) VOLT

3.5 V

2.5 V

SET POINT

1.5 V

B2b
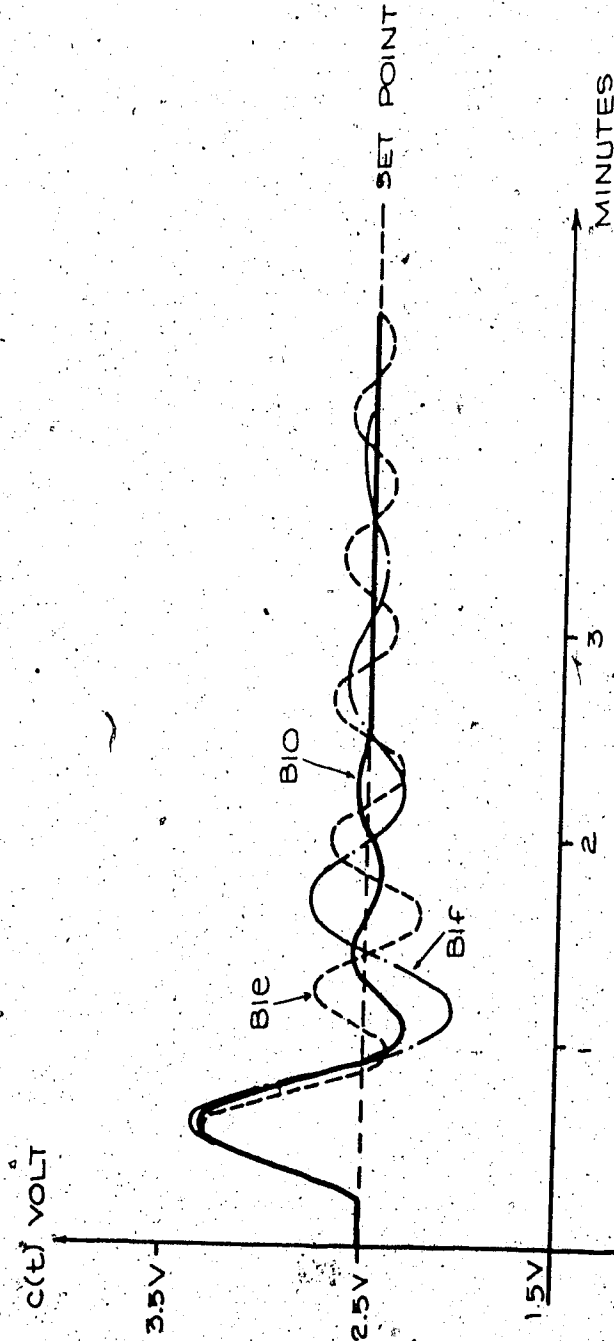
B2a

B2O

MINUTES

2   3

FIG 5-14   COMPARISON OF OPTIMUM TUNING WITH ITS
DEVIATIONS IN GAIN K_c FOR A 2ND ORDER
PLANT WITH $\theta_o \omega_n = 1.1$ AND $\xi = 1$.

$$\text{PLANT} = \frac{K_e\,\theta_0 S}{\frac{S^2}{\omega_n^2} + \frac{2\xi S}{\omega_n} + 1}$$

PERFORMANCE CRITERION = IAE

B2O TUNING = T_{io}, K_{co}, T_{do}

B2c TUNING = $\frac{3}{2} \times T_{io}$, K_{co}, T_{do}

B2d TUNING = $\frac{1}{2} \times T_{io}$, K_{co}, T_{do}

SET POINT

B2O
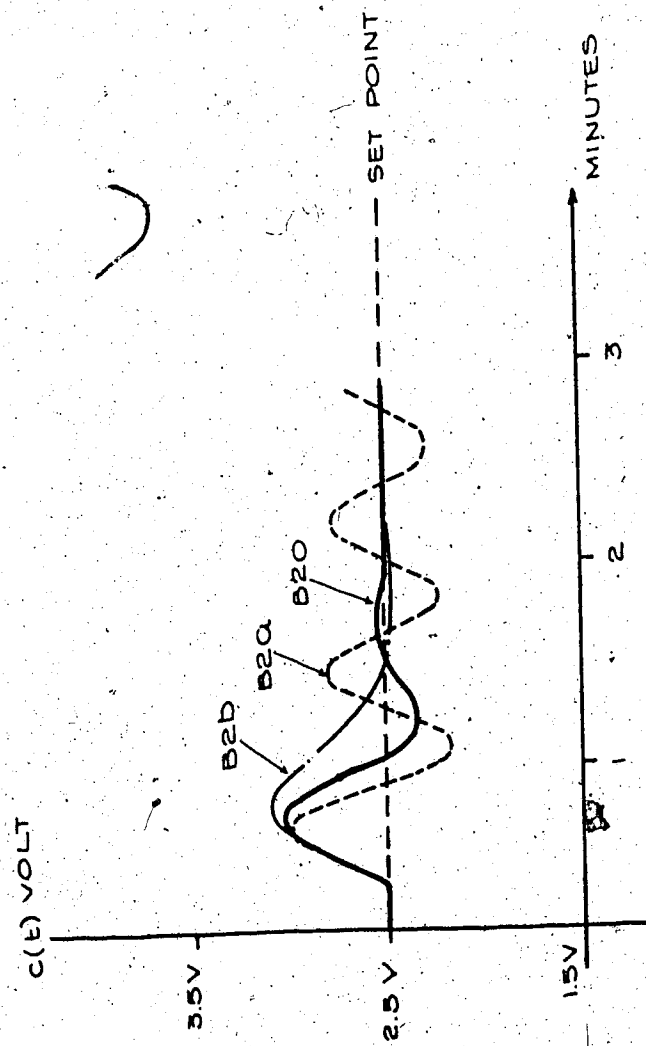
B2C

B2d

$c(t)$ VOLT.

3.5V

2.5V

1.5V

1   2   MINUTES

FIG 5-15   COMPARISON OF OPTIMUM TUNING WITH ITS DEVIATIONS IN T_i FOR A 2ND ORDER PLANT WITH $\theta_0\omega_n = 1.1$ AND $\xi = 1$.

88

PLANT $\frac{K_c \theta_o \cdot S}{\frac{S^2}{\omega_n^2} + \frac{2\xi S}{\omega_n} + 1}$

PERFORMANCE CRITERION = IAE

B2O TUNING = TdO, KcO, $\frac{1}{T_iO}$

B2e TUNING = $\frac{3}{2} \times$TdO, KcO, $\frac{1}{T_iO}$

B2f TUNING = $\frac{1}{2} \times$TdO, KcO, $\frac{1}{T_iO}$

FIG. 5-16   COMPARISON OF OPTIMUM TUNING WITH ITS DEVIATIONS IN Td FOR A 2ND ORDER PLANT WITH $\theta_o \omega_n \approx 1.1$ AND $\xi = 1$.

FIG 5-17   COMPARISON OF OPTIMUM TUNING WITH ITS
DEVIATIONS IN GAIN. K_C FOR A 2ND ORDER PLANT
WITH $\Theta_0 W_n = 4.0$ $\xi = 0.5$

$$Pl. T: \frac{K_c \cdot \theta_o S}{\frac{S^2}{\omega_n^2} + \frac{2\xi S}{\omega_n} + 1}$$

PERFORMANCE CRITERION: IAE

B3O TUNING: $\frac{1}{T_iO}$, K_cO, TdO

B3C TUNING: $\frac{3}{2} \times \frac{1}{T_iO}$, K_cO, TdO
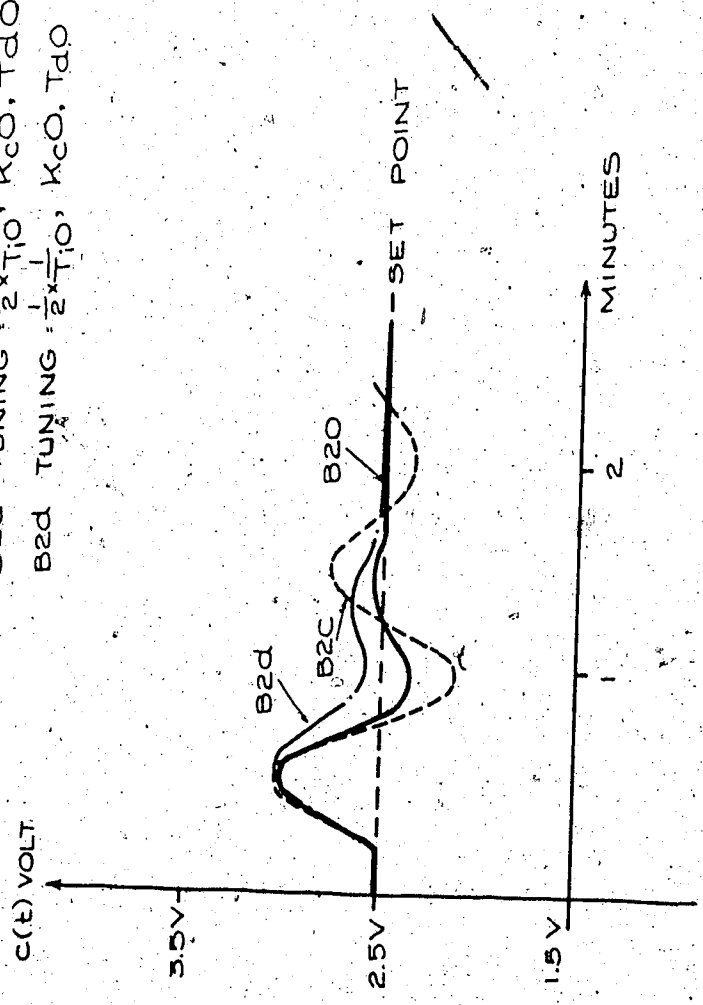
B3d TUNING: $\frac{1}{2} \times \frac{1}{T_iO}$, K_cO, TdO
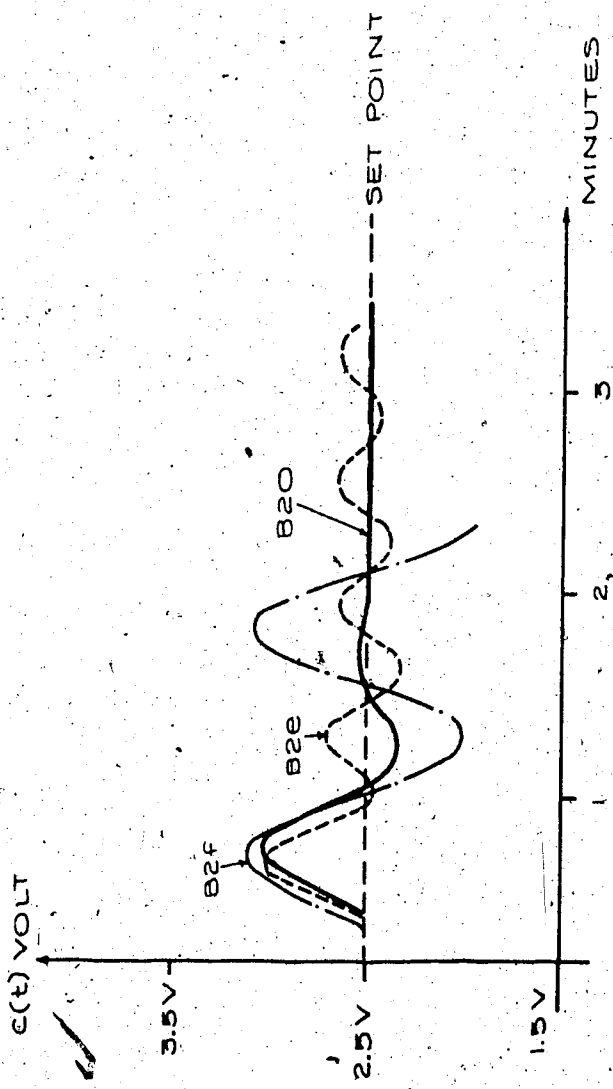
FIG 5.18 COMPARISON OF OPTIMUM TUNING WITH ITS DEVIATIONS IN T_i FOR A 2ND ORDER PLANT WITH θ_o $\omega_n=4$ AND $\xi=0.5$.

92

PLANT: $\dfrac{Ke \cdot \theta_0 S}{\dfrac{S^2}{\omega_n^2} + \dfrac{2\xi S}{\omega_n} + 1}$

PERFORMANCE CRITERION: IAE

B3O TUNING TdO, KcO, $\overline{T}_{iO}$

B3e TUNING $\frac{3}{2} \times$TdO, KcO, $\overline{T}_{iO}$

B3f TUNING $\frac{1}{2} \times$TdO, KcO, $\overline{T}_{iO}$

FIG. 5.19 — COMPARISON OF OPTIMUM TUNING WITH ITS DEVIATIONS, IN Td FOR A 2ND ORDER PLANT WITH θ_0 ω_n= 4.0
ξ, ξ=0.5

PLANT $\dfrac{Ke\theta_0 S}{\dfrac{S^2}{\omega_n^2} + \dfrac{2\xi S}{\omega_n} + 1}$

PERFORMANCE CRITERION : IAE

B4O TUNING = K_cO, TdO, $\dfrac{1}{TiO}$

B4a TUNING = $\dfrac{3}{2} \times K_cO$, TdO, $\dfrac{1}{TiO}$

B4b TUNING = $\dfrac{1}{2} \times K_cO$, TdO, $\dfrac{1}{TiO}$

FIG 5·20 · COMPARISON OF OPTIMUM TUNING WITH ITS DEVIATIONS IN GAIN K_c FOR A 2ND ORDER PLANT WITH $\theta_0 \omega = 4.0$ AND $\xi = 1$.

PLANT $\dfrac{Ke^{-\theta_o S}}{\dfrac{S^2}{\omega_n^2} + \dfrac{2\xi S}{\omega_n} + 1}$

PERFORMANCE CRITERION: $I\Delta E$

B4O TUNING $\dfrac{1}{T_iO}$, KcO, TdO

B4C TUNING $= \dfrac{3}{2} \times \dfrac{1}{T_iO}$, KcO, TdO

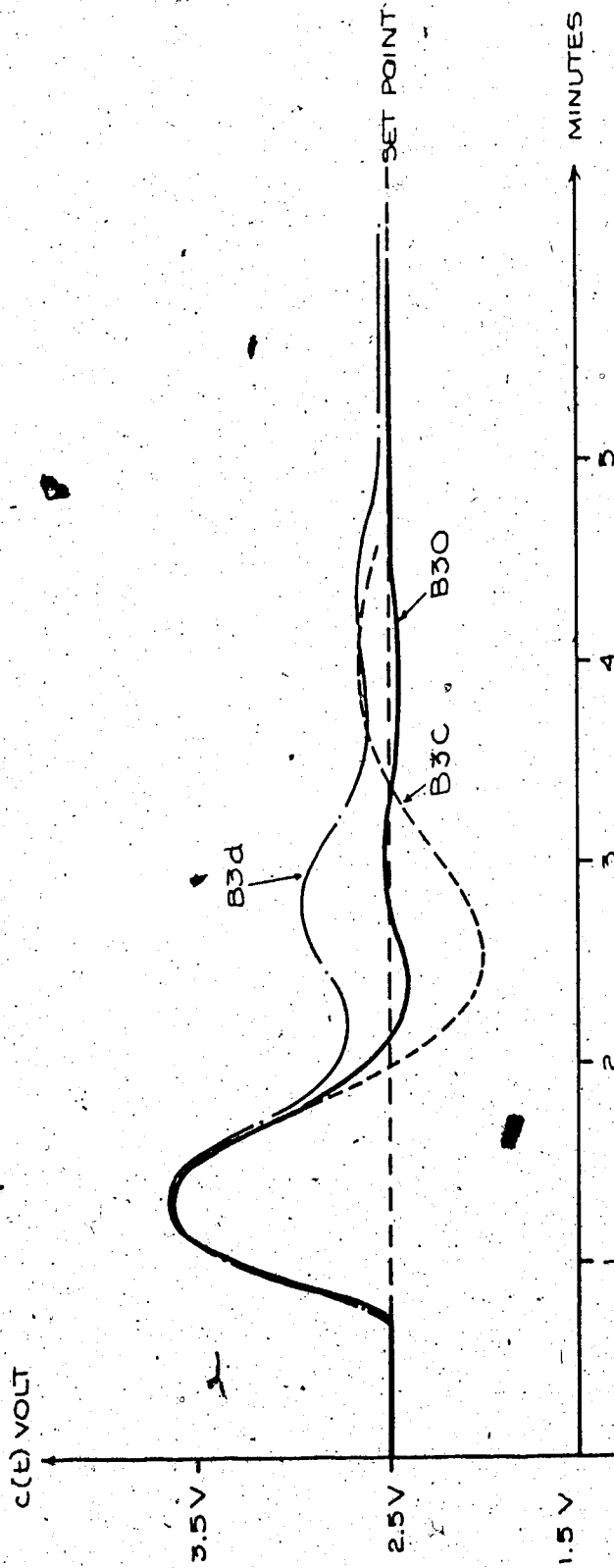B4d TUNING $= \dfrac{1}{2} \times \dfrac{1}{T_iO}$, KcO, TdO

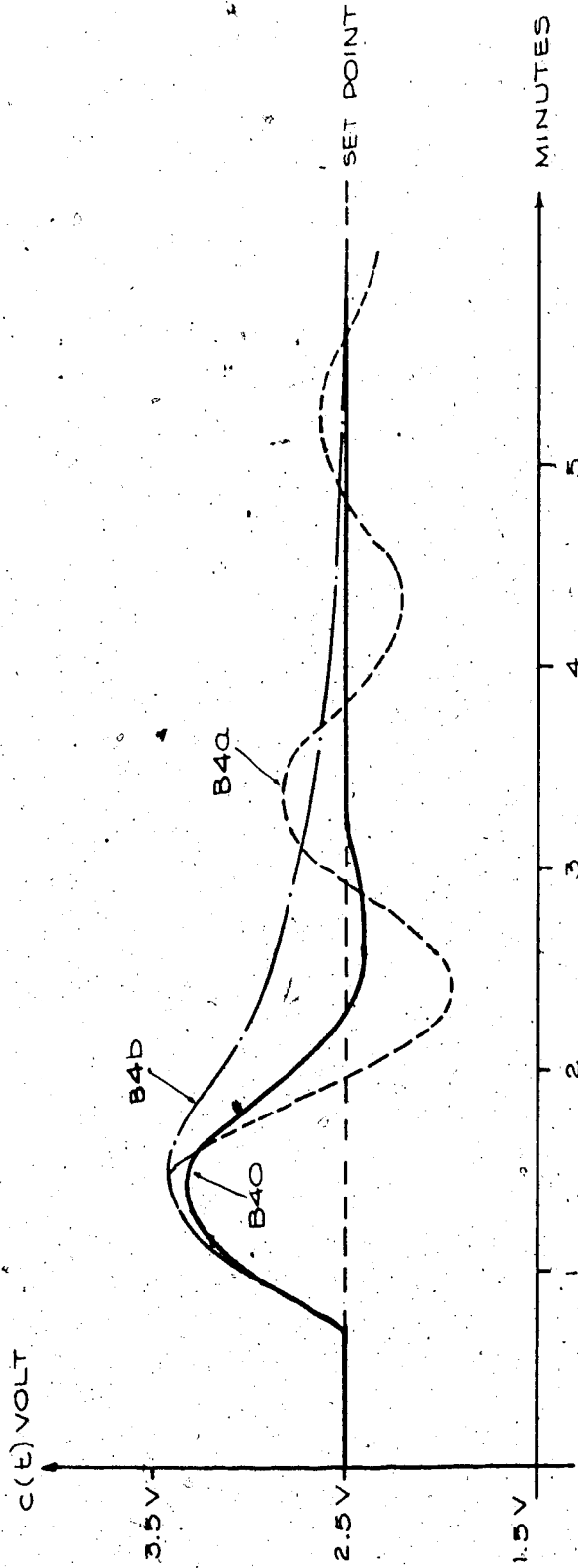FIG 5·21 COMPARISON OF OPTIMUM TUNING WITH ITS DEVIATIONS IN T_i FOR A 2ND ORDER PLANT WITH $\theta_o \omega_n = 4.0$ AND $\xi = 1$.

PLANT $\dfrac{Ke^{-\theta_0 S}}{\dfrac{S^2}{\omega_n^2} + \dfrac{2\xi S}{\omega_n} + 1}$

PERFORMANCE CRITERION : IAE

B4O TUNING $Td_O, K_CO, \dfrac{1}{T_{iO}}$

B4e TUNING $\dfrac{3}{2} Td_O, K_CO, \dfrac{1}{T_{iO}}$
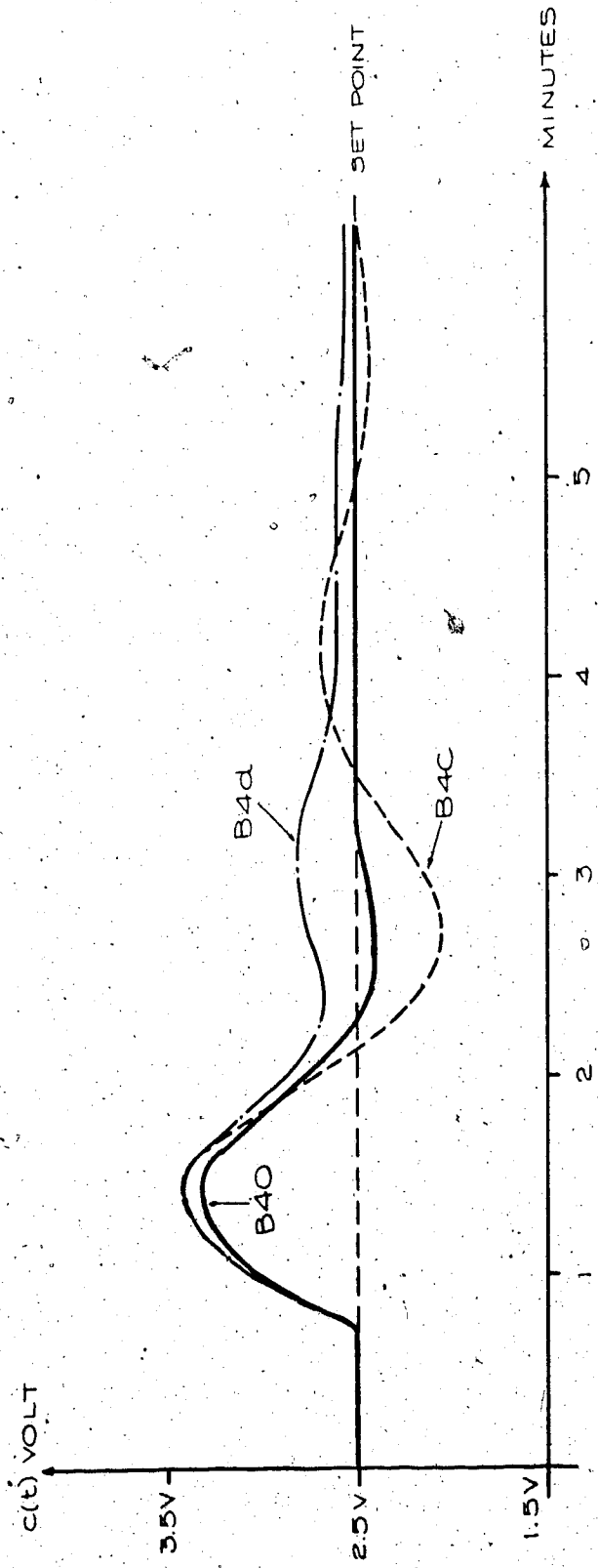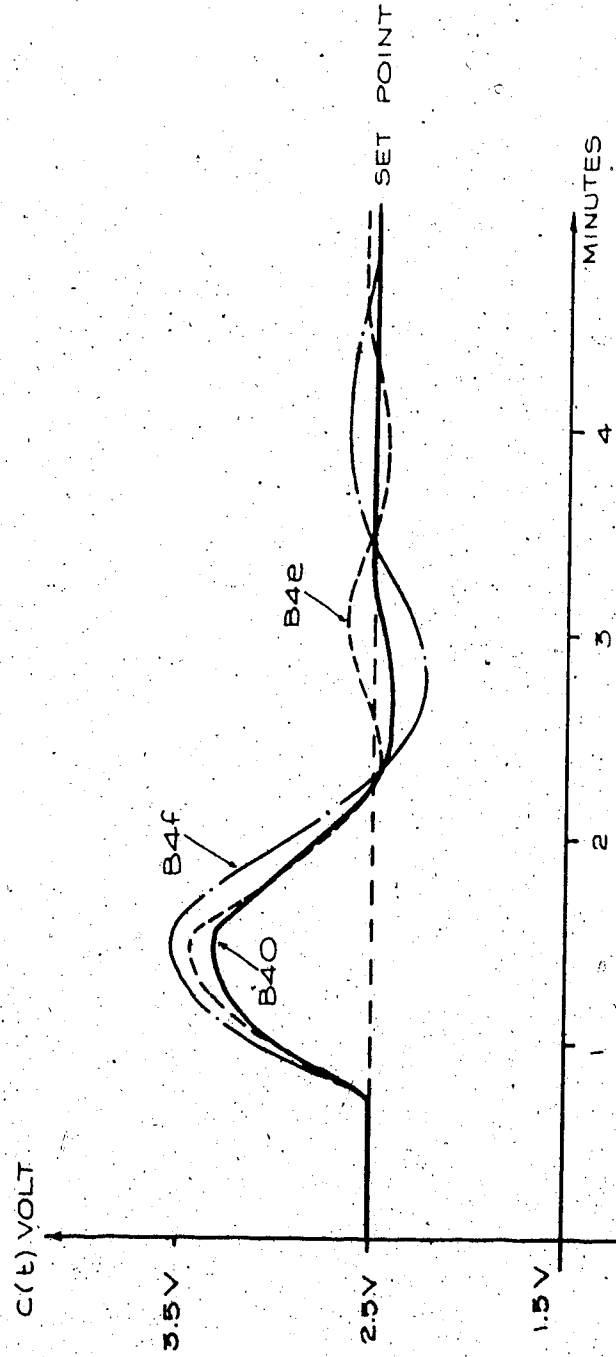
B4f TUNING $\dfrac{1}{2} Td_O, K_CO, \dfrac{1}{T_{iO}}$

FIG 5 - 22   COMPARISON OF OPTIMUM TUNING WITH ITS DEVIATIONS IN Td FOR A 2ND ORDER PLANT WITH $\theta_0 \omega_n = 4.0$, ξ, $\xi = 1$.

Test of reset inhibiting action

Extensive trial of reset inhibition was carried out. In figure 5-23 the responses of a particular first order plant with dead time under a set point change are shown. Between the two curves, one is under the effect of reset inhibition.

It is obvious from figure 5-23 that the designed controller has an excellent reset inhibiting feature.

Extreme situations were also tried. With $KK_c = 2$, $\frac{1}{T_i} = 10$ repeats /minute and $T_d = 0$ minutes, the same first order plant in figure 5-23 was put under a set point change and reset inhibition. Overshoot was found in the response. This was because of the extremely high value of $\frac{1}{T_i}$. Even when error started to diminish, the integrator still charged up fast enough to cause an overshoot.

However, an extreme parameter combination like this case is unlikely to happen in real situations. The purpose of integral action is to provide offset free on-line control. Its capacity to cancel offset is determined by the integrator output range instead of the integral time: T_i. The parameter $\frac{1}{T_i}$ only determines the integrator's speed to acquire its offset cancelling capacity. With critical processes such as batch sintering, batch brazing, diffusion, crystal growing etc., manual start up (very slow) is used to avoid overshoot. This suggests the speed to arrive at steady state is of lower priority than to avoid overshoot.

PLANT $\quad \dfrac{Ke - \theta_0 S}{\tau_S + 1}$
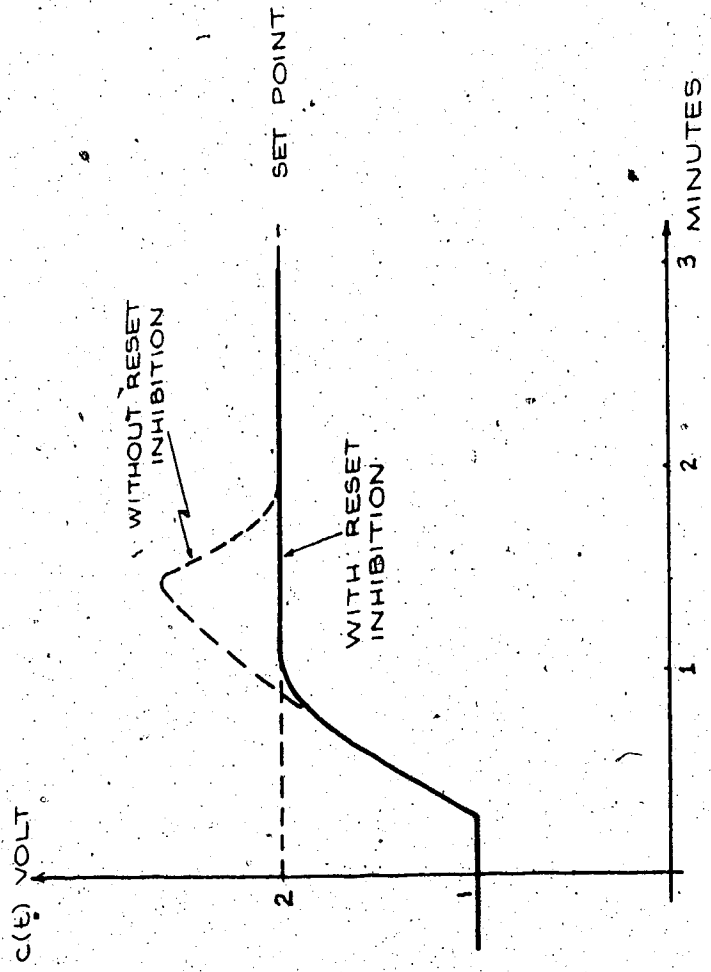
MODE OF CONTROL - PID

FIG 5-23 THE RESPONSE OF A 1st ORDER PLANT WITH DEAD TIME AND THE EFFECT OF RESET INHIBITING.

Therefore, when reset inhibition is needed, it is recommended to have the parameter $\frac{1}{T_1}$ set towards lower values. The relationship between K_c, T_d and T_1 for an optimum control under reset inhibition, is complicated enough to warrant another investigation.

Test of bumpless transfer

Various processes were allowed to come to steady state under manual control. With the set point value set equal to output value $c(t)$, the control was suddenly returned to automatic. The resultant responses observed were bumpless.

Conclusion

The objective to build a near ideal PID controller was achieved with negligible interrelationship between the three parameters. The PID algorithm adopted in the design was exactly the same algorithm which A.M. Lopez used for his optimum tuning study. Hence, Lopez's optimum tuning graphs can be readily applicable to this particular PID controller. As the three parameters are practically independent of each other, tuning the controller becomes a straightforward task. The recordings in figure 5-2 to 5-22 proved that this controller, when used in conjunction with the optimum tuning graphs, produces superior responses than those supposedly non optimally tuned results.

The low drift integrated circuits used in this design, make it possible to abandon the DC to AC and AC to DC processing of signal as was necessary in the old days.

The reset inhibiting feature is very satisfactory except in extreme cases. But as explained in the previous section, most of the

time these extreme cases do not exist. A lower $\frac{1}{T_i}$ value can always circumvent this problem without impairing the controller capability. The reset inhibiting feature is expected to increase this controller's versatility.

The manual control functions properly. The transfer from manual to automatic control is always bumpless. Other features such as selected meter read-out, analog and digital set point adjustment, power supply indicators, etc. are all meant to increase the convenience in using this unit.

References

1. L.M. Zoss, B.C. Delahooke, "Theory and applications of industrial process control", Delmar Publishers, Inc.

2. J.G. Ziegler, N.B. Nichols, "Optimum settings for automatic controllers." Transactions of the A.S.M.E. Nov., 1942.

3. J.S. Anderson, "Optimal Controller Adjustment" Instrument Practice. Sept., 1970.

4. A.M. Lopez, P.W. Murill, C.L. Smith, "Tuning P.I. and P.I.D. Digital Controllers." Instruments and Control Systems, Feb., 1969.

5. M. Athans, "On the Design of P.I.D. Controllers Using Optimal Linear Regulator Theory." Automatica, Vol. 7, 1971.

6. A.M. Lopez, "Optimization of System Response." Ph.D. Dissertation, Louisiana State University, 1968.

7. C.J. Swartwout, "An Electronic Approach to Process Control." Instruments, Vol. 26, 1953.

8. Handbook of Automation, Computation and Control. Vol. 3, Section D. John Wiley and Sons Inc., 1961.

9. M. Athans, P.L. Falb, "Optimal Control." McGraw Hill, New York, 1966.

10. Ogata , "Modern Control Engineering", Prentice Hall, Inc., 1970.

11.   K.T. Parker, "Design of Proportional Integral and Derivative Controllers by the use of Optimal-Linear-Regulator Theory. Proc. IEEE, Vol. 119, No. 7, July 1972.

12.   G.F. Ohlson, "Reset Inhibiting Improves Control." Instrument and Control Systems, May 1965.

13.   T.L. Magliozzi, "Control System Prevents Surging in Centrifugal-flow Compressors." Chemical Engineering, May 8, 1967.

14.   Fisher Controls, "TL101 Process Controller, Installation and Operation Instruction." Form 4081, Nov. 1972.

15.   ITT Barton Co., "Trutrac Process Controller: Models A2DA, A2RA and A2CA" Barton Product Bulletin 4110/DB1-1, 4110/DB2.

16.   Burr Brown, "Operational Amplifiers, Design and Applications". McGraw-Hill, 1971. Editors: Tobey ; Graeme and Huelsman

17.   J.A. Miller, A.M. Lopez, O.S. Smith, P.W. Murill, "A Comparison of Controller Tuning Techniques." Control Engineering, Dec. 1967.

18.   P.W. Murill, C.L. Smith, "The Adjustments of Controllers." Louisiana State University, Technical Report, THEMIS-LSU-T-TR-19.

19.   P.W. Murill, "Automatic Control of Process." International Textbook Company, 1967.

20.   D.A. Spitz, "Optimal Process Control of a Single Variable." Instrument and Control Systems, Aug. 1968.

21.   J.M. Meyer, "Short-cut Process Response Approximation."

          Louisiana State University, Research Report.

22.   D. Graham, R.C. Lathrop, "The Synthesis of Optimum Transient

          Response: Criterion and Standard Form." Trans. AIEE

          Vol. 72, Nov. 1953.

23.   G.A. Bekey, "Optimization of Multiparameter Systems by

          Hybrid Computer Techniques." Part I and II Simulation,

          February and March 1964.

24.   A.M. Lopez, J.A. Miller, O.S. Smith, P.W. Murill,

          "Tuning Controllers with Error Integral Criteria"

          Instrumentation Technology Nov. 1967.

25.   O'Connor and Denn, "Three Mode Control as an Optimal

          Control", Chemical Engineering Science 1972, Vol. 27

          pp. 121-127.

26.   M.R. Chidambara, "Chemical Process Control - A Technique

          for Adaptive Tuning of Controllers", International

          Journal of Control, 1970, Vol. 12, No. 6, pp. 1057-1074.

Level detector with Hysterisis

The circuit of the level detector with hysteresis is shown
in figure AI-1.

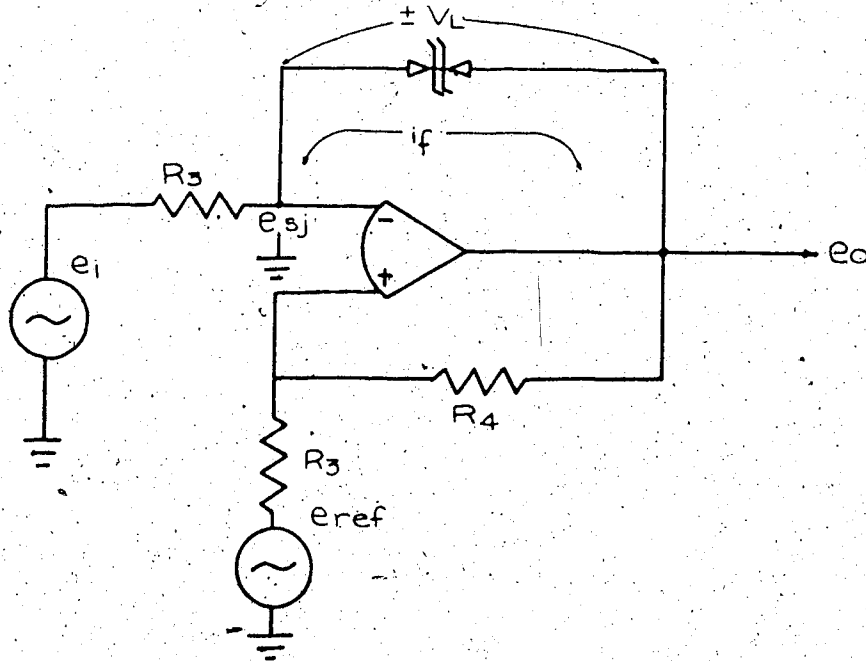

Figure AI-1 Level detector with hysteresis

The output voltage,

$$e_o = \pm V_L + e_{sj} \tag{1}$$

But

$$e_{sj} = \frac{(e_o - e_{ref})}{R_4 + R_3} \times R_3 + e_{ref} \tag{2}$$

Substitute equation 1 into equation 2

$$e_{sj} = \frac{(\pm V_L + e_{sj} - e_{ref})}{R_4 + R_3} R_3 + e_{ref}$$

or

$$e_{sj} = \pm V_L \frac{R_3}{R_4} + e_{ref} \qquad (3)$$

Substitute equation 3 into equation 1

$$e_o = \pm V_L \pm V_L \frac{R_3}{R_4} + e_{ref}$$

Or

$$e_o = \pm V_L \left(\frac{R_4 + R_3}{R_4}\right) + e_{ref} \qquad (4)$$

Initially, if e_i is smaller than e_{sj}, the current i_f will flow from e_o towards e_{sj} and e_i. V_L under this situation will take on a positive sign. Using equation 3:

$$e_{sj} = + V_L \frac{R_3}{R_4} + e_{ref}$$

and

$$e_o = + V_L \left(\frac{R_4 + R_3}{R_4}\right) + e_{ref} \qquad (5)$$

If e_i grows and exceeds the value $e_{sj} = + V_L \frac{R_3}{R_4} + e_{ref}$, the current i_f will reverse its direction and V_L will take on a negative sign. In other words,

$$e_{sj} = - V_L \frac{R_3}{R_4} + e_{ref}$$

$$e_o = - V_L \left(\frac{R_3 + R_4}{R_4}\right) + e_{ref} \qquad (6)$$

From this moment on, so long as e_i is greater than the value e_{sj} ($e_{sj} = - V_L \frac{R_3}{R_4} + e_{ref}$), the output will remain at the value of

$$- V_L \left(\frac{R_4 + R_3}{R_4}\right) + e_{ref}.$$

If e_i varies its direction and becomes less than e_{sj}

$(-V_L \frac{R_3}{R_4} + e_{ref} = e_{sj})$, the output e_o will switch back to the value:

$+ V_L \left(\frac{R_4 + R_3}{R_4}\right) + e_{ref}.$ So long as e_i is smaller than $+ V_L \frac{R_3}{R_4} + e_{ref}$,

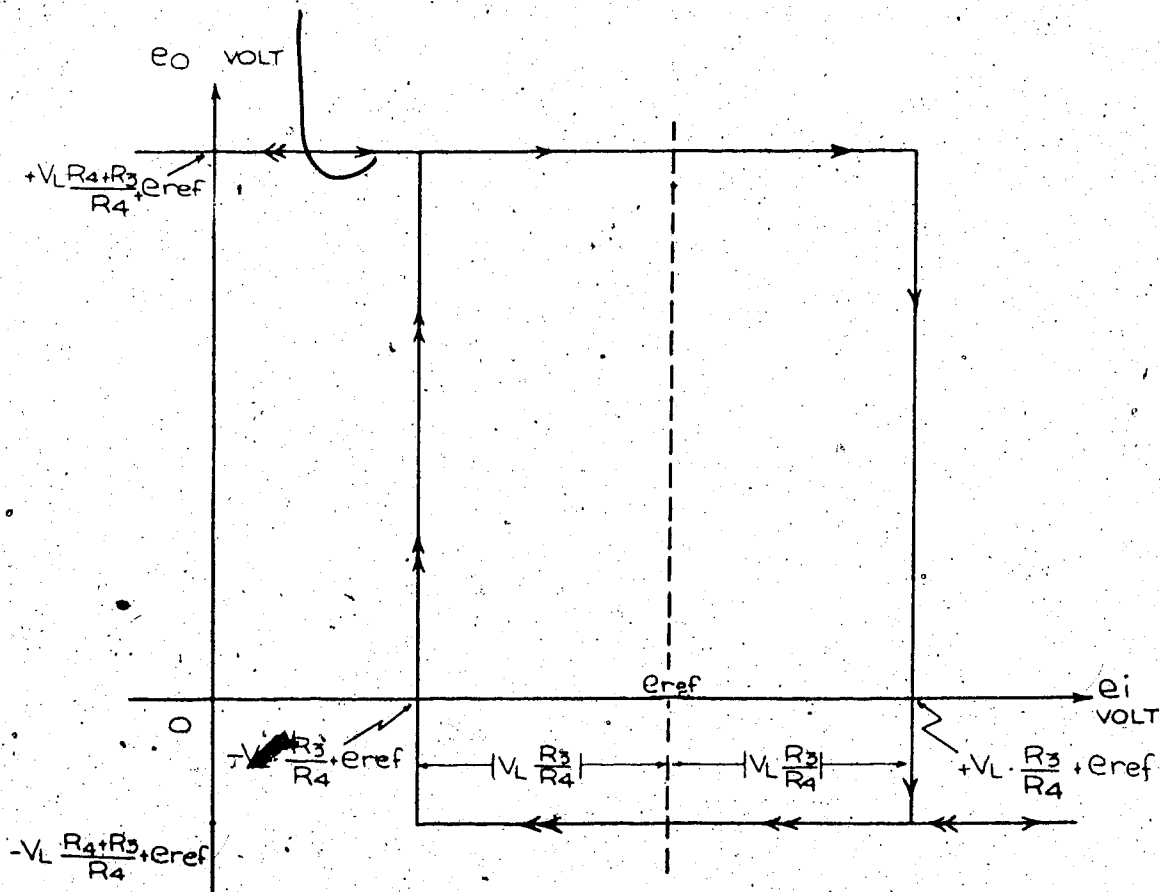the output value will remain the same. The complete situation is

depicted in figure AI-2.

Figure AI-2 Voltage output versus voltage input of the

level detector circuit with hysterisis

Figure AI-2 shows that the value $\left| V_L \frac{R_3}{R_4} \right|$ is actually a threshold

level. The value e_i has to exceed e_{ref} plus or minus this threshold

level, in order to enable a change of state. Once the state is

changed, the output will be kept in that state, unless e_i reverses its direction and exceeds the opposite threshold point. With this hysterisis, the changes of states at the output will be the results of substantial changes of e_i. Noise and errors of values smaller than the threshold will not cause unwanted changes of state.

One special case of this circuit occurs when the reference voltage e_{ref} equals zero. The circuit becomes a zero crossing detector with hysterisis. Its voltage output and input is shown in figure AI-3.
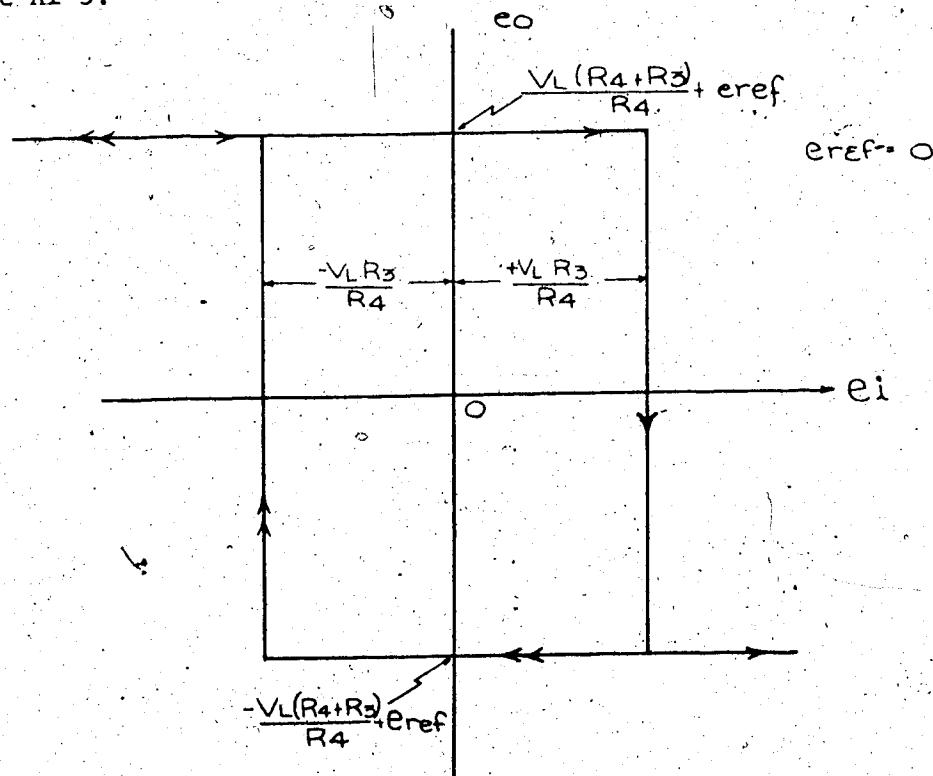

$$\frac{V_L(R_4+R_3)}{R_4} + e_{ref}$$

$e_{ref} = 0$

$$\frac{-V_L R_3}{R_4}$$

$$\frac{+V_L R_3}{R_4}$$

$$\frac{-V_L(R_4+R_3)}{R_4} + e_{ref}$$

Figure AI-3 e_o vs. e_i of the zero crossing detector

with hysterisis

Note the symmetry in figure AI-3. The two states of output e_o are equal in magnitude but opposite in sign. This symmetrical output e_o

can be used as logic commands on symmetrical COS-MOS switches such as RCA's CD4016.

In general, when e_{ref} does not equal zero, unsymmetrical output will occur in figure AI-2. If a symmetrical output is needed one can use a special circuit to transform the output in figure AI-2 into a symmetrical one. This transforming circuit is simply a voltage amplifier with voltage limiters. It is shown in figure AI-4.
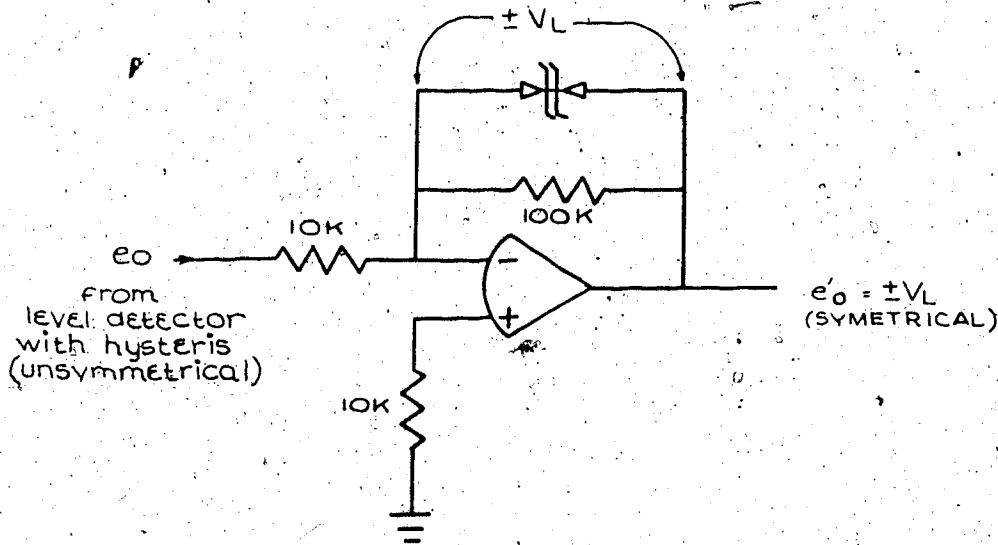

Figure AI-4 Transforming an unsymmetrical signal into

a symmetrical one

Appendix II

The Generation of Dead Time

If a signal x(t) passes through a device which is nothing but a pure time delay generator, then the output y(t) should be exactly the same as input x(t), only delayed by θ_o units of time. This situation is depicted in figure AII-1.
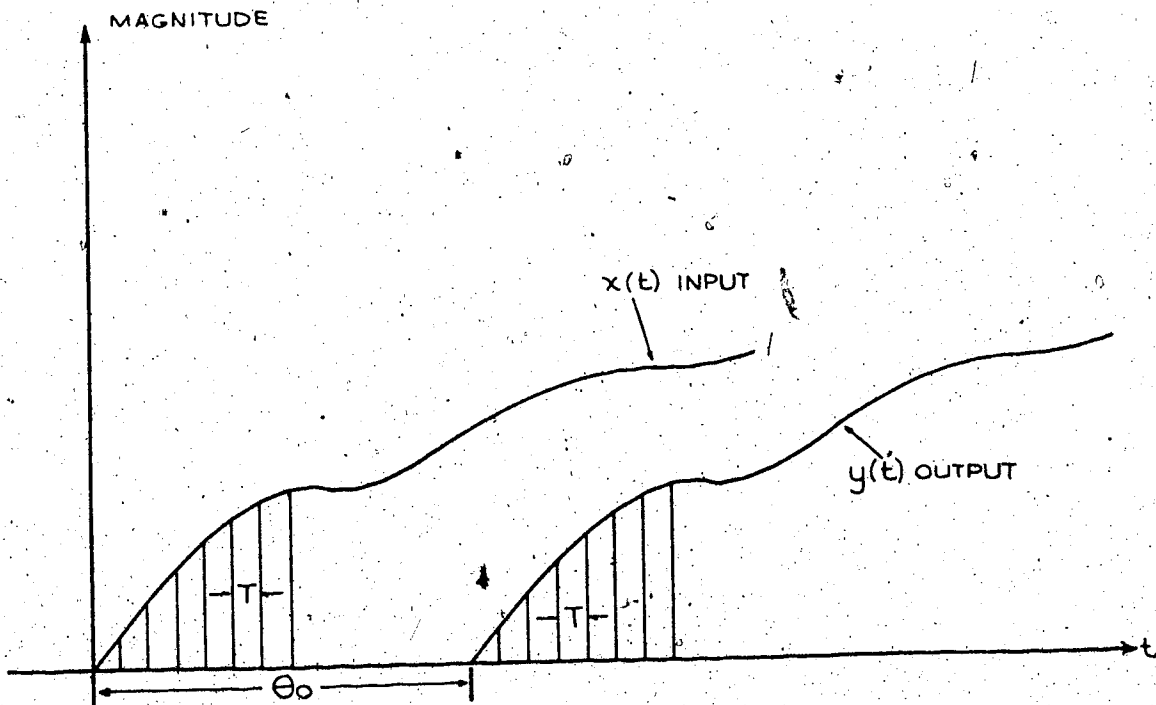

Figure AII-1 $y(t) = x(t-\theta_o)$, T= sampling period

$$\theta_o = 3072 \times T$$

This pure time delay generator can be simulated as in figure AII-2:
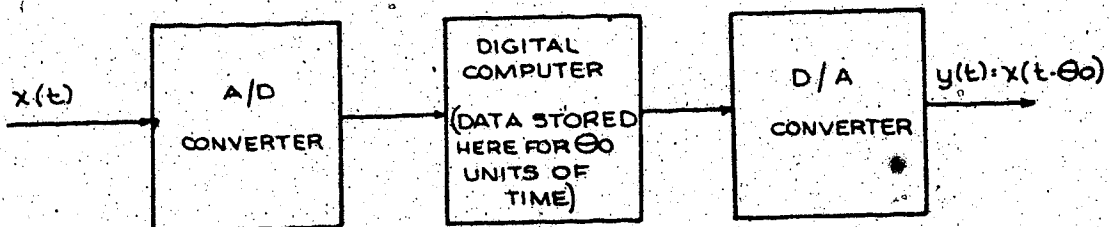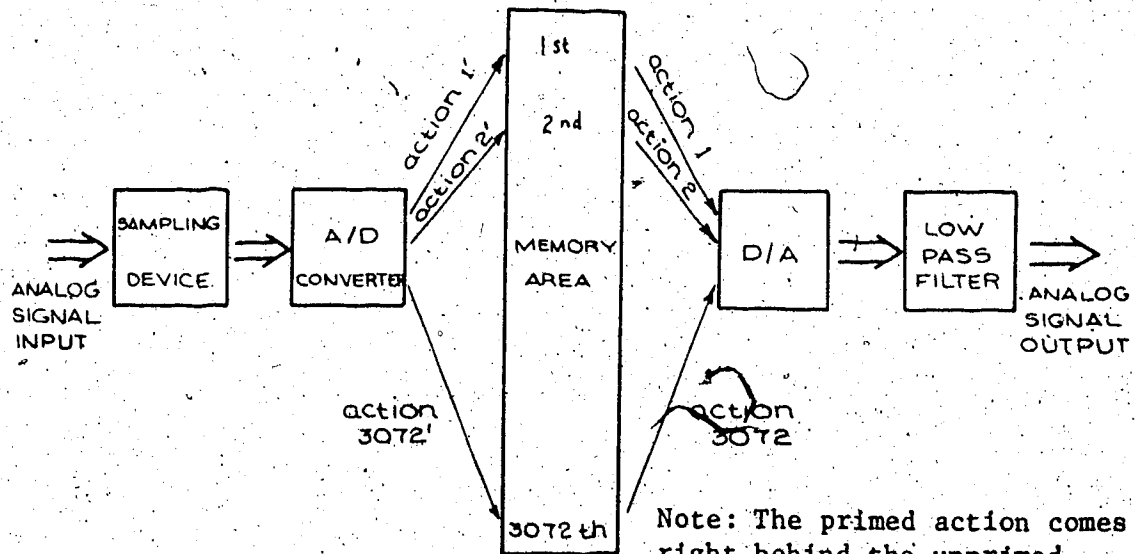

Figure AII-2 A simulated pure time delay generator

The control of the dead time delay generator is done by a computer

program. At the starting point, the control program will clear all

the core content in a specified memory area. Then, starting from

the first address in that memory area, the program brings out the

content of that address. The content is converted to an analog

signal and sent out as output $y(t)$. Since the contents of the

memory is cleared initially, $y(t)$ is zero at this instant. Next,

the program will command the A/D converter to bring in the first

sample of input $x(t)$ in digital format. This first sample of input

is subsequently stored into the first address of the memory area.

After this, the program will wait for "T" seconds, before it repeats

the above sequence for address number two. The total number of

addresses in the specified memory area is 3072. When the program

comes to the last address (the 3072th address), T x 3072 seconds have

elapsed. Then the program will go back to the first address and send

out its content. However, the content in the first address is actually

the input signal sampled at T x 3072 seconds ago. The program will

run through the memory area repeatedly. If θ_o is specified, the

value of "T" can be programed in such a way that T x 3072 equals θ_o

units of time. In other words, for any θ_o value, one should sample it

into 3072 intervals. The number 3072 is three quarters of the total

memory address in a 4K PDP8 computer. Also, it is an extremely high

rate of sampling for this particular purpose where θ_o usually

exceeds tens of seconds. The flow and format of information is shown

in figure AII-2.

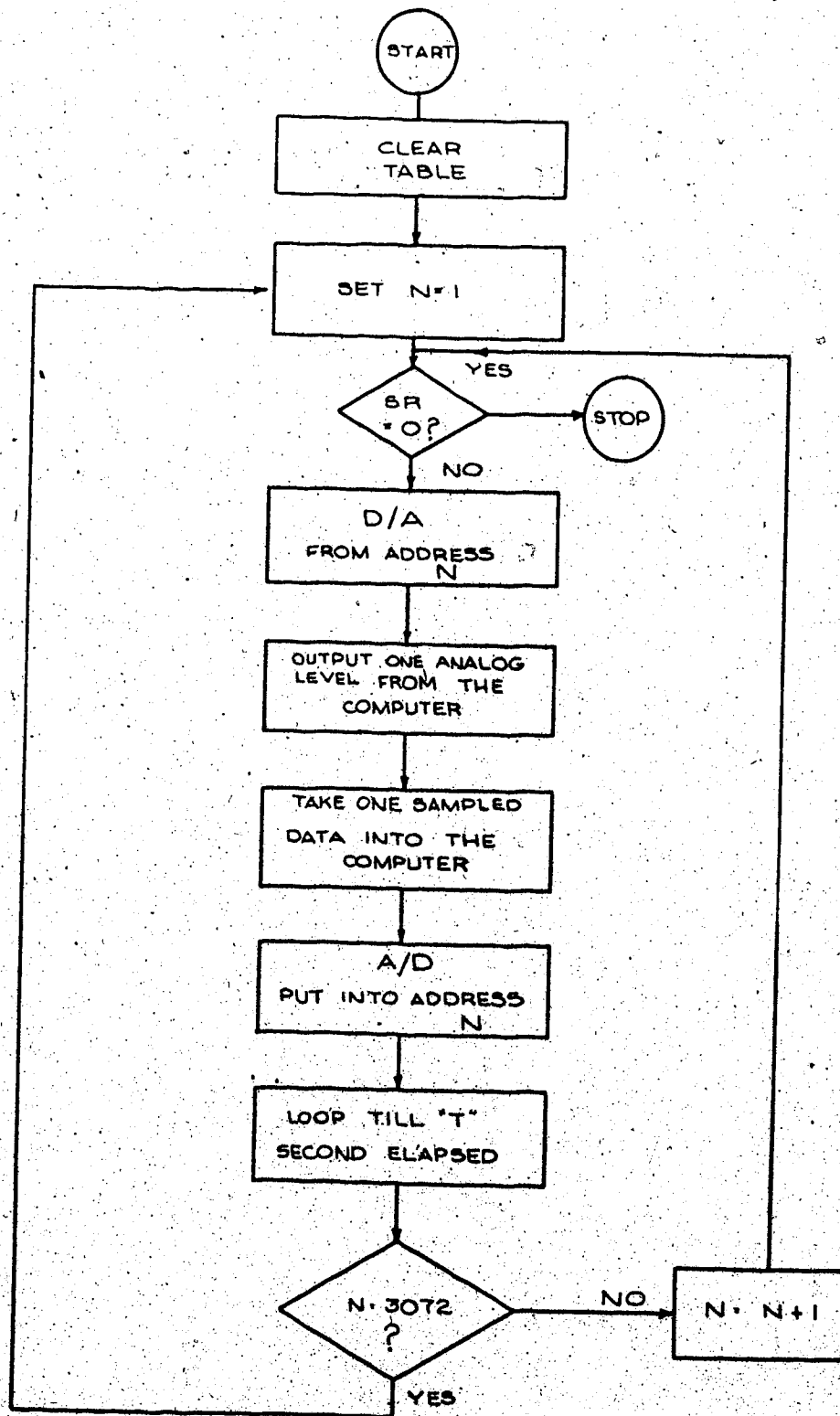Figure AII-2 The flow and format of information in

a pure time delay generator

FIG AII-3 The flow chart for a dead time delay program.

```
ATOD      0231
CLEAR     0200
CONST     0267
COUNT     0270
DACHN     0272
DTOA      0220
IMDEX     0011
INDEX     0010
KONST     0273
KONST1    0274
KOUNT     0275
KOUNT1    0276
LOPI      0250
NINDE     0266
NULO      0210
OLOP      0217
TABLE     1000
TEST      0260
TTABLE    0271
```

```
                    *10
0010    0000    INDEX,  0
0011    0000    IMDEX,  0
                    *200
0200    7300    CLEAR,  CLA CLL
0201    1267            TAD CONST
0202    3270            DCA COUNT
0203    1271            TAD TTABLE
0204    3010            DCA INDEX
0205    3410            DCA I INDEX
0206    2270            ISZ COUNT
0207    5205            JMP .-2
0210    1271    NULO,   TAD TTABLE
0211    3010            DCA INDEX
0212    1271            TAD TTABLE
0213    3011            DCA IMDEX
0214    7300            CLA CLL
0215    7404            OSR
0216    3274            DCA KONST1
0217    7300    OLOP,   CLA CLL
0220    1410    DTOA,   TAD I INDEX
0221    6462            6462
0222    6464            6464
0223    7200            CLA
0224    1272            TAD DACHN
0225    6451            6451
0226    6454            6454
0227    6441            6441
0230    5227            JMP .-1
```

```
0231   7300   ATOD,    CLA CLL
0232   1272            TAD DACHN
0233   6412            6412
0234   6421            6421
0235   6433            6433
0236   6411            6411
0237   5236            JMP .-1
0240   6421            6421
0241   6422            6422
0242   6411            6411
0243   5242            JMP .-1
0244   6421            6421
0245   7200            CLA
0246   6434            6434
0247   3411            DCA I IMDEX
0250   1273   LOPI,    TAD KONST
0251   3275            DCA KOUNT
0252   1274            TAD KONST1
0253   3276            DCA KOUNT1
0254   2276            ISZ KOUNT1
0255   5254            JMP .-1
0256   2275            ISZ KOUNT
0257   5252           ~JMP .-5
0260   7300   TEST,    CLA CLL
0261   1010            TAD INDEX
0262   1266            TAD NINDE
0263   7440            SZA
0264   5217            JMP OLOP
0265   5210            JMP NULO
0266   1001   NINDE,   1001
0267   2000   CONST,   2000
0270   0000   COUNT,   0
0271   0777   TTABLE,  TABLE-1
0272   0001   DACHN,   0001
0273   7774   KONST,   7774
0274   0000   KONST1,  0
0275   0000   KOUNT,   0
0276   0000   KOUNT1,  0
              *1000
1000   0000   TABLE,   0
```

OPTIMAL TUNING GRAPHS BASED ON INTEGRALS OF ERROR CRITERIA

A.M. Lopez in his Ph.D. dissertation had set up a multi-parameter optimization program to find out the optimum settings of a controller for particular control loops under specified performance criterion.

The performance criteria chosen were of the integral of error type. The plants chosen could be either first order plant with dead time delay or second order plant with dead time delay. The multiparameter optimization technique used was a modified steepest ascent method known as optimum gradient [23].

Both the control loop simulation and the optimization program were carried out on an IBM 7040 digital computer. The result was a set of tuning relationship graphs and equations.

For a first order plant with dead time delay:

$$G(S) = \frac{K\,e^{-\theta_o S}}{\tau S + 1}$$

the optimum PID controller settings for ISE, IAE and ITAE performance criteria are shown in figure AIII-1. In addition, equations in table AIII-1 were developed to fit the curves in figure AIII-1. For a second order plant with dead time delay:

$$G(S) = \frac{K\,e^{-\theta_o S}}{\dfrac{S^2}{\omega_n^2} + \dfrac{2\xi S}{\omega_n} + 1}$$

the optimum PID controller settings for ISE, IAE and ITAE performance criteria are shown in figure AIII-2 to figure AIII-10.

For the optimum controller settings for one mode and two

mode controlling and the computer programs please refer to A.M. Lopez's

Ph.D. dissertation [6].

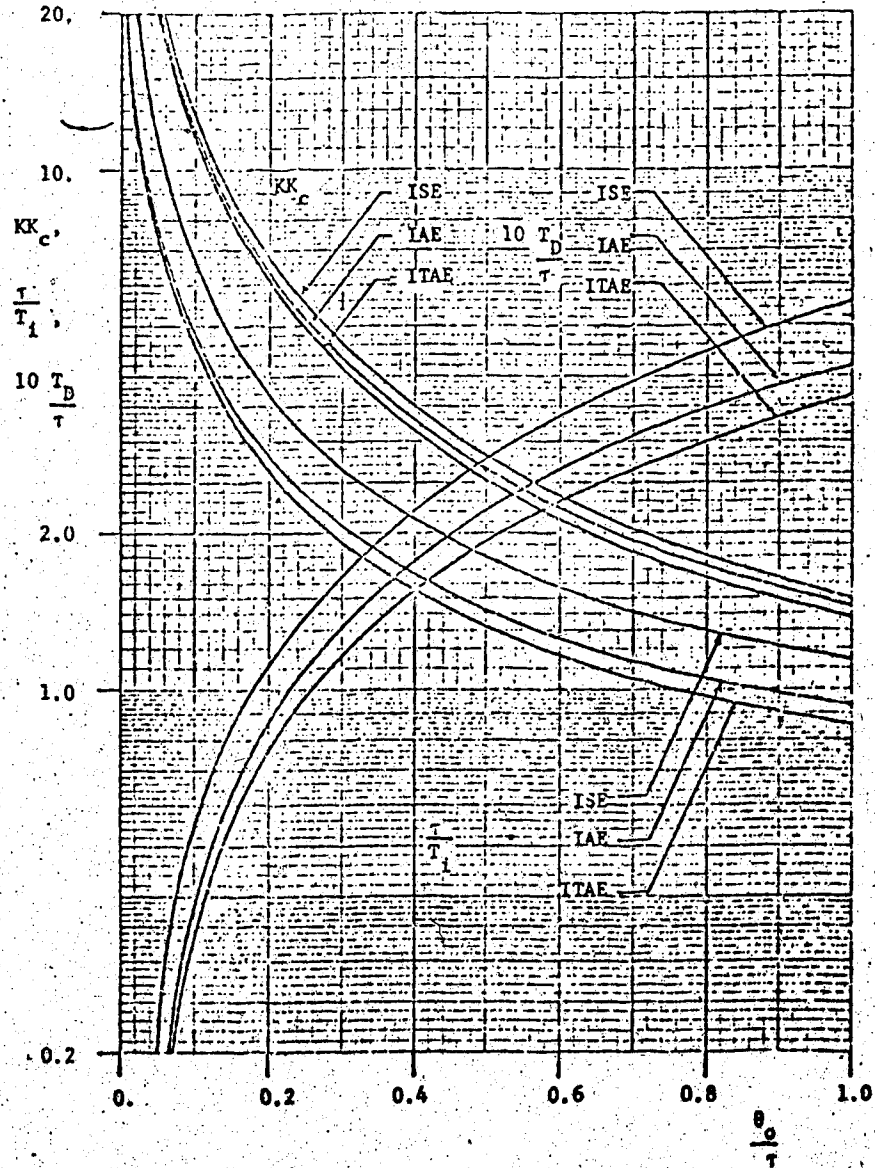All graphs and tables in this Appendix are extracted for A.M. Lopez's Ph.D.

thesis.

Figure AⅢ-1   PID Controller Settings to Minimize Error Integrals.

TABLE A III - 1

Tuning Equations for PID Controllers.

Controller Algorithm:

$$m(t) = K_c \left(1 + \frac{1}{T_i P} + T_D P\right) e(t)$$

Tuning Equations:

$$KK_c = a\left(\frac{\theta_o}{\tau}\right)^b$$

$$\frac{T}{T_i} = c\left(\frac{\theta_o}{\tau}\right)^d$$

$$\frac{T_D}{\tau} = e\left(\frac{\theta_o}{\tau}\right)^f$$

Criterion	a	b	c	d	e	f
ISE	1.495	-0.945	1.101	-0.771	0.560	1.006
IAE	1.435	-0.921	0.878	-0.749	0.482	1.137
ITAE	1.357	-0.947	0.842	-0.738	0.381	0.995
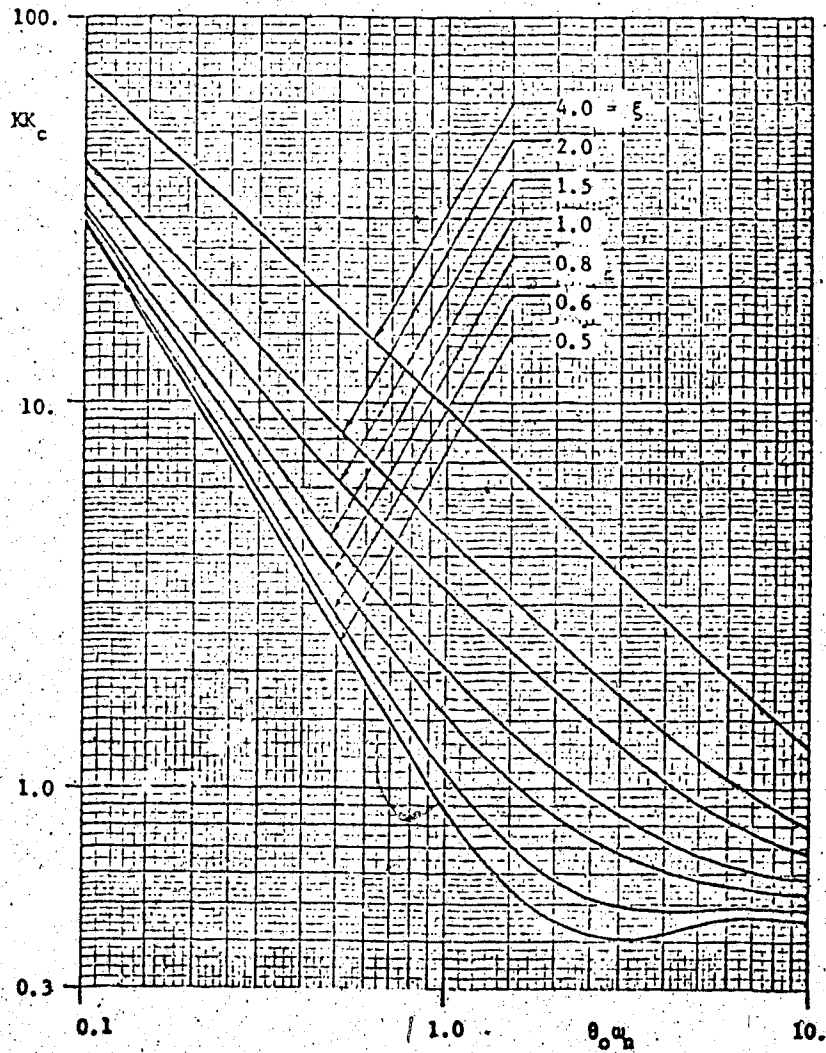
Figure AIII-2 Optimum Gain for PID Control. ISE Criterion.
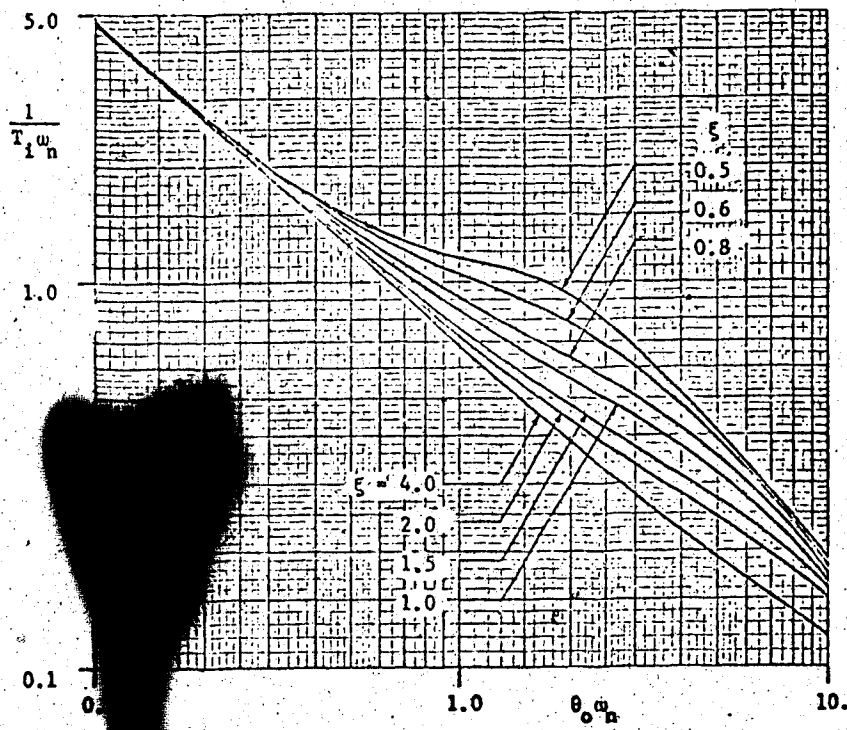
Figure AIII-3. Optimum Reset Setting for PID Control.
ISE Criterion.
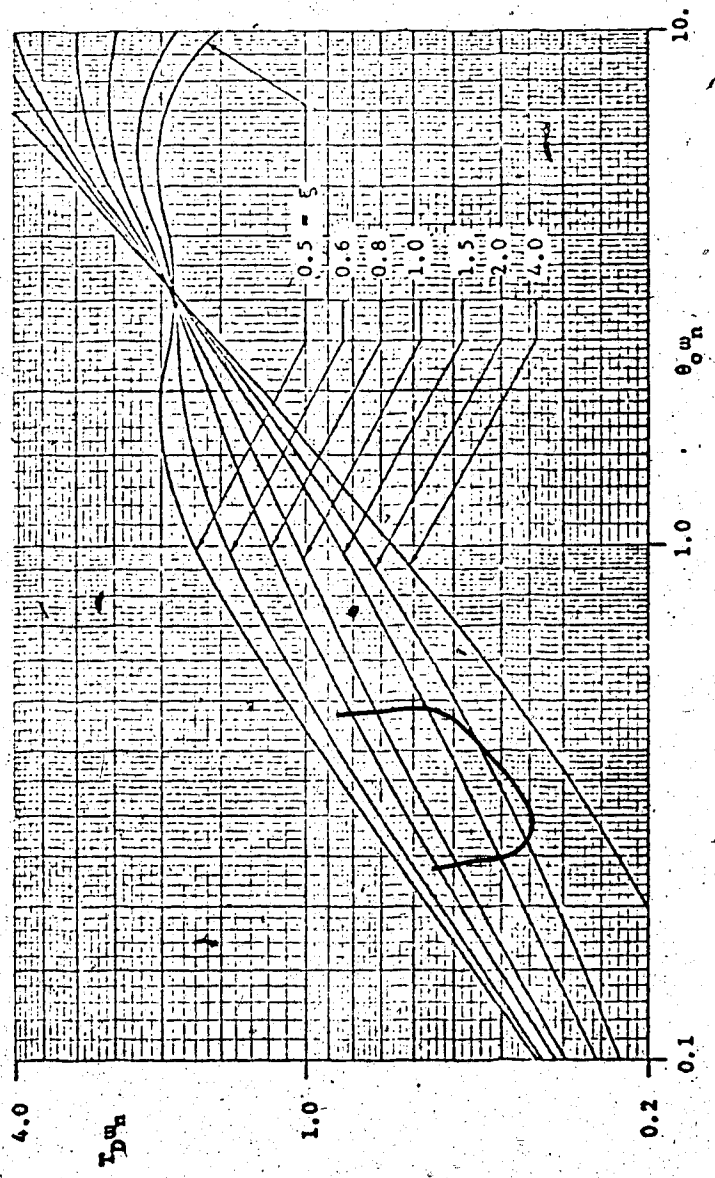
Figure A III-4 Optimum Derivative Setting for PID Control. IBE Criterion.
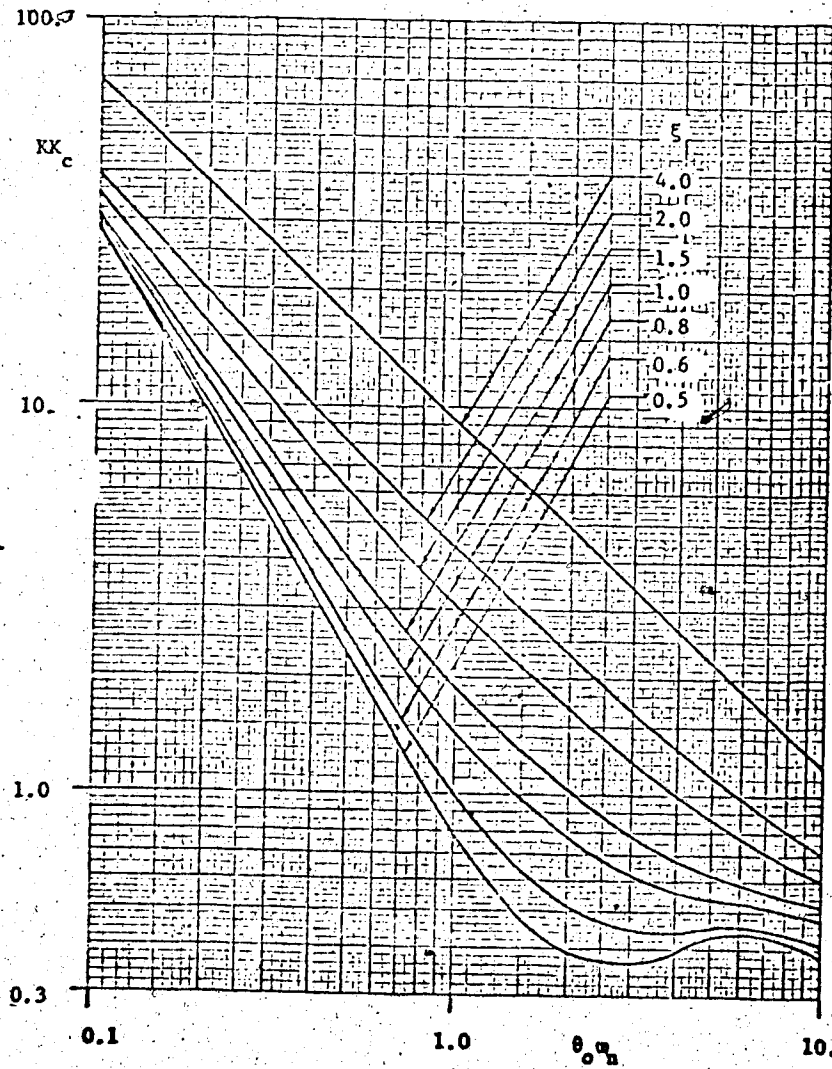
Figure AIII-5   Optimum Gain for PID Control.   IAE Criterion.

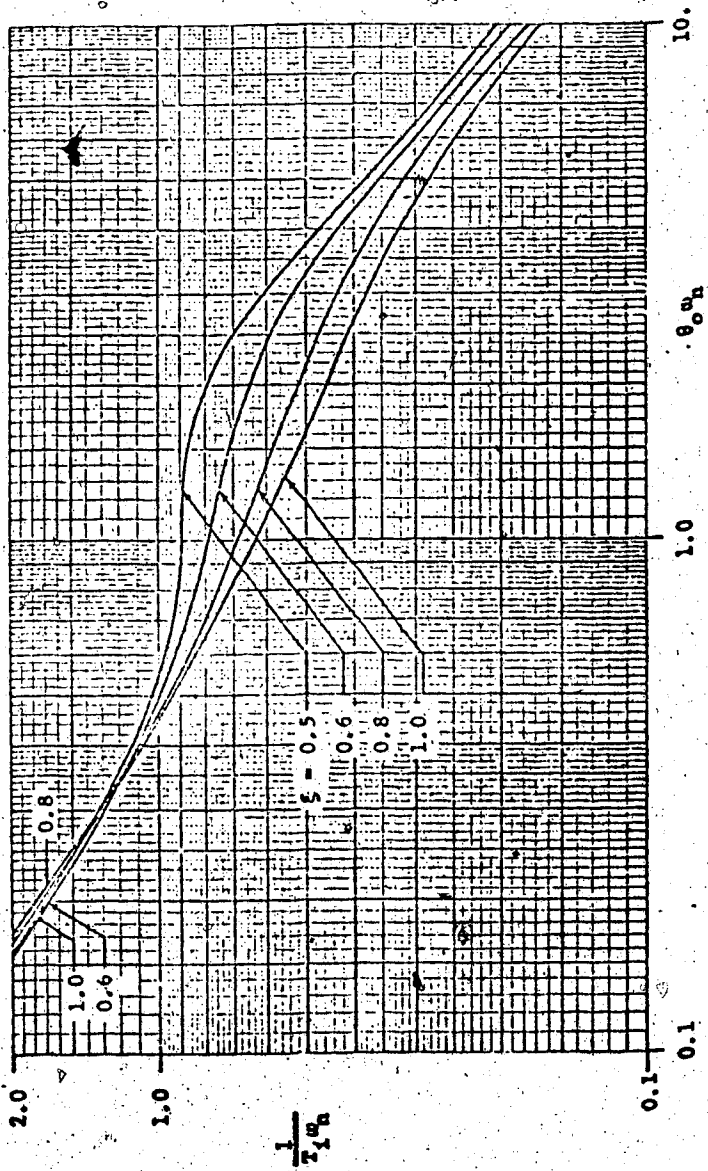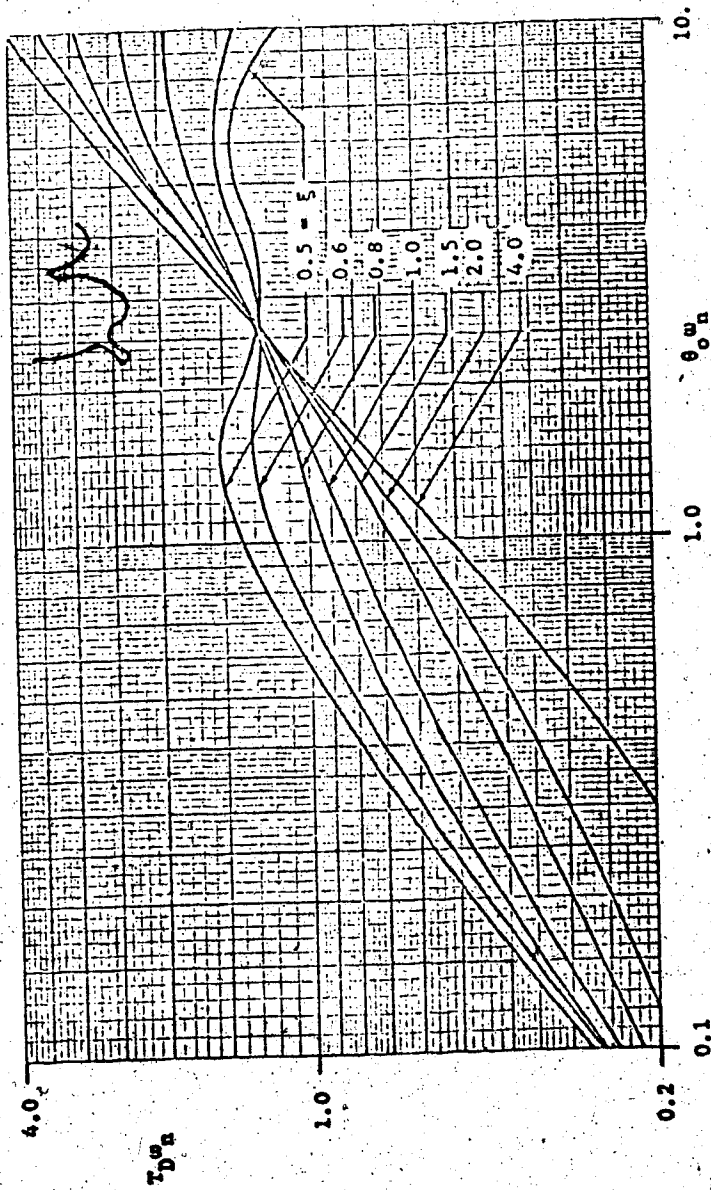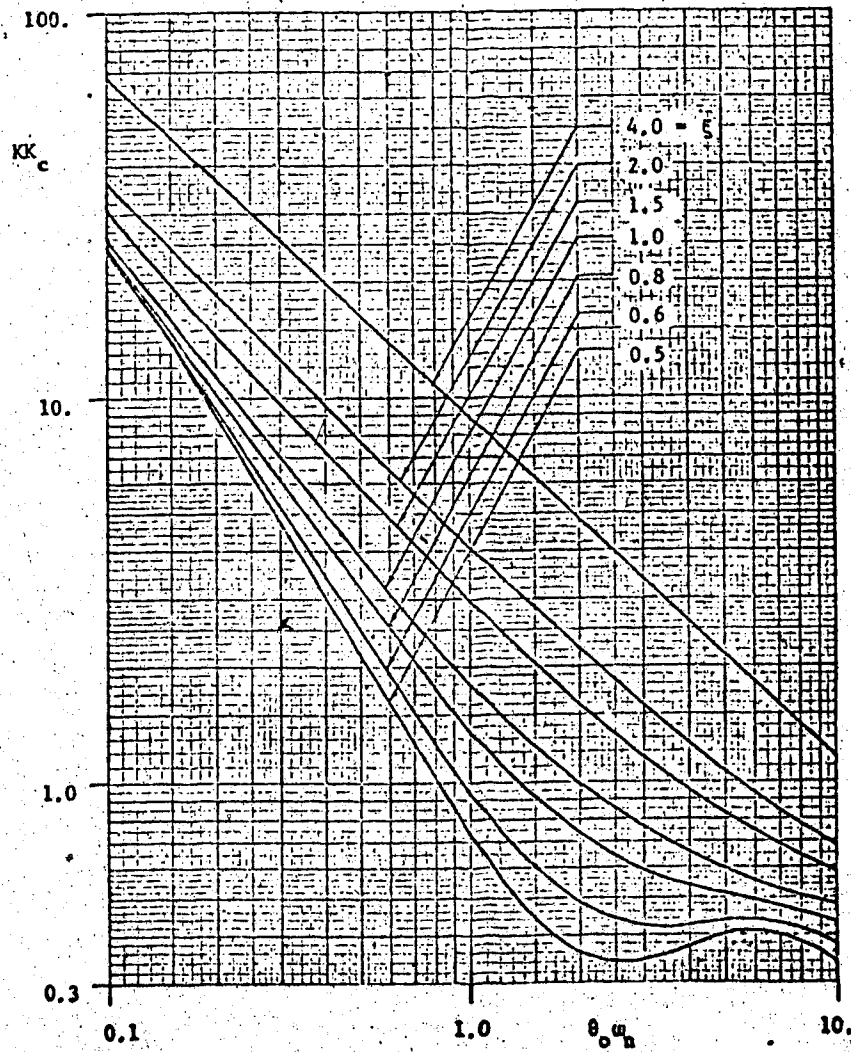Figure AIII-6a. Optimum Reset Setting for PID Control. IAE Criterion. ($\xi \geq 1.0$)

122
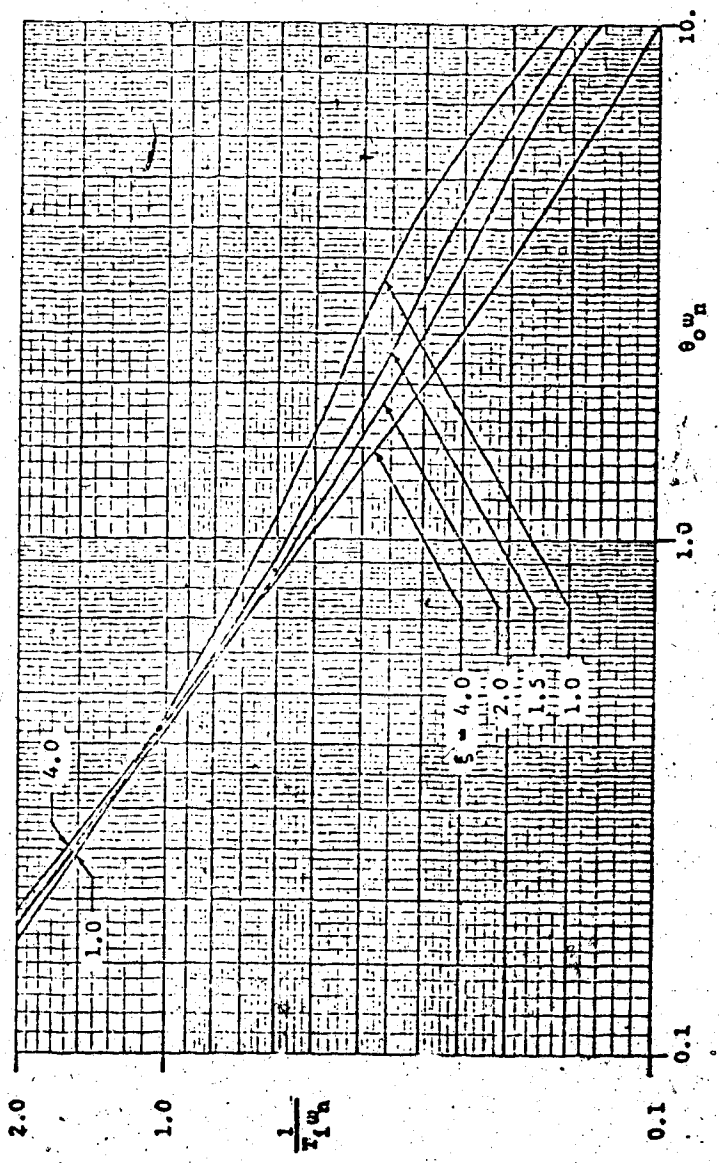
Figure AIII-6b Optimum Reset Setting for PID Control. IAE Criterion. $(\zeta \leq 1.0)$

Figure AⅡ - 7 Optimum Derivative Setting for PID Control. IAE Criterion.

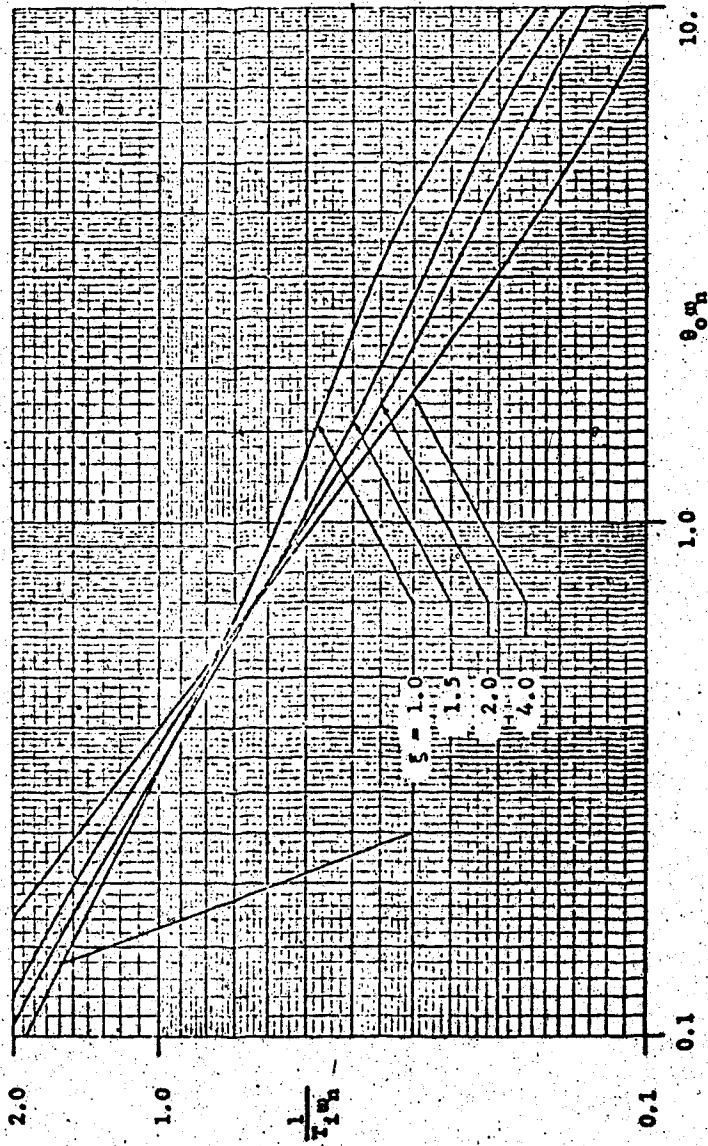Figure A III-8 Optimum Gain for PID Control. ITAE Criterion.

Figure AⅢ-9a Optimum Reset Setting for PID Control. ITAE Criterion ($\zeta \geq 1.0$)
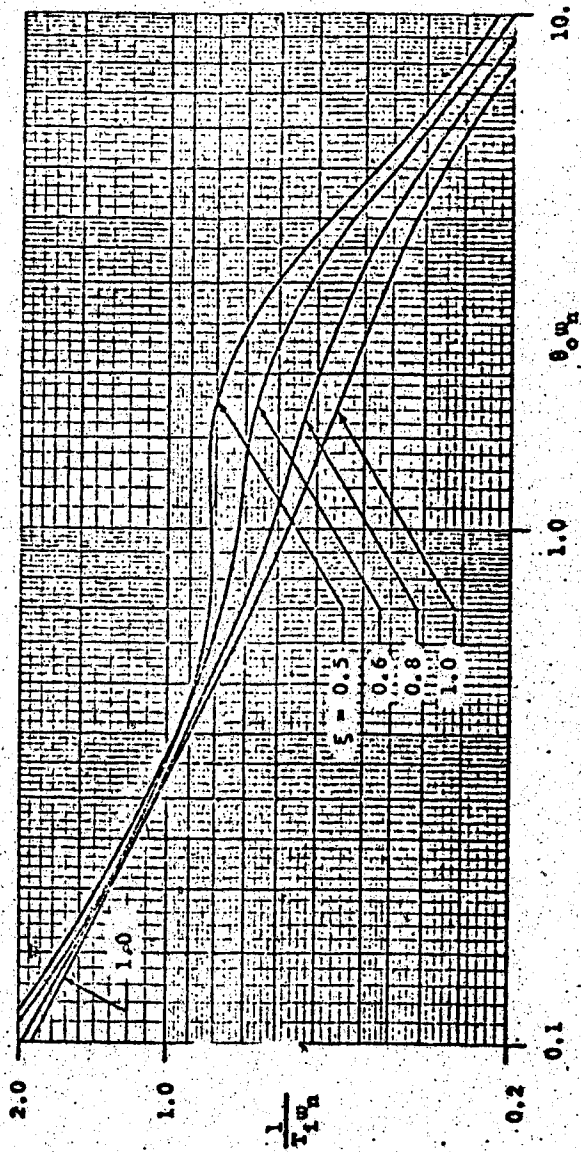
125

126

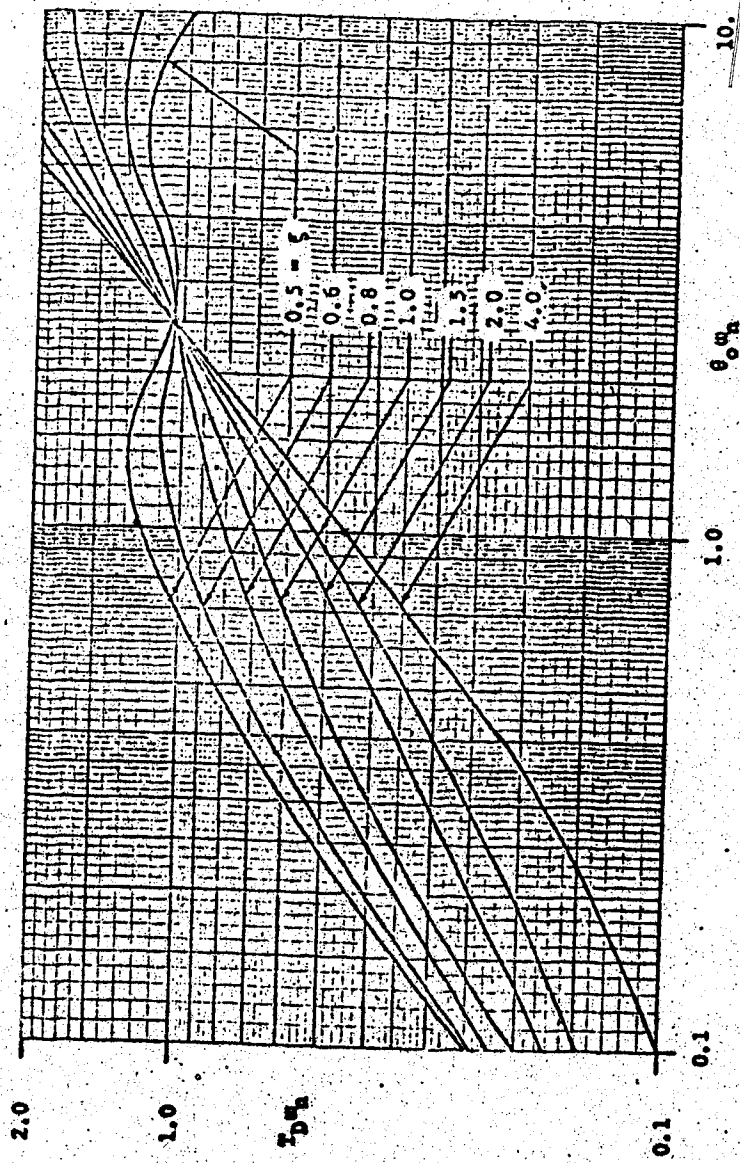Figure A III-9b   Optimum Reset Setting for PID Control, ITAE Criterion ($\xi \leq 1.0$)

Figure AIII-10 Optimum Derivative Setting for PID Control.— ITAE Criterion.